INVESTIGATION OF NOVEL TOPOLOGICAL INDICES AND THEIR APPLICATIONS IN ORGANIC CHEMISTRY

A THESIS SUBMITTED TO
THE GRADUATE SCHOOL OF NATURAL AND APPLIED SCIENCES
OF
MIDDLE EAST TECHNICAL UNIVERSITY

BY

SELÇUK GÜMÜŞ

IN PARTIAL FULFILLMENT OF THE REQUIREMENTS
FOR
THE DEGREE OF DOCTOR OF PHILOSOPHY
IN
CHEMISTRY

SEPTEMBER 2009

Approval of the thesis:

INVESTIGATION OF NOVEL TOPOLOGICAL INDICES AND THEIR APPLICATIONS IN ORGANIC CHEMISTRY

submitted by **SELÇUK GÜMÜŞ** in partial fulfillment of the requirements for the degree of **Doctor of Philosophy in Chemistry Department, Middle East Technical University** by,

Prof. Dr. Canan Özgen _____
Dean, Graduate School of **Natural and Applied Sciences**

Prof. Dr. M. Ahmet Önal _____
Head of Department, **Chemistry**

Prof. Dr. Lemi Türker _____
Supervisor, **Chemistry Dept.**, **METU**

Examining Committee Members:

Prof. Dr. Cihangir Tanyeli _____
Chemistry Dept., METU

Prof. Dr. Lemi Türker _____
Chemistry Dept., METU

Prof. Dr. Canan Ünaleroğlu _____
Chemistry Dept., Hacettepe University

Prof. Dr. Yılmaz Yıldırır _____
Chemistry Dept., Gazi University

Prof. Dr. Özdemir Doğan _____
Chemistry Dept., METU

Date: 10.09.2009

I hereby declare that all information in this document has been obtained and presented in accordance with academic rules and ethical conduct. I also declare that, as required by these rules and conduct, I have fully cited and referenced all material and results that are not original to this work.

Name, Last name: Selçuk GÜMÜŞ

Signature:

ABSTRACT

INVESTIGATION OF NOVEL TOPOLOGICAL INDICES AND THEIR APPLICATIONS IN ORGANIC CHEMISTRY

Gümüş, Selçuk
Ph.D., Department of Chemistry
Supervisor: Prof. Dr. Lemi Türker

September 2009, 144 Pages.

Numerical descriptors, beginning with Wiener, and then named topological indices by Hosoya, have gained gradually increasing importance along with other descriptors for use in QSAR and QSPR studies. Being able to estimate the physical or chemical properties of a yet nonexistent substance as close as possible is very important due to huge consumption of time and money upon direct synthesis. In addition, one may face safety problem as in the case of explosives. There have been almost hundred topological indices so far in the chemical graph theory literature. However, there is no topological index which is generalizable to all kinds of molecules. In the present study, a novel topological index (TG Index) has been developed and applied to a wide range of organic molecules including explosives for modeling their physical, structural and molecular orbital properties. The index yielded quite successful correlation data with most of the properties considered in this study.

Keywords: TG Index, topological indices, T(A) graphs, physico-chemical properties, detonation parameters.

ÖZ

YENİ TOPOLOJİK İNDEKSLERİN ARAŞTIRILMASI VE ORGANİK KİMYADAKİ UYGULAMALARI

Gümüş, Selçuk
Doktora, Kimya Bölümü
Tez Yöneticisi: Prof. Dr. Lemi TÜRKER

Eylül 2009, 144 Sayfa

Wiener ile başlayıp, Hosoya tarafından topolojik indeks olarak adlandırılan sayısal tanımlayıcılar, QSAR ve QSPR çalışmalarındaki kullanımından dolayı gittikçe artan bir önem kazanmıştır. Bilinmeyen bir maddenin fiziksel ve kimyasal özelliklerinin olabildiğince yakın olarak tahmini direk olarak sentezlenmesinin getireceği büyük zaman ve para kaybını önlemek açısından çok önemlidir. Buna ek olarak, patlatıcılarda güvenlik problemleri de ortaya çıkar. Bu zamana kadar yüz kadar topolojik indeks kimyasal grafik teori literatüründe yer almıştır. Ancak, her çeşit moleküle uygulanabilecek şekilde genelleştirilmiş bir topolojik indeks yoktur. Bu çalışmada, yeni bir topolojik indeks (TG İndeks) üretilmiş ve patlayıcıları da içeren geniş bir çerçevede organic moleküllerin fiziksel, yapısal ve moleküler özelliklerinin modellenmesi için uygulanmıştır. İndeks çalışmada ele alınan özelliklerin birçoğuyla oldukça başarılı korelasyon göstermiştir.

Anahtar kelimeler: TG İndeks, topolojik indeksler, T(A) grafikleri, fiziko-kimyasal özellikler, patlama parametreleri.

To My Family

ACKNOWLEDGEMENTS

I would like to express my sincere feelings of gratitude and appreciation to my supervisor Prof. Dr. Lemi TÜRKER for directing me in this interesting study and for his skillful guidance, endless support, encouragement and patience throughout this tedious work. It has been more than a decade since I started working with him. Every moment of this period was very valuable for my academic career and living life.

I want to thank Middle East Technical University and Van Yüzüncü Yıl University for cooperation for the ÖYP program.

I also give my thanks to Dr. Taner ATALAR and Yakup ÇAMUR for their friendship and help during some computational calculations. Moreover, I want to thank the present members of D-250 Research Group: Çağlar ÇELİK BAYAR and Hamza TURHAN for their friendship.

I also wish to express my deepful thanks to the entire members organic chemistry research group.

Finally, my sincere appreciation and gratitude is devoted to my wife, Ayşegül for her love, endless encouragement and moral support, which makes everything possible.

TABLE OF CONTENTS

LIST OF TABLES

TABLES

LIST OF FIGURES

FIGURES

LIST OF ABBREVIATIONS

Å	Angstrom
A(G)	Adjacency matrix of graph G
AM1	Austin Model 1
B3LYP	Becke's three parameter exchange hybrid functional with Lee, Yang, Parr (LYP) correlation functional
B3P86	Becke's three parameter hybrid functional combined with Perdew86 nonlocal correlation
B3PW91	Becke's three parameter hybrid functional and Perdew and Wang's 1991 gradient-corrected correlation functional
BHandHLYP	Becke's half-and-half method with. LYP correlation added
bp	Boiling point
CC	Coupled cluster theory
cc-PVDZ	The polarized valence double-zeta correlation-consistent basis set
cc-PVTZ	The polarized valence triple-zeta correlation-consistent basis set
CCSD	Coupled cluster theory with single and double excitations
CCSDT	Coupled cluster theory with single and double excitations and inclusion of connected triples excitations
CI	Configuration interaction
CISD	Configuration interaction single-and-double-excitation
d	Density
D	Detonation velocity
D(G)	Distance matrix of graph G
DFT	Density functional theory
E(G)	Edge set of graph G

F	Platt number
FLASH	Flash point
G	Graph
G2	Gaussian 2 basis set
G3	Gaussian 3 basis set
GIAO	Gauge invariant atomic orbital
GTO	Gaussian type orbital
GVB	Generalized valence bond
HC	Heats of combustion
HEDM	High energy density material
HF	Hartree-Fock theory
HMO	Hückel molecular orbital
HMX	1,3,5,7-tetranitro-1,3,5,7-tetraazacyclooctane
HOMO	Highest occupied molecularo
HV	Molar heat of vaporization
LSD	Local spin-density
LUMO	Lowest unoccupied molecular orbital
M	The average molecular weight of the gaseous products
M_1	First Zagreb index
M_2	Second Zagreb index
MINDO	Modified intermediate neglect of differential overlap
MM2	Molecular mechanics
MNDO	Modified neglect of diatomic overlap
mp	Melting point
MPn	Møller-Plesset nth-order perturbation theory
MR	Molar refraction
MV	Molar volume
MW	Molecular weight
N	Moles of gaseous detonation products per gram of explosive
N_2	Gordon-Scantlebury index
NICS	Nucleus independent chemical shift

P	Detonation pressure
PC	Critical pressure
PES	Potential energy surface
PM3	Parameterization method-3
P_{oct}	Partition coefficient in octanol-water solvent system
PR	Parachor
Q	Chemical energy of detonation
QSAR	Quantitative structure activity relationship
QSPR	Quantitative structure property relationship
RDX	1,3,5-trinitro-1,3,5-triazacyclohextane
SCF	Self-consistent field
ST	Surface tension
STO	Slater type orbital
S_w	Aqueous solubility
T(A)	Türker graphs for alternant hydrocarbons
TC	Critical temperature
TG	Türker-Gümüş index
V	Volume
V(G)	Vertex set of graph G
VIRC	Second virial coefficients
VISC	Viscosity
VWN3	Vosko, Wilk, Nusair's local correlation functional
W	Wiener index
Z	Hosoya index
α	Polarizability
χ	Connectivity index
χ_m	Molar susceptibility
$\Delta\varepsilon$	Frontier molecular orbital energy gap
ΔH_f	Heat of formation
ΔH_{rxn}	Heat of reaction

CHAPTER 1

INTRODUCTION

The mathematization of chemistry has a long and colorful history extending back well over two centuries. At any period in the development of chemistry the extent of mathematization process roughly parallels the progress of chemistry as a whole. In 1874 one of the greatest pioneers of chemical structure theory, Alexander Crum Brown (1838-1922) prophesied [1] that "...chemistry will become a branch of applied mathematics but will never become cease to be an experimental science. Mathematics may enable us retrospectively to justify results obtained by experiment, may point out useful lines of research and even sometimes predict entirely novel discoveries." Indeed, even before these words were uttered, combinatorial methods were being employed for the enumeration of isomeric species [2]. During the first decades of the 20. century algebraic equations were used to predict the properties of substances, calculus was employed in the description of thermodynamic and kinetic behavior of chemical systems, and graph theory was adapted for the structural characterization of molecular species.

In the present century the applications of mathematics have come thick and fast. The advent of quantum chemistry in the 1920s brought in its wake a host of mathematical disciplines that chemists felt obliged to master. These included several areas of linear algebra, such as matrix theory and group theory, as well as calculus. Group theory has now become so widely accepted by chemists that it is now used routinely in areas such as crystallography and molecular structure analysis. Graph theory seems to be following in the

footsteps of group theory and is currently being expoilted in a wide range of applications involving the classification, symmetrization, enumeration and design of systems of chemical interest. Topology has found important applications in the areas as diverse as the characterization of potential energy surfaces.

All of these and numerous other applications of mathematics that have been made in the chemical domain have brought us to a point where we can fairly say that mathematics plays an indispensable role in modern chemistry.

1.1. Introduction To Graph Theory

Graph theory is a branch of discrete mathematics that deals with the way objects are connected [3]. Thus, the connectivity in the system is a fundamental quality of graph theory. The principle concept in graph theory is that of a *graph*.

Graph theory is related to topology, matrix theory, group theory, set theory, probability, combinatorics and numerical analysis. It has been used in such diverse fields as economics [4], theoretical physics [5], psychology [6], nuclear physics [7], computer science [8], geography [9], biology [10], etc.

Chemical graph theory is a branch of mathematical chemistry that is concerned with the analysis of all consequences of connectivity in a chemical graph. Chemical graph serves as a convenient model for any real or abstract chemical system (molecule or reaction scheme in a chemical transformation) [11,12]. In other words, chemical graph theory is concerned with all aspects of the application of graph theory to chemistry.

Past decades have witnessed a remarkable growth of chemical graph theory [13-20]. There are many reasons for the increasing popularity of graph theory in chemistry [11-20]. First, there is hardly any concept in the natural sciences which is closer to the notion of graph than the structural (constitutional) formula of the chemical compound [21], because a graph is, simply said, a mathematical model [22] which may be used directly to represent a molecule when the only property considered is the internal

connectivity, i.e., whether or not a chemical bond joins two atoms in a molecule. Since almost all discussions in chemistry are carried out by means of graphical display of compounds and reactions, chemists manipulate graphs on a daily basis without being aware of this fact. Thus, it appears that the natural language of chemistry by which chemists communicate is provided by (chemical) graph theory. Secondly, graph theory provides simple rules by which chemists may obtain many qualitative predictions about the structure and reactivity of various compounds. All these predictions can be reached using nothing more than pencil and paper. Furthermore, the obtained results have in many cases a general validity and may be formulated as theorems and/or rules which can then be applied to a variety of similar problems without any further numerical or conceptual work. Third, graph theory may be used as a foundation for the representation, classification and categorization of a very large number of chemical systems [23-26]. Fourth, graphs appear as useful tools devices for computer-assisted synthesis and design [27,28]. Fifth, the development of simple valance-bond resonance-theoretical schemes is mostly influenced by the graph-theoretical work on the enumeration of valence structures [29,30]. One more reason must be mentioned can be the explosive use of graph-theoretical invariants in the structure-property-activity relationships [31-34]. Perhaps this is an area of chemistry in which graph theory could be the most useful theoretical tool.

In relating graph-theoretical terms and chemical terms, a certain caution is needed, because on set of terms is taken from the abstract theory and the other from the concrete models used in chemistry. Thus, in one case, for example, trees may be used to represent acyclic structures and in another, certain reaction schemes.

1.1.1. Definition of a Graph

The central concept in graph theory is that of *graph*. A simple graph G is defined as an ordered pair [V(G),E(G)], where V = V(G) is a nonempty set of elements called vertices (or points) of G and E = E(G), called edges (or

lines) is a set of unordered pairs of distinct elements of V(G). Sets V(G) and E(G) are called the vertex-set and the edge-set of G, respectively. In most cases of chemical interest the vertex and the edge sets are finite. The number or elements (N) in V(G) is called the order G and the number of elements (M) in E(G) is the size of G.

A very attractive feature of graph theory is that a graph can be visualized by means of a diagram when the vertices are drawn as small circles or dots and the edges as lines or curves joining the appropriate circles. An example of a simple graph is given in Figure 1. A graph G is *labeled* when its vertices are distinguished from one another by labels which may be letters or numbers. Therefore, the graph shown in Figure 1 is a diagram of the labeled simple graph G whose vertex-set V(G) is the set $\{v_1,v_2,v_3,v_4\}$(or in the simple notation {1,2,3,4}) and whose edge-set E(G) consists of pairs $\{v_1,v_2\}$, $\{v_2,v_3\}$, $\{v_2,v_4\}$ and $\{v_3,v_4\}$ (or in the simple notation {1,2}, {2,3}, {2,4} and {3,4} or $\{e_{12}, e_{23}, e_{24}, e_{34}\}$).

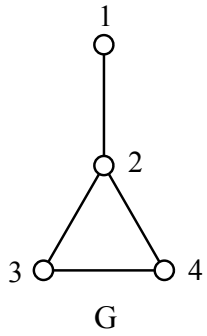

Figure 1. A diagram of a simple graph

Many results which can be proved for simple graphs may be extended without difficulty to more general graphs in which two vertices may have more than one edge joining them. In addition, it is often convenient to remove any restriction that any edge must join two distinct vertices, to allow the existence

of *loops*, i.e., edges joining vertices to themselves. General graphs may be split into two classes: (1) multigraphs [35] (in which multiple edges are allowed) (see Figure 2, G_1) and (2) loop-multigraphs [22] or pseodographs [35] (in which both multiple edges and loops are allowed) (see Figure 2, G_2).

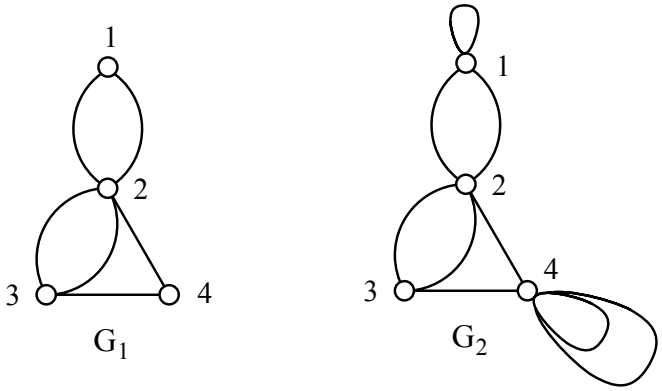

Figure 2. Diagrams of a multigraph G_1 and a loop-multigraph G_2.

A special class of graphs is a class of *directed graphs*. A directed graph is a nonempty set of elements (vertices) and is a family of ordered pairs of elements of *directed edges*.

Another important concept in graph theory is adjacency. Two vertices of a graph are set to be *adjacent* if there is an edge joining them. In other words, these two vertices are called to be *incident* to the edge connecting them. Similarly, two distinct edges are adjacent if they have at least one vertex in common. In graph G_1 of Figure 2, vertices 1 and 2 are adjacent whereas 1 and 3 are not.

A *subgraph* G' of a graph G is a graph having all its vertices and edges contained in G [35]. Subgraphs can be obtained by the removal of edges or vertices or both. A graph can also be its own subgraph.

1.1.2. Eulerian Graphs and the Story of the Königsberg Bridge Problem

The city of Königsberg in Prussia (now Kaliningrad, Russia) was set on both sides of the Pregel River, and included two large islands which were connected to each other and the mainland by seven bridges.

The problem was to find a walk through the city that would cross each bridge once and only once. The islands could not be reached by any route other than the bridges, and every bridge must have been crossed completely every time (one could not walk halfway onto the bridge and then turn around to come at it from another side).

To start with, Euler pointed out that the choice of route inside each landmass is irrelevant. The only important feature of a route is the sequence of bridges crossed. This allowed him to reformulate the problem in abstract terms (laying the foundations of graph theory), eliminating all features except the list of landmasses and the bridges connecting them. In modern terms, one replaces each landmass with an abstract "vertex", and each bridge with an abstract connection, an "edge", which only serves to record which pair of vertices (landmasses) is connected by that bridge (Figure 3). Therefore, he ended up with the first multigraph in the history of graph theory [36].

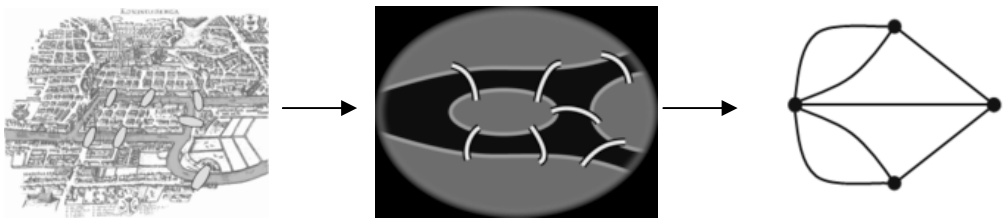

Figure 3. The seven bridges of Königsberg and its graph theoretical representation.

Euler shows that the existence of a walk in a graph which traverses each edge once depends on the degrees of the nodes. The degree of a node is the

number of edges touching it. Euler's argument shows that a necessary condition for the walk of the desired form to exist is that the graph be connected and have exactly zero or two nodes of odd degree. This condition turns out also to be sufficient - a result stated by Euler [36]. Such a walk is now called an *Eulerian path* or *Euler walk* in his honor.

On the other hand, if a circuit which includes every vertex of a graph only once, the connected graph is named as a *Hamiltonian graph* [12].

1.1.3. The Concept of a Chemical Graph

In chemistry graphs can represent different chemical objects: molecules, reactions, crystals, polymers, clusters, etc. The common feature of chemical systems is the presence of atoms and bonds between them. When a molecule is converted to the corresponding chemical graph, atoms and bonds are represented as vertices and edges (either single or multiple), respectively.

In order to simplify the handling of molecular graphs, *hydrogen-depleted graphs* [37], i.e., graphs depicting only molecular skeletons without hydrogen atoms and their bonds, are often used. The hydrogen-suppressed graphs are almost universally used in chemical graph theory, because the neglect of the hydrogen atoms and their bonds in most cases cannot be the cause of any ambiguity. An example of converting a chemical structure into a hydrogen-suppressed chemical graph has been illustrated in Figure 4.

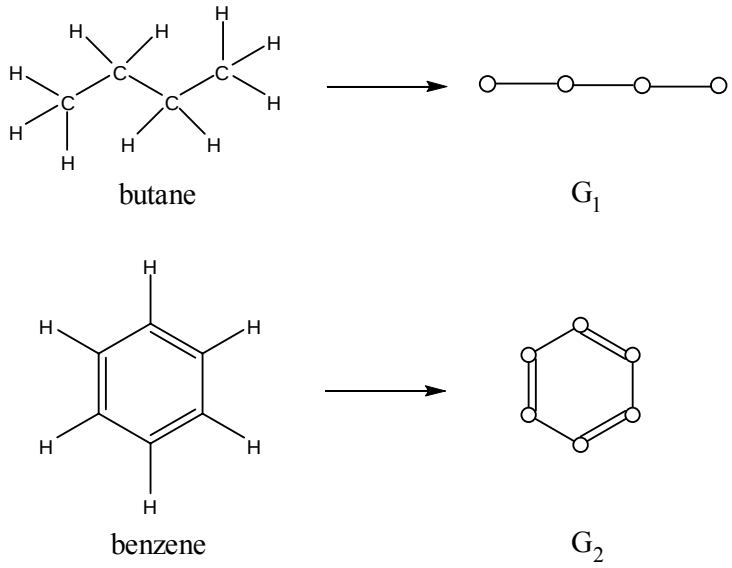

Figure 4. The hydrogen-depleted graphs depicting butane and benzene.

Molecular graphs depicting constitutional formulae of molecules represent their *topology* [12,35]. Each connected simple graph is associated with a topological space. Since the molecular graph is uniquely derived from the molecular constitution, each molecule is associated with topological space via its molecular graph.

1.2. Graph-Theoretical Matrices

Graphs may be associated with several matrices [35]. The adjacency matrix and the distance matrix are the most frequently pronounced matrices in chemical graph theory. They are also referred to as topological matrices [38]. They may be used for identifying certain properties of graphs.

1.2.1. The Adjacency Matrix

The most important matrix representation of a graph is the vertex-adjacency matrix [12]. This matrix finds important use in both chemistry and physics [35].

The adjacency matrix A(G) of a labeled connected graph G with N vertices is the square N x N symmetric square matrix which contains information about the internal connectivity of vertices in G. It is defined as,

$$A_{ij} = \begin{cases} 1 & \text{if vertices } v_i \text{ and } v_j \text{ are adjacent} \\ 0 & \text{otherwise} \end{cases}$$

$$A_{ii} = 0$$

Therefore, a nonzero entry appears in A(G) only if an edge connects vertices i and j. Figure 5 shows an example for the construction of the adjacency matrix for methylcylopropane. Note that, the adjacency matrix is symmetrical about the principle diagonal.

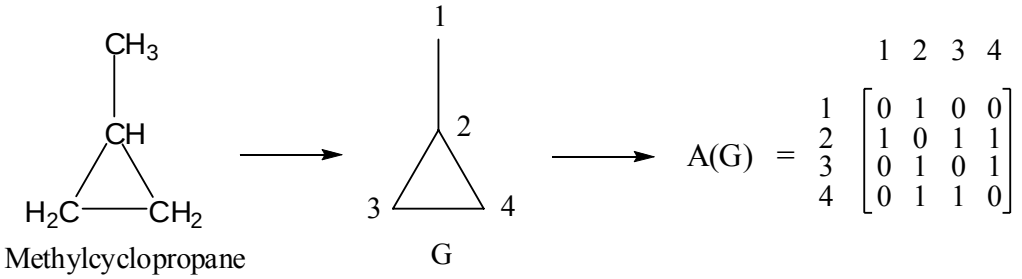

Figure 5. The adjacency matrix of methylcyclopropane.

1.2.2. The Distance Matrix

The *distance matrix* is a more complicated and also a richer structure than the adjacency matrix [35,38]. It is a graph theoretical (topological) matrix less common than the adjacency matrix, but it has been increasingly used in the last decades in many different areas of chemistry and physics [39].

The distance matrix D(G) of a labeled connected graph G is a real symmetric N x N matrix whose elements are defined as follows;

$$D_{ij} = \begin{cases} l_{ij} & \text{if } i \neq j \\ 0 & \text{if } i = j \end{cases}$$

where l_{ij} is the length of the shortest path, i.e., the minimum number of edges, between the vertices v_i and v_j. The length can also be called as the distance between the vertices v_i and v_j. In Figure 6 the distance matrix for methyl cyclopropane is given. Note that, the distance matrix is also symmetrical about the principle diagonal as in the case of adjacency matrix.

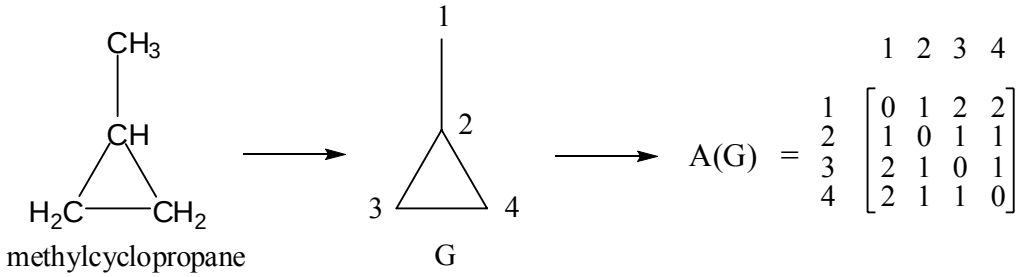

Figure 6. The distance matrix of methylcyclopropane.

1.3. Topological Indices

Topological indices are numbers associated with constitutional formulas by mathematical operations on the graphs representing these formulas. The necessity of having to use such tools as topological indices originates in the fact that physico-chemical properties are expressed as numbers and thus have a metric enabling scientists to make comparisons and correlations. In order to evaluate quantitatively the degree of similarity or dissimilarity of chemical structures or to find correlations between structures

and properties (QSAR or QSPR) one needs to translate structures into numbers. For electronic factors, quantum chemistry or linear free energy relationships provide such numerical data. For steric factors or hydrophobicity/hydrophilicity there are well-established numerical data. For shape, however, topological indices provided a simple solution.

Ever since structure theory became able to explain the isomerism phenomenon and to predict what substances with a given molecular formula can exist, chemists have tried to predict the properties of these substances before they were synthesized. After some of these substances were prepared, the predictions could be checked and the prediction methods could be validated or improved.

Probably the first chemist who attempted such predictions was Kopp who published his results in 1844 [40]. His methods were primitive because the structure theory was just emerging. With the advent of quantum theory and more recently with the help of computer-assisted semiempirical or *ab initio* calculations, the theoretical background of molecular chemistry reached a satisfactory level for understanding chemical reactivity and for describing transition states. It was Erich Hückel who for the first time thought about applying to molecules the π-electron approximation and invented the equivalence between the eigenvalues of the adjacency matrix of a graph symbolizing the σ-electron framework and the energy levels of π-electrons in conjugated systems [41]. Thus, topological or graph theoretical data are deeply associated with the core of quantum chemistry [42].

Most of the proposed topological indices are related to either vertex adjacency relationship (connectivity) in the molecular graph or to graph theoretical (topological) distances. Therefore, the origin of topological indices can be traced either to the adjacency matrix of a molecular graph or to the distance matrix of a molecular graph. Furthermore, since the distance matrix can be generated from adjacency matrix [43], most of the topological indices are really related to the latter matrix [44].

Here are some of the most famous topological indices whose computations are based on either connectivity or the adjacency in the molecular graph.

1.3.1. Wiener Index

Harold Wiener is accepted to be the "founding father" of topological indices. He proposed one of the first molecular descriptors of topological nature for acyclic saturated hydrocarbons (alkanes) [45,46]. He called the sum of the number of bonds linking all pairs of atoms as the *path number*. Due to the contradiction that paths can be in different lengths, the misnomer of the molecular descriptor has been renamed as *Wiener Index* and denoted by W. It was later shown by Hosoya that W is the half-sum of all entries in the distance matrix. The formula for the Wiener index is as follows;

$$W = \tfrac{1}{2} \sum_{i=1}^{n} \sum_{j=1}^{n} dij \qquad (1)$$

Index W is important not only because it was the first topological index to be invented, but also because it is simple to compute and yet is quite successful for many applications. Its main drawback is its high degeneracy, which is the fact that many non-isomeric graphs share the same W value.

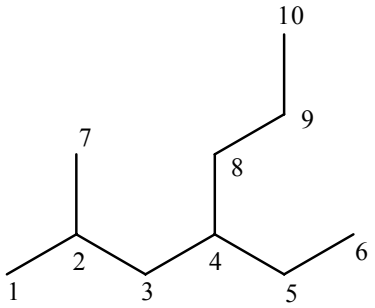

G

$$d(G) = \begin{bmatrix} 0 & 1 & 2 & 3 & 4 & 5 & 2 & 4 & 5 & 6 \\ 1 & 0 & 1 & 2 & 3 & 4 & 1 & 3 & 4 & 5 \\ 2 & 1 & 0 & 1 & 2 & 3 & 2 & 2 & 3 & 4 \\ 3 & 2 & 1 & 0 & 1 & 2 & 3 & 1 & 2 & 3 \\ 4 & 3 & 2 & 1 & 0 & 1 & 4 & 2 & 3 & 4 \\ 5 & 4 & 3 & 2 & 1 & 0 & 5 & 3 & 4 & 5 \\ 2 & 1 & 2 & 3 & 4 & 5 & 0 & 4 & 5 & 6 \\ 4 & 3 & 2 & 1 & 2 & 3 & 4 & 0 & 1 & 2 \\ 5 & 4 & 3 & 2 & 3 & 4 & 5 & 1 & 0 & 1 \\ 6 & 5 & 4 & 3 & 4 & 5 & 6 & 2 & 1 & 0 \end{bmatrix}$$

$$\sum_{k=1}^{10} \sum_{l=1}^{10} = 268 \longrightarrow W(G) = 134$$

Figure 7. A graph G depicting 2-methyl-4-propylhexane and the computation of Wiener number, W for G.

1.3.2. Platt Number and the Gordon-Scantlebury Index

Platt was also interested in devising a scheme for predicting physical parameters (molar volumes, boiling points, heats of formation, heats of vaporization) of alkanes. Practically simultaneously with Wiener, Platt [47,48] introduced index *F*, which is equal to the total sum of the edge-degrees in a graph G. The edge-degree of an edge e, D(e), is the number of its adjacent edges. This index was named as the Platt Number. The Platt number for a graph G is defined by

$$F = \sum_{i=1}^{M} D(e_i) \qquad (2)$$

One may also regard the edge-degrees as the edge-weights. Then, the Platt number may be considered as the sum of the weighted distances of the length one.

Dr. Manfred Gordon, who developed application of graph theory in polymer chemistry, proposed with Dr. Scantlebury in 1964 an index called N_2, defined [49] as the number of distinct ways a path P_2 of length two (a chain fragment on three vertices) can be superimposed on the molecular graph. It can be demonstrated that $F = 2N_2$ indicating once again that during this period several independent chemists arrived at similar ideas.

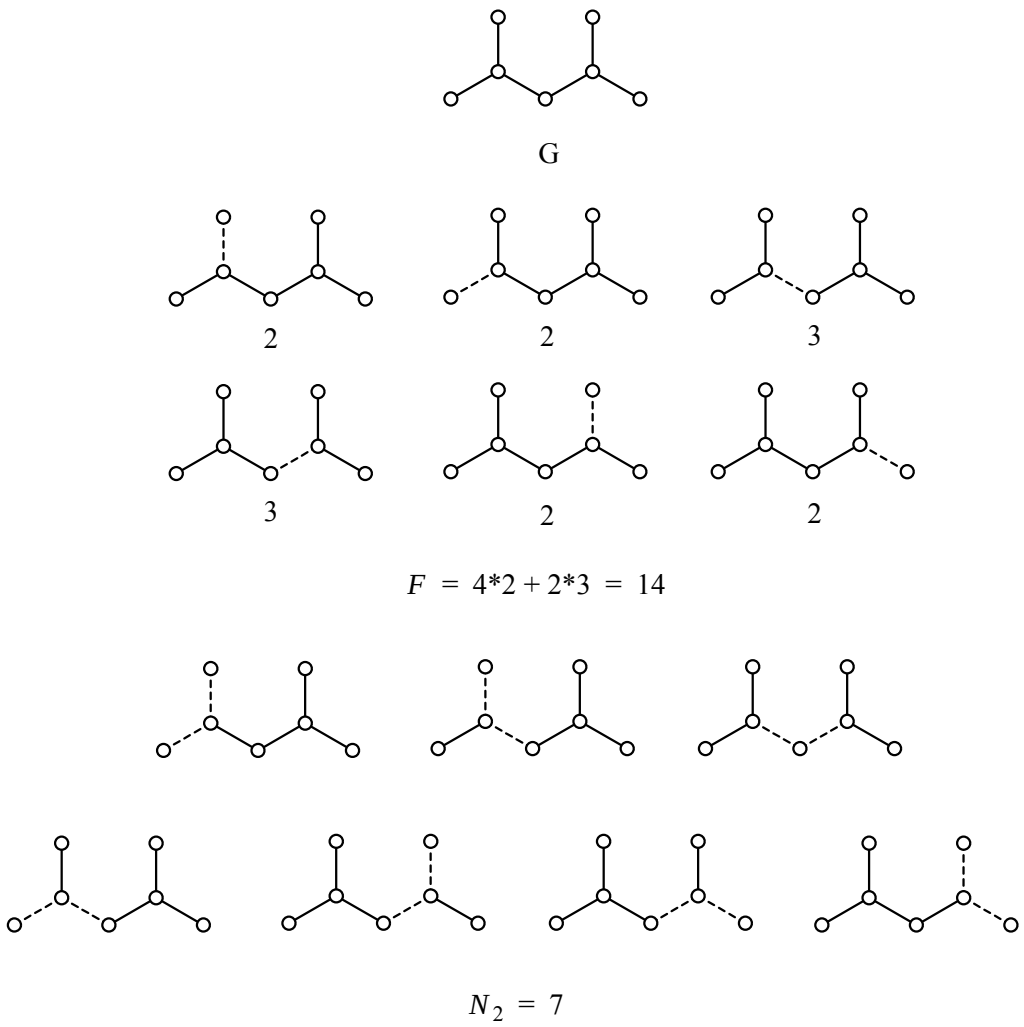

Figure 8. A graph G depicting 2,4-dimethylpentane and the computation of Platt number, *F* and Gordon-Scantlebury Index, N_2 for G. Note that $F = 2N_2$ is confirmed.

1.3.3. Hosoya Index

In the early seventies, Haruo Hosoya proposed another molecular descriptor called *Z* [50]. Its definition is

$$Z = \sum_{k=0}^{[n/2]} p(G,k) \qquad (3)$$

where *p*(G,k) is the number of ways in which *k* edges of a graph may be chosen so that no two of them are adjacent, and the Gauss square half brackets indicate the smallest integer not exceeding the number included in these brackets. The number *e* of edges equals *p*(G,1) and by definition *p*(G,0) is 1. The sum of these absolute values is equal to *Z*. Hosoya coined the term *topological index* which, although occasionally disputed, has become accepted by the scientific community. The index *Z* was shown to possess excellent correlation ability with many physical properties.

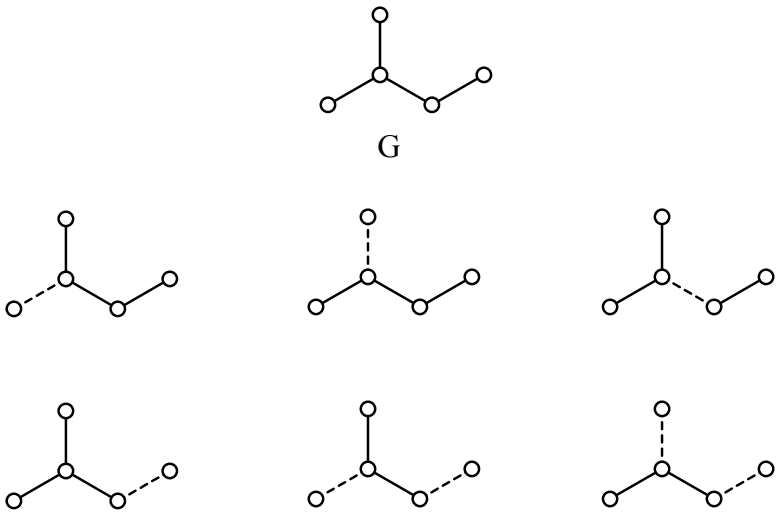

$$Z = G(0) + G(1) + G(2) = 1 + 4 + 2 = 7$$

Figure 9. A graph G depicting 2-methylbutane and the computation of Hosoya Index, *Z*.

1.3.4. Zagreb Group Indices

Around 1975, chemists who had been interested in the applications of the chemical graph theory in Zagreb, proposed [51] two topological indices derived from the adjacency matrix.

$$M_1 = \sum_i D^2(i) \qquad (4)$$

$$M_2 = \sum_{(i,j)} D(i)D(j) \qquad (5)$$

This group consisted of quantum chemists and mathematicians Nenad Trinajstic, Ivan Gutman and Milan Randic. It can be shown that the Platt, Gordon-Scantlebury, and the first Zagreb group indices are related by:

$$F = 2N_2 = M_1 - e \qquad (6)$$

where e is the sum of the degrees of all vertices. By means of the adjacency matrix, the Zagreb group indices can also be expressed as:

$$M_1 = \sum_i [A^2]_{ii}[A^2]_{ii} \qquad (7)$$

$$M_2 = \sum_{(i,j)} [A^2]_{ii}[A^2]_{jj} \qquad (8)$$

because $D_i = [A^2]_{ii}$.

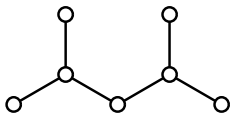

G

$$M_1 = 4*(1)^2 + 1*(2)^2 + 2*(3)^2 = 26$$

$$M_2 = 4*(1*3) + 2*(3*2) = 24$$

Figure 10. A graph G depicting 2,4-dimethylpentane and the computation of Zagreb group indices, M_1 and M_2.

1.3.5. The Connectivity Index

The connectivity index χ of a graph was introduced by Randic [52] and is similar to Zagreb group indices. It was obtained after a search for the specific index to quantify the notion of chemical branching, unlike the indices M_1 and M_2, which appeared in the topological formula for the π-electron energy of conjugated systems. Nevertheless, the connectivity index has found considerable application in both Quantitative Structure Property Relationship

(QSPR) and Quantitative Structure Activity Relationship (QSAR) [12]. Actually, the χ is the most used topological index in QSPR and QSAR up to date. The connectivity index of a graph was defined by Randic as a bond additive quantity [52].

$$\chi = \sum_{(i,j)} [D(i)D(j)]^{-1/2} \qquad (9)$$

Therefore, the connectivity index may be viewed as a sum of bond weights given in terms of $[D(i)\ D(j)]^{-1/2}$. This index may also be redefined by means of the adjacency matrix of a graph:

$$\chi = \sum_{(i,j)} [(A^2)_{ii}(A^2)_{jj}]^{-1/2} \qquad (10)$$

For carbon compounds, the first equation can be given in closed form. In the graphs representing the skeletons of carbon compounds there are possible only four types of vertices according to their valencies. These give rise to 10 edge types (bond types) whose connectivity weights are given in Table 1.

Table 1. Connectivity weights for edge types in the graphs corresponding to carbon compounds [12].

Edge type (D(i),D(j))	Connectivity Weight $[D(i)D(j)]^{-1/2}$
1,1	1.0000
1,2	0.7071
1,3	0.5773
1,4	0.5000
2,2	0.5000
2,3	0.4082
2,4	0.3536
3,3	0.3333
3,4	0.2887
4,4	0.2500

If the number of each edge type is denoted by b_{ij} (i = 1-4, j = 1-4) and if the corresponding weights are used (see Table 1) then, χ becomes;

$$\chi = b_{11} + 0.7071\, b_{12} + 0.5773\, b_{13} + 0.5\,(b_{14} + b_{22}) + 0.4882\, b_{23} + 0.3536\, b_{24} + 0.3333\, b_{33} + 0.2887\, b_{34} + 0.25\, b_{44}$$

In this way, the computation of the connectivity index for carbon compounds transforms into the enumeration of their bond types.

In the case of polycyclic graphs representing the carbon skeletons of polycyclic conjugated hydrocarbons there are possible only vertices of two types, according to their valencies. They give rise to three edge types: b_{22}, b_{23} and b_{33}. Thus, the above equation is used accordingly.

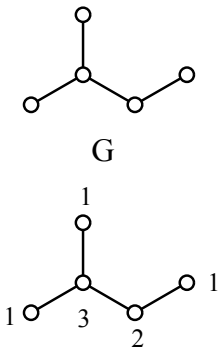

$\chi = 2* 0.5773 + 0.7071 +0.4082 = 2.2699$

Figure 11. A graph G depicting 2-methylbutane and the computation of Connectivity index, χ.

To sum up, one should reiterate that since the advent of topological indices more than six decades ago (when the term "topological index" had not yet been advanced) much progress has been made. Novel topological indices attracted the attention of the scientific community because QSAR and QSPR studies which must rely on numerical descriptors are interdisciplinary. The pharmaceutical industry contributed to the increased interest in molecular descriptors because of the necessity to reduce the expenses connected both with synthesis and clinical testing of medicinal drugs.

As summarized above, there have been many topological indices reported in the literature since the beginning of 70s. However, there has not been any topological index which covers all the necessities, that is, being unique for each and every molecule, easy to calculate, applicable to all kinds of molecular structures, correlate as many properties as possible and etc. Therefore, not only the famous topological indices are needed to be improved but also novel topological indices are needed to be invented.

CHAPTER 2

METHOD OF CALCULATION

2.1. The TG Index

2.1.1. T(A) Graphs

It is known that within the constraints of the Hückel molecular orbital theory (HMO), the adjacency matrix A [53] of a graph G(v;e) is identical to the secular matrix for the electronic system isomorphic to the graph [54,55] and there exists a vector X and a number λ such that

$$AX = \lambda X \qquad (11)$$

where X is the eigenvector (invariant vector) and λ an eigenvalue of graph G(v;e). On the other hand, eigenvalues of matrix A^2 (with multiplicities taken into account) fulfill the reaction below [56].

$$A^2X = \lambda^2X \qquad (12)$$

where, the matrix A^2 is symmetric as the adjacency matrix A. It is proved that an A^2-matrix is associated with certain graphs (known as T(A) graphs [57]) in which every vertex i has certain number of self-loops having weight λ, equal to d_i in number, and off-diagonal relations with the necessary number of edges having weight λ [57]. They have a quite great importance in the area of graph theory since they can be used in the construction of isospectral graphs of

alternant hydrocarbons [57]. Figure 12 shows the T(A) graphs of 1,3,5-hexatriene molecule.

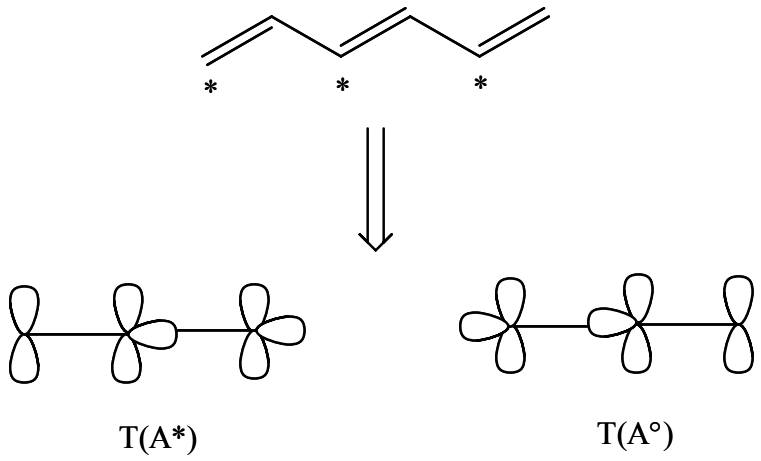

Figure 12. 1,3,5-hexatriene molecule and its T(A) graphs.

The T(A) graphs display simultaneously the degrees of vertices and the nearest neighbor relations including molecular symmetry implicitly. The starred and unstarred set of atoms are grouped as T(A*) and T(A°) graphs, respectively.

2.1.2. Calculation of the TG Index

In the present study a research has been performed to investigate a novel topological index which can be calculated easily. Ideally, a good topological index should show low degeneracy and high correlation ability. In other words, a good topological index should be unique for each and every molecule, correlate as many properties as of known molecules so that the properties of unknown species can be predicted before synthesis.

TG Index (Türker-Gümüş Index) is a novel topological index developed by Türker and Gümüş which is constructed on the basis of T(A)

graphs. Moreover, the calculation of the topological index makes use of the concepts of both, the connectivity (branching) which was introduced by Randic [52], and the path distances, introduced by Wiener [46,58].

However, the application of the T(A) graphs in the case of the TG index is somewhat different from the original [57,59]. T(A) graphs, as pointed out earlier, have been drawn and used to predict some properties of the completely conjugated systems. Nevertheless, it has been shown here that T(A) graphs can be exerted to all kinds of molecules independent from being totally conjugated, saturated or unsaturated. In fact, it can be implemented on both hydrocarbons and heteroatom containing species.

The TG index is defined by the following equation;

$$TG = \left(\sum_{i}^{N}\sum_{j}^{N} D^{*}_{ij}\right)\left(\sum_{i}^{M}\sum_{j}^{M} D^{\circ}_{ij}\right) \qquad (13)$$

The calculation of the index is based on a novel type of matrix presently introduced that is the distance-degree matrix (D_{ij}). This matrix represents the connectivity in the structure under consideration, so that the distance between the vertices as well as the degrees of the vertices in the parent structure are taken into account.

The calculation of the topological index is presented by an example in Figure 13. One can calculate the index by following the required steps;

a) Consider a hydrogen-depleted molecular graph (A).
b) Star the molecule alternatingly (as in the case of alternant hydrocarbons).
c) Obtain $T(A^{*})$ and $T(A^{\circ})$ graphs, as shown in Figure 13 and Refs [57,59], (the number of self loops is determined by the degree of the corresponding vertex in the original graph (A)).
d) Number the vertices of the newly obtained $T(A^{*})$ and $T(A^{\circ})$ graphs.

e) Construct the distance-degree matrix (This is a newly developed matrix which has not been pronounced in the literature up to date.), for both $T(A^*)$ and $T(A°)$ graphs as follows;

$$\overset{*}{D} = \begin{bmatrix} l_{11}d_1 & l_{12}d_2 & l_{13}d_3 & l_{14}d_4 & l_{15}d_5 \\ l_{21}d_1 & l_{22}d_2 & l_{23}d_3 & l_{24}d_4 & l_{25}d_5 \\ l_{31}d_1 & l_{32}d_2 & l_{33}d_3 & l_{34}d_4 & l_{35}d_5 \\ l_{41}d_1 & l_{42}d_2 & l_{43}d_3 & l_{44}d_4 & l_{45}d_5 \\ l_{51}d_1 & l_{52}d_2 & l_{53}d_3 & l_{54}d_4 & l_{55}d_5 \end{bmatrix} \qquad \overset{o}{D} = \begin{bmatrix} l_{11}d_1 & l_{12}d_2 & l_{13}d_3 \\ l_{21}d_1 & l_{22}d_2 & l_{23}d_3 \\ l_{31}d_1 & l_{32}d_2 & l_{33}d_3 \end{bmatrix}$$

Since the distance between the same atom is zero, all the diagonal elements of the matrix should be zero by definition, independent from the degree of that vertex.

f) The elements of the matrix are obtained numerically as follows; Considering the D_{35} element of the matrix,

$D_{35} = l_{35}$ (the distance between 3 and 5) x d_5 (the degree of 5) = 1 x 1 = 1

g) Sum all the elements of the each matrix to obtain

$$\sum_{i}^{N}\sum_{j}^{N} D^{*}_{ij} \qquad \text{and} \qquad \sum_{i}^{M}\sum_{j}^{M} D^{\circ}_{ij}$$

Summation of half or all of the matrix elements has been frequently pronounced in the literature [46,58,60,61].

h) Use the equation above to calculate the TG index for compound A.

The construction of the T(A) graphs during the formulation of the TG index makes it quite different from previously published indices. The physical meaning behind this lays on the success of the T(A) graphs for the prediction of isospectral graphs [59] (see section 2.1.1).

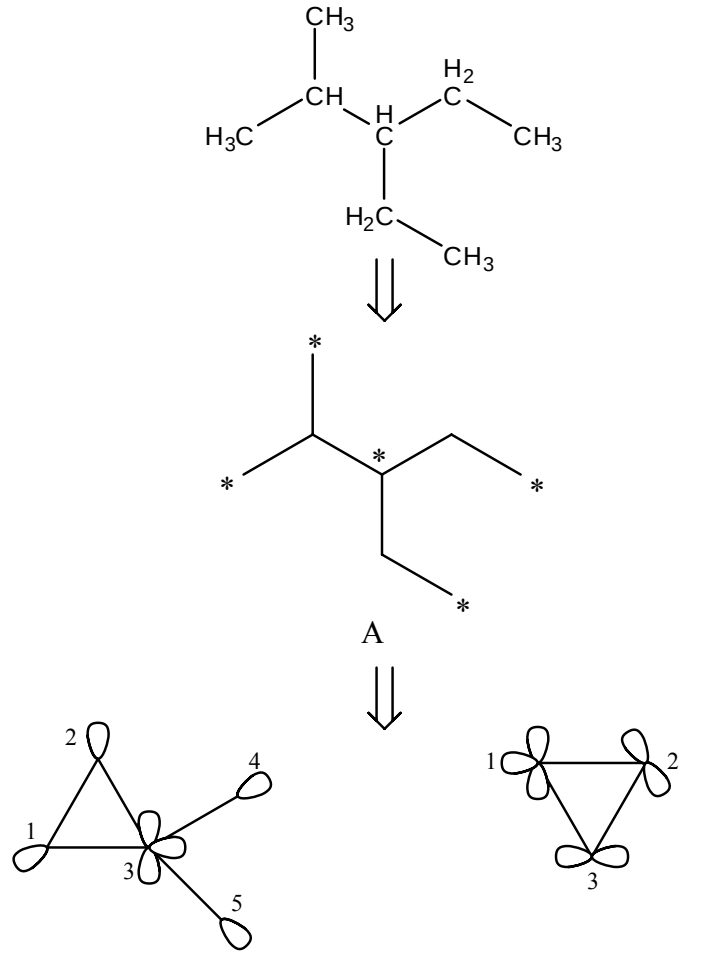

Figure 13. Illustration of how to calculate the TG index

One drawback of calculation method of TG index is that the index cannot be calculated for linear compounds having less than four vertices. Moreover, we cannot compute the TG index for isopropane and neopentan because their T(A˚) graph has only one vertex which make the TG index not applicable. In addition to those specific cases, TG index of structures having odd-membered rings cannot be computed because they are nonalternant systems and they do not have any T(A) graphs.

2.1.3. The TG Index for Heterosystems

The TG index can be applied to hydrocarbons or the other systems consisting of exclusively carbon and hydrogen atoms which can be represented by simple molecular graphs in chemical graph theory [12]. However, introduction of a heteroatom to the system completely affects the physical, chemical and electronic properties of a certain molecule. Therefore, the method of calculation of the TG index for the heteroatom containing systems is somewhat different.

Organic compounds containing heteroatoms and/or multiple bonds can be represented as vertex- and edge-weighted molecular graphs [12]. Early applications of weighted molecular graphs are connected with the computation of polynomials and spectra of the heteroconjugated compounds [62]. Methods using graphs weighted with Hückel parameters may be employed to compute Hückel molecular orbitals, but the results are general and may be applied to any weighted molecular graphs. Efforts were devoted to developing parameters suited for the computation of a large number of topological indices [63-69]. Apart from such general procedures, there are special weighing methods developed for a single type of topological index [31,32,70-72].

In the case of the TG index, vertex-weighted molecular graphs have been used. The calculation of the TG index for 2-ethyl-3-methylbutan-1-ol has been illustrated in Figure 14.

Different schemes for assigning the numerical value to *w* are available [73-79]. However, there is no unique recipe for selecting the numerical value of *w*. The pragmatic approach is to consider *w* as the variable parameter whose optimal value is the result of the fitted procedure in the structure-property-activity modeling.

2.1.4. The *Z* Weighting Scheme

A general approach of computing parameters for vertex-weighted graphs was developed by Trinajstic and coworkers by weighting the contributions of the atoms and bonds with parameters based on the atomic number *Z* [80]. This method was applied to the computation of many topological indices [63-68]. In the atomic number weighting scheme *Z* the vertex parameter $Vw(Z)_i$ of the vertex v_i (representing atom i of a molecule) is defined as:

$$Vw(Z)_i = 1\text{-}Z_C/Z_i = 1\text{-}6/Z_i \qquad (14)$$

where Z_i is the atomic number *Z* of the atom i and $Z_C = 6$ is the atomic number *Z* of carbon. If the heteroatom parameter for the atoms are calculated by the equation given above, negative values are obtained for atoms having lower *Z* than that of carbon, such as -0.2 for boron. Carbon has a $Vw(Z)_i$ parameter equal to zero, while for the remaining atoms one can observe a steady increase of the *Vw* weight with the increase of the corresponding *Z* number.

Having *Z* based vertex weighting scheme developed by Trinajstic and coworkers [80] as basis, we have generated a novel vertex weighting scheme which takes carbon as a reference and its parameter is represented by one (1). The $Vw(Z)_i$ parameters for the remaining atoms are defined by the following formula:

$$Vw(Z)_i = 1 \qquad \text{for carbon} \qquad (15)$$

$$Vw(Z)_i = 1+Z_C/Z_i \qquad Z_i > Z_C \qquad (16)$$

Table 2 gives a list of $Vw(Z)_i$ parameters for the heteroatoms computed with the novel Z based vertex weighting scheme developed by Türker and Gümüş, and with that of Trinajstic et al. [80]. In contrast to the method of Trinajstic et al., there exist no parameters with negative value and there is a steady decrease of the Vw weight with the increase of the corresponding Z number.

Table 2. Vertex parameters ($Vw(Z)_i$) based on atomic number (Z) for selected atoms ([a]: Türker and Gümüş, [b]: Trinajstic et al. [80])

Atom	***Z***	***Vw(Z)*[a]**	***Vw(Z)*[b]**
C	6	1.000	0.000
N	7	1.857	0.143
O	8	1.750	0.250
F	9	1.667	0.333
Si	14	1.429	0.571
P	15	1.400	0.600
S	16	1.375	0.625
Cl	17	1.353	0.647
As	33	1.182	0.818
Se	34	1.176	0.824
Br	35	1.171	0.829
Te	52	1.115	0.885
I	53	1.113	0.887

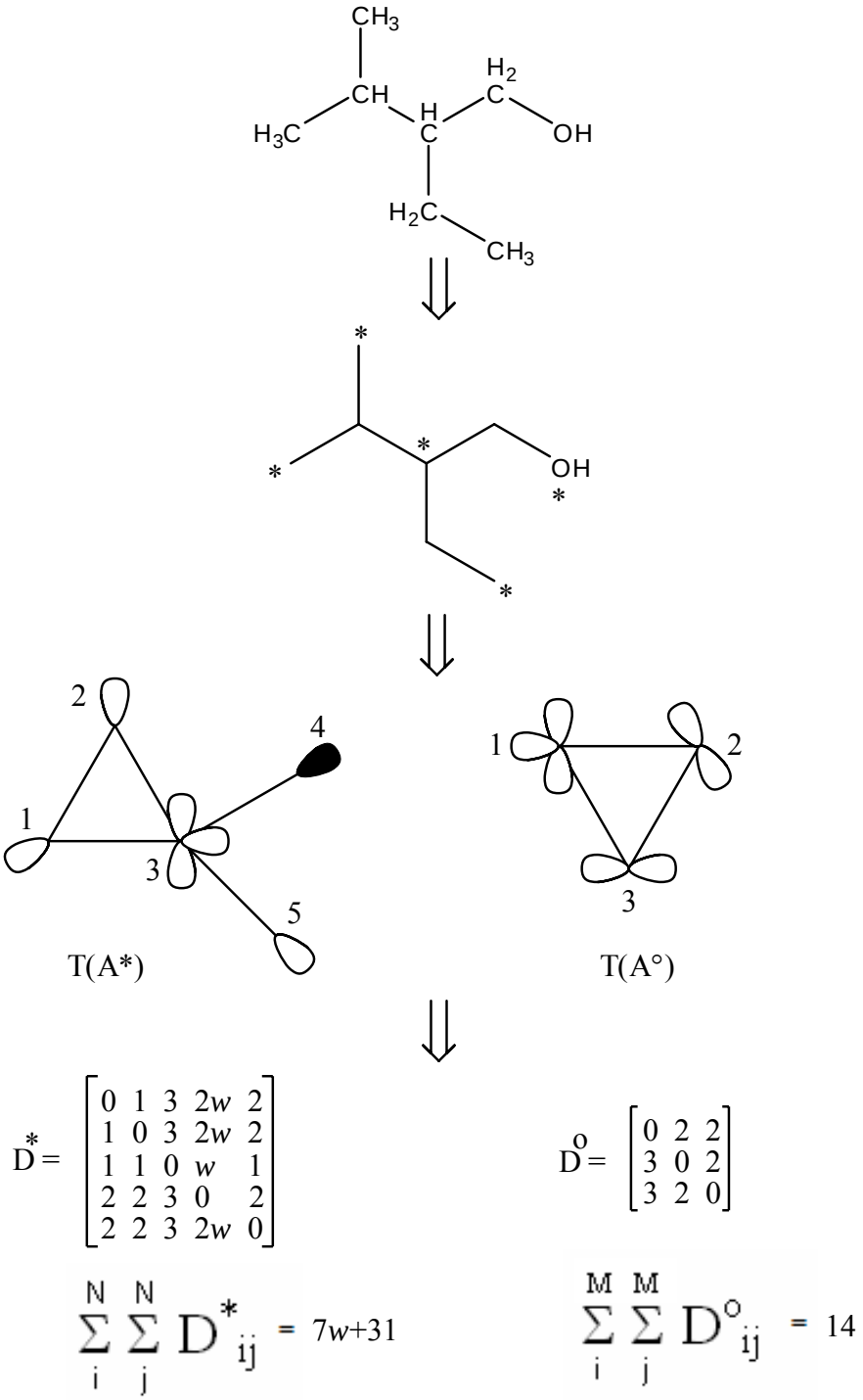

Figure 14. Illustration of how to calculate TG index for a heteroatom containing system.

2.2. Computational Chemistry

Computational chemistry is a branch of chemistry that uses computers to assist in solving chemical problems. It uses the results of theoretical chemistry, incorporated into efficient computer programs, to calculate the structures and properties of molecules and solids. While its results normally complement the information obtained by chemical experiments, it can in some cases predict hitherto unobserved chemical phenomena. It is widely used in the design of new drugs, explosives and materials.

Structure (i.e. the expected positions of the constituent atoms), absolute and relative (interaction) energies, electronic charge distributions, dipoles and higher multipole moments, vibrational frequencies, reactivity or other spectroscopic quantities, and cross sections for collision with other particles can be obtained with the aid of computational chemistry applications.

The methods employed cover both static and dynamic situations. In all cases the computer time and other resources (such as memory and disk space) increase rapidly with the size of the system being studied. That system can be a single molecule, a group of molecules, or a solid. Computational chemistry methods range from highly accurate to very approximate; highly accurate methods are typically feasible only for small systems. *Ab initio* methods are based entirely on theory from first principles. Other (typically less accurate) methods are called empirical or semi-empirical because they employ experimental results, often from acceptable models of atoms or related molecules, to approximate some elements of the underlying theory.

Both *ab initio* and semi-empirical approaches involve approximations. These range from simplified forms of the first-principles equations that are easier or faster to solve, to approximations limiting the size of the system (for example, Periodic boundary conditions), to fundamental approximations to the underlying equations that are required to achieve any solution to them at all. For example, most *ab initio* calculations make the Born-Oppenheimer approximation, which greatly simplifies the underlying Schrödinger Equation by freezing the nuclei in place during the calculation. In principle, *ab initio*

methods eventually converge to the exact solution of the underlying equations as the number of approximations is reduced. In practice, however, it is impossible to eliminate all approximations, and residual error inevitably remains. The goal of computational chemistry is to minimize this residual error while keeping the calculations tractable.

There are two different aspects to computational chemistry:

- Computational studies can be carried out in order to find a starting point for a laboratory synthesis, or to assist in understanding experimental data, such as the position and source of spectroscopic peaks.
- Computational studies can be used to predict the possibility of so far entirely unknown molecules or to explore reaction mechanisms that are not readily studied by experimental means.

Thus, computational chemistry can assist the experimental chemist or it can challenge the experimental chemist to find entirely new chemical objects. Several major areas may be distinguished within computational chemistry:

- The prediction of the molecular structure of molecules by the use of the simulation of forces, or more accurate quantum chemical methods, to find stationary points on the energy surface as the position of the nuclei is varied.
- Identifying correlations between chemical structures and properties (see QSPR and QSAR).
- Computational approaches to help in the efficient synthesis of compounds.
- Computational approaches to design molecules that interact in specific ways with other molecules (e.g. drug design and catalysis)

The first step to making the theory more closely mimic the experiment is to consider not just one structure for a given a chemical formula, but all possible structures. Many aspects of chemistry can be reduced to questions about potential energy surfaces (PES) [81]. A PES displays the energy of a molecule as a function of its geometry. It can resemble a hilly landscape, with

valleys and mountain peaks. Real PESs have many dimensions, but key feature can be represented by a 3 dimensional PES, as depicted in Figure 15.

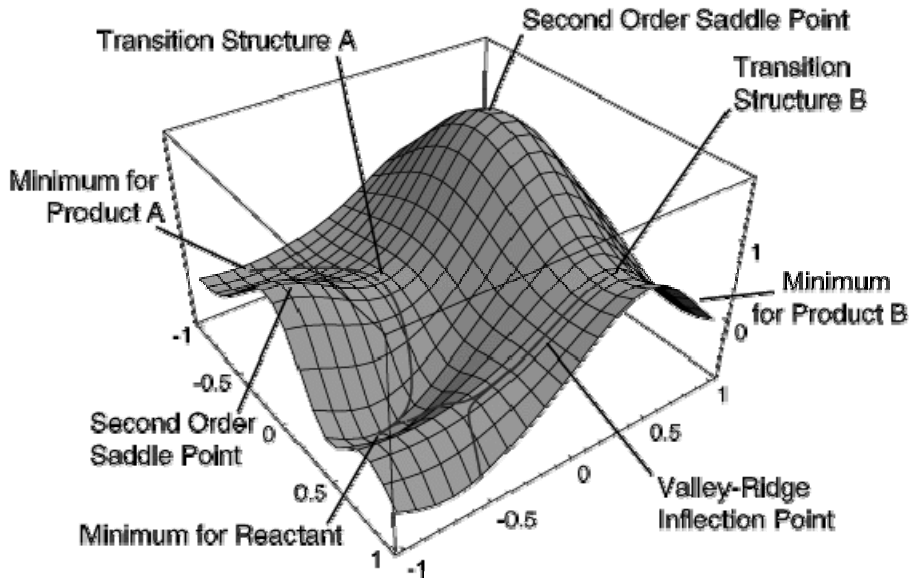

Figure 15. A simplified PES in three dimensions. (Reprinted from "An Introduction to Theoretical Chemistry" Jack Simons, Cambridge University Press, 2003.)

The form of a potential energy surface for a specific number of nuclei and electrons, can be calculated by solving the Schrödinger equation for every possible set of atomic coordinates. The transition state of a reaction corresponds to a maximum in the reaction coordinate and a minimum in all other coordinates, i.e. the highest point on the lowest energy path being a first-order saddle point. A reaction path connects reactants and products through a mountain pass. Energetic of reactions can be calculated from the energies or altitudes of the minima for reactants and products. The structure, energetics, properties, reactivity, spectra and dynamics of molecules can be readily

understood in terms of potential energy surfaces. Except in very simple cases, the potential energy surface cannot be obtained from experiment.

The most important methods of computational chemistry are *ab-initio*, semi-empirical and Density Functional Theory. The details of all will be given in the following sections.

2.2.1. Semiempirical Methods

Semiempirical quantum chemistry methods are based on the Hartree-Fock formalism, but make many approximations and obtain some parameters from empirical data. They are very important in computational chemistry for treating large molecules where the full Hartree-Fock method without the approximations is too expensive. The use of empirical parameters appears to allow some inclusion of electron correlation effects into the methods.

Within the framework of Hartree-Fock calculations, some pieces of information (such as two-electron integrals) are sometimes approximated or completely omitted. In order to correct for this loss, semi-empirical methods are parameterized, that is their results are fitted by a set of parameters, normally in such a way as to produce results that best agree with experimental data, but sometimes to agree with *ab initio* results.

Semiempirical methods follow what are often called empirical methods where the two-electron part of the Hamiltonian is not explicitly included. Therefore, semiempirical calculations are much faster than their *ab initio* counterparts. Their results, however, can be very wrong if the molecule being computed is not similar enough to the molecules in the database used to parameterize the method.

Semi-empirical calculations have been most successful in the description of organic chemistry, where only a few elements are used extensively and molecules are of moderate size.

Here are some of the semiempirical methods embedded in most of the computational chemistry package programs; MINDO, MNDO, AM1 and PM3.

2.2.1.1. Parameterization Method-3 (PM3)

The Parameterization Method-3 (PM3) [82] has been preferred for predicting properties of organic systems extensively. The PM3 method uses the same formalism and equations as the AM1 method. The only difference lie in the philosophy and methodology used during the parameterization: whereas AM1 takes some of the parameter values from spectroscopical measurements, PM3 treats them as optimizable values. It is more accurate than AM1 for hydrogen bond angles, but AM1 is more accurate for hydrogen bond energies. The PM3 and AM1 methods are also more popular than other semiempirical methods due to the availability of algorithms for including solvation effects in these calculations.

2.2.2. *Ab initio* Methods

Ab initio chemistry involves calculating molecular properties using quantum chemistry based methods. The term *ab initio* indicates that the calculation is derived from first principles and does not rely on any empirical data. A variety of *ab initio* methods exist and although these calculations are computationally expensive, they allow chemists to make predictions of molecular properties of new and existing compounds. The ever increasing level of computer power available to researchers makes the application of *ab initio* methods more practical for larger molecular systems.

2.2.2.1. The Hartree-Fock (HF) Theory

In computational physics and computational chemistry, the Hartree-Fock (HF) method is an approximate method for the determination of the ground-state wavefunction and ground-state energy of a quantum many-body system [83,84].

The Hartree-Fock method is also called, especially in the older literature, the self-consistent field method (SCF). The solutions to the resulting non-linear equations behave as if each particle is subjected to the mean field

created by all other particles. The equations are almost universally solved by means of an iterative, fixed-point type algorithm.

During HF calculations the many-electron Schrödinger equation is broken into many simpler one-electron equations. Each one-electron equation is solved to yield a single-electron wave function, called an orbital, and energy, called an orbital energy. The orbital describes the behavior of an electron in the net field of all the other electrons.

These orbitals are then combined into a determinant. This is done to satisfy two requirements of quantum mechanics. One is that the electrons must be indistinguishable. By having a linear combination of orbitals in which each electron appears in each orbital, it is only possible to say that an electron was put in a particular orbital but not which electron it is. The second requirement is that the wave function for fermions (an electron is a fermion) must be antisymmetric with respect to interchanging two particles. Thus, if electron 1 and electron 2 are switched, the sign of the total wave function must change and only the sign can change. This is satisfied by a determinant because switching two electrons is equivalent to interchanging two columns of the determinant, which changes its sign [83,84].

The Hartree-Fock method uses the variation theorem which states that for a time-independent Hamiltonian operator, any trial wavefunction will have an energy expectation value that is greater than or equal to the true ground state wavefunction corresponding to the given Hamiltonian. Because of this, the Hartree-Fock energy is an upper bound to the true ground state energy of a given molecule [83,84].

2.2.2.2. Electron Correlation

Electronic correlation refers to the interaction between electrons in a quantum system whose electronic structure is being considered. HF calculations do not include electron correlation. This means that HF takes into account the average effect of electron repulsion, but not the explicit electron-electron interaction. Within HF theory the probability of finding an electron at

some location around an atom is determined by the distance from the nucleus but not the distance to the other electrons as shown in Figure 16. This is not physically true, but it is the consequence of the central field approximation, which defines the HF method.

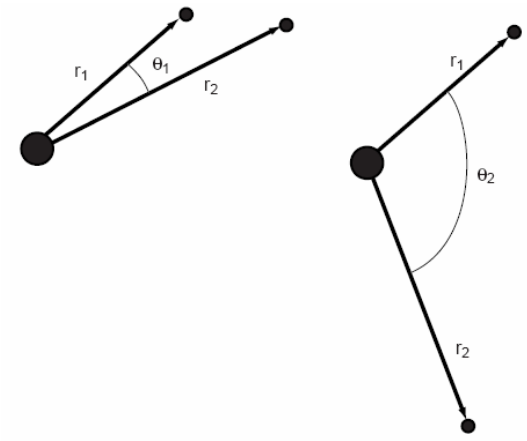

Figure 16. Two arrangements of electrons around the nucleus of an atom having the same probability within HF theory, but not in correlated calculations. (Reprinted from "Computational Chemistry" D. Young, Wiley-Intersience, New York, 2001.)

A number of types of calculations begin with a HF calculation and then correct for correlation. Some of these methods are Møller-Plesset [85] perturbation theory (MPn, where n is the order of correction), the generalized valence bond (GVB) method, multi-configurational self-consistent field (MCSCF), configuration interaction (CI), and coupled cluster theory (CC) [86-88]. Correlation is important such that the accuracy of computed energies and molecular geometries generally improved by including correlation. For organic molecules, correlation is an extra correction for very-high-accuracy work, but is not generally needed to obtain quantitative results. In general, *ab initio*

calculations give very good qualitative results and can yield increasingly accurate quantitative results as the molecules in question become smaller.

The advantage of *ab initio* methods is that they eventually converge to the exact solution once all the approximations are made sufficiently small in magnitude. In general, the relative accuracy of results is:

$$HF << MP2 < CISD \approx MP4 \approx CCSD < CCSD(T) < CCSDT < Full\ CI$$

Taking enormous amounts of computer CPU time, memory, and disk space can be considered as the major drawbacks of HF methods. In fact these requirements are much greater in correlated calculations. In practice, extremely accurate solutions are only obtainable when the molecule contains a dozen electrons or less. However, results with an accuracy rivaling that of many experimental techniques can be obtained for moderate-size organic molecules. The minimally correlated methods, such as MP2 is often used when correlation is important to the description of large molecules.

2.2.3. Density Functional Theory

Density functional theory (DFT) methods are often considered to be *ab initio* methods for determining the molecular electronic structure, even though many of the most common functionals use parameters derived from empirical data, or from more complex calculations. In DFT, the total energy is expressed in terms of the total one-electron density rather than the wave function. Hence the name density functional theory comes from the use of functionals of the electron density. DFT is among the most popular and versatile methods available in condensed-matter physics, computational physics, and computational chemistry.

In this type of calculation, there is an approximate Hamiltonian and an approximate expression for the total electron density. DFT methods can be very accurate for little computational cost. Some methods combine the density functional exchange functional with the Hartree-Fock exchange term and are known as hybrid functional methods.

The idea of expressing the energy of a system as a function of total electron density was implied for the first time in the late 1920s, by Fermi [89] and Thomas, [90]. Even though these theories were able to relate the energy and other properties of the system with the electron density, a formal proof of this notion came only in the 1960s, when Hohenberg and Kohn published a theorem [91] demonstrating that the ground-state energy of a nondegenerate electronic system and the correspondent electronic properties are uniquely defined by its electron density. After the proof of such relationship between the electronic properties and the electron density scientists worked on searching for functionals able to connect these two quantities.

The kinetic energy has a large contribution to the total energy. Therefore even the 1% error in the kinetic energy of the Thomas-Fermi-Weizsacker model prevented DFT from being used as a quantitative predictive tool. Thus DFT was largely ignored until 1965 until when Kohn and Sham [92] formulated the problem of calculating the ground state energy as a functional of the electron density as solving a set of single particle Schrödinger equations by introducing a fictitious system of non-interacting electrons moving in an effective potential chosen such that its ground state electron density is the same as the one of the true system. The ansatz of Kohn and Sham was to write the energy functional in terms of a functional for the kinetic energy. With this new formulasim they were able to treat the majority of the kinetic energy exactly. Therefore, the basic principles of today's most successful and popular computational chemistry calculation method, Density Functional Theory (DFT) was founded.

The Kohn-Sham orbitals in each iteration are normally expressed in terms of a set of basis functions. In this sense, solving the Kohn-Sham equations corresponds to determining the coefficients in a linear combination of basis functions, in a similar way to what is done in Hartree-Fock calculations. The choice of the basis set is therefore of great importance also in DFT calculations.

The exchange-correlation energy is generally divided into two separate terms, an exchange term and a correlation term, although the legitimacy of such separation has been the subject of some doubt. The exchange term is normally associated with the interactions between electrons of the same spin, whereas the correlation term essentially represents those between electrons of opposite spin. These two terms are themselves also functionals of the electron density. The corresponding functionals are known as the exchange functional and the correlation functional, respectively. Hybrid functionals are a class of approximations to the exchange-correlation energy functional in density functional theory (DFT) that incorporate a portion of exact exchange from Hartree-Fock theory with exchange and correlation from other sources. The exact exchange energy functional is expressed in terms of the Kohn-Sham orbitals rather than the density, so is termed an implicit density functional. The hybrid approach to construct density functional approximations was introduced by Axel Becke in 1993 [93]. Hybridization with Hartree-Fock (exact) exchange provides a simple scheme for improving many molecular properties, such as atomization energies, bond lengths and vibration frequencies, which tend to be poorly described with simple *ab initio* functionals [94]. Here are some examples of the hybrid density functionals, B3LYP [95], B3P86 [96], B3PW91 [97], BHandHLYP [98].

2.2.4. Basis sets

A basis set is a set of functions used to create the molecular orbitals, which are expanded as a linear combination of such functions with the weights or coefficients to be determined. Usually these functions are atomic orbitals, in that they are centered on atoms, but functions centered in bonds or lone pairs, and pairs of functions centered in the two lobes of a p orbital, have been used. Additionally, basis sets composed of sets of plane waves down to a cutoff wavelength are often used, especially in calculations involving systems with periodic boundary conditions.

In modern computational chemistry, quantum chemical calculations are typically performed within a finite set of basis functions. In these cases, the wavefunctions under consideration are all represented as vectors, the components of which correspond to coefficients in a linear combination of the basis functions in the basis set used. The operators are then represented as matrices, (rank two tensors), in this finite basis.

When molecular calculations are performed, it is common to use a basis composed of a finite number of atomic orbitals, centered at each atomic nucleus within the molecule. Initially, these atomic orbitals were typically Slater orbitals, which corresponded to a set of functions which decayed exponentially with distance from the nuclei. Later, it was realized by F. Boys that these Slater-type orbitals could in turn be approximated as linear combinations of Gaussian orbitals instead. Because it is easier to calculate overlap and other integrals with Gaussian basis functions, this led to huge computational savings [99].

Today, there are hundreds of basis sets composed of Gaussian-type orbitals (GTOs). The smallest of these are called *minimal basis sets*, and they are typically composed of the minimum number of basis functions required to represent all of the electrons on each atom. The largest of these can contain literally dozens to hundreds of basis functions on each atom.

A minimum basis set (e.g. STO-3G) is one in which, on each atom in the molecule, a single basis function is used for each orbital in a Hartree-Fock calculation on the free atom.

The most common addition to minimal basis sets is probably the addition of polarization functions, denoted (in the names of basis sets developed by Pople [100]) by an asterisk, * or (d). Two asterisks, ** or (d,p), indicate that polarization functions are also added to light atoms (hydrogen and helium). Another common addition to basis sets is the addition of diffuse functions, denoted in Pople-type sets (e.g. 3-31G, 6-31G) by a plus sign, +, and in Dunning-type sets [101] (e.g. cc-PVDZ, cc-PVTZ) by "aug" (from "augmented"). Two plus signs indicate that diffuse functions are also added to

light atoms (hydrogen and helium). These are very shallow Gaussian basis functions, which more accurately represent the "tail" portion of the atomic orbitals, which are distant from the atomic nuclei. These additional basis functions can be important when considering anions and other large molecular systems.

2.2.5. Methods Employed

The computational calculations have been applied in order to investigate the structural, electronic, physicochemical and explosive properties of corresponding series of molecules presently considered. The results of these calculations have been correlated by the novel topological index (The TG Index).

All of the computational calculations in this thesis have been performed using G.03W [102], Spartan 06 [103] and Hyperchem 7.0 [104] package programs. The details about the applied methods and the calculated properties will be explained on the corresponding parts of the thesis.

CHAPTER 3

RESULTS AND DISCUSSION

The physical and chemical properties of a substance are strongly related to its both geometrical and electronic structures. The qualitative and quantitative structure-property and structure-activity (QSPR and QSAR, respectively) relations of substances can be investigated by the application of certain numerical descriptors, so-called topological indices. Every topological index represents a unique structure. There has been much effort to design topological indices and the investigation of structure-property and structure-activity relationships date back to a couple of decades ago.

As it is explained earlier in this thesis, topological indices are used to characterize features of chemical structures in numerical form. Most of the existing topological indices usually start either with the vertex adjacency matrix A or with the distance matrix D. Despite large achievements in this field having been attained, existing topological index approaches to QSPR/QSAR need further improvement. Therefore, it is desirous to find new topological indices for modeling different properties.

The present research has emerged with the idea to develop a novel topological index with the desired features. The calculation of the TG Index is quite simple besides it comprises the most important graph theoretical terms, adjacency and connectivity together with the application of the T(A) graphs. The other objectives for a good topological index are that it should be unique for each and every molecule and correlate well with the properties of the applied molecules so that it can be used to predict the desired properties of the

yet nonexistent compounds. The following sections will represent the application of the TG index over a series of conjugated unsaturated, unsaturated and saturated hydrocarbons, heteroatom containing species (alcohols and amines) and explosives.

3.1. Graphical Matrices and the TG Index

The most useful and popular matrices have been described in the introduction part of the present thesis. Apart from the matrices constructed by numbers related to the chemical structure, there exist graphical matrices whose elements are subgraphs of the main graph rather than numbers.

The advantage of a graphical matrix lies in the fact that it allows many possibilities of numerical realizations. In order to obtain a numerical form of a graphical matrix, one needs to select a graph invariant and replace all graphical elements by the corresponding numerical values of the selected invariant. In this way, the numerical form of the graphical matrix is established. There are two main types of these matrices obtained by; i) consecutive removal of the edges connecting vertices i and j, ii) consecutive removal of the adjacent vertices i and j, and the incident edges from the graph [60]. For both cases, the matrices can be formed by a) drawing subgraphs for only incident vertices and the other elements are zero, b) drawing subgraphs for all vertices.

In the present case, the distance-degree matrix can be represented by the first type of the graphical matrices with some modifications from the original definition. Up to date no graphical matrix was constructed indicating the direction of the path and the degrees of the vertices with self loops. Each of the matrix elements of the graphical representation of the TG index should be directed subgraphs. The necessity for using the directed subgraphs in the present case force us to construct the complete graphical matrix, in contrast to the systems in the literature where formation of the half of the square matrix is just enough. Because the other half will obviously be exactly the same. In that sense, the TG index is more informative than the previously observed graphical matrices. The graphical matrix for 3-ethyl-2-methylpentane can be seen in

Figure 17. For convenience, only the degrees of the related vertices have been indicated.

The graphical form of the distance-degree matrix make it easier to construct the numerical matrix. Therefore, for the calculation of the TG index of large systems where there is a possibility of making a mistake, it is first preferable to form the graphical representation and then reform the distance-degree matrix with numbers.

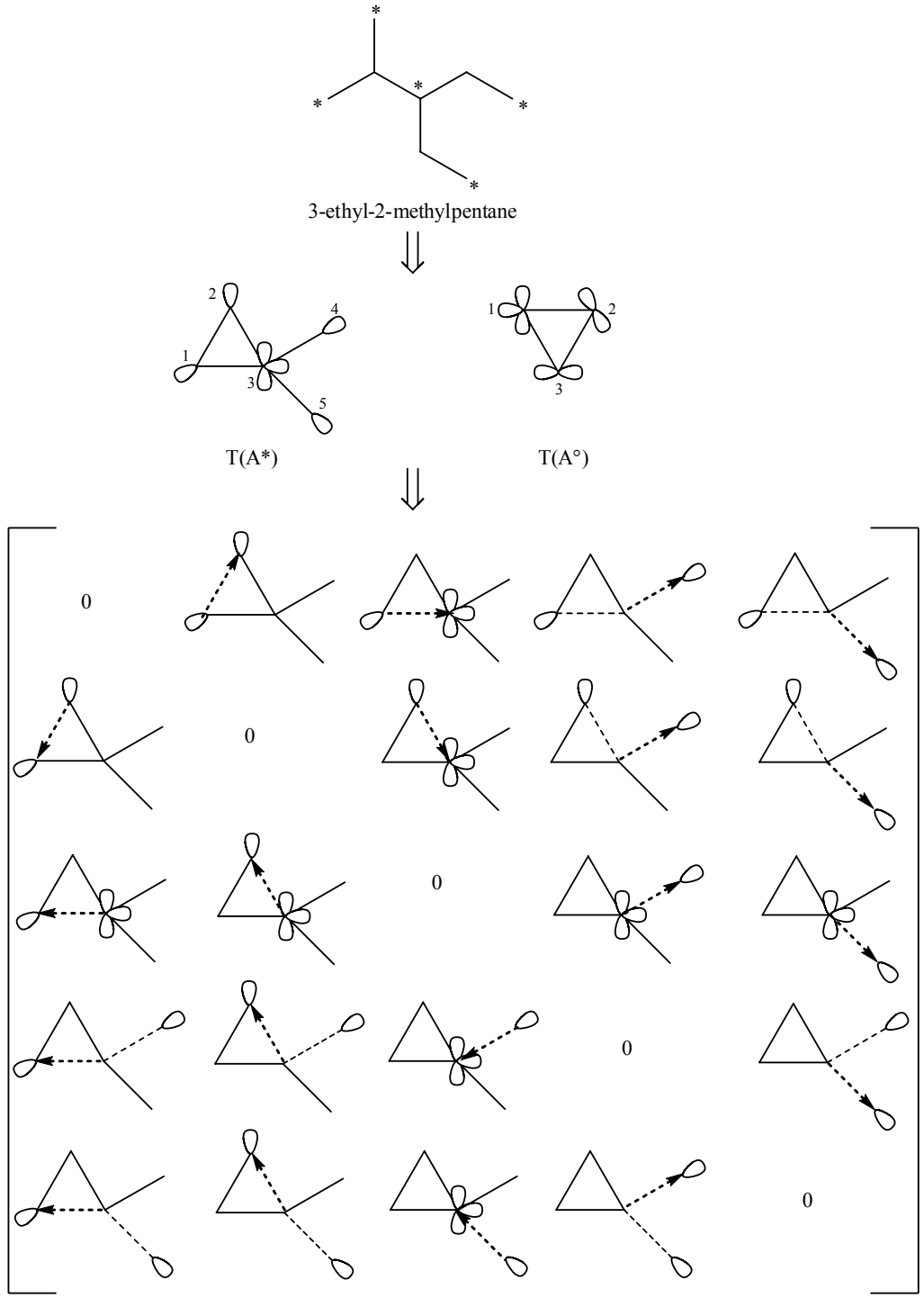

Figure 17. The graphical representation of TG Index by the application of graph theoretical matrices. This is the graphical matrix representation for T(A*) graph of 3-ethyl-2-methylpentane

3.2. Applications of the TG Index

3.2.1. Linear Conjugated Hydrocarbons (Polyenes)

Since T(A) graphs have been defined for construction of isospectral graphs of the alternant hydrocarbons, it is meaningful to start the application of the index on linear conjugated hydrocarbons (linear polyenes).

A linear polyene is a chain of conjugated carbon-carbon double bonds with an unbranched π-electron system. The conventional representation of alternating double and single bonds corresponds to the resonance structure of major importance in the ground state. Polyenes are distinguished from symmetrical cyanines and aromatic compounds by the fact that these other compounds have at least two resonance structures which contribute significantly to their ground state.

A more quantitative distinction between linear polyenes and other classes of compounds concerns the presence of bond length alternation in polyenes as determined by X-ray crystallography [105,106]. The bond alternation between lengths of 1.36 and 1.45 Å has a number of theoretical and spectroscopic consequences that have been very important historically. The linear structure of these molecules permits the existence of relatively unhindered geometrical isomers.

Linear polyenes were first prepared and studied spectroscopically in 1930s. Their spectral properties had an important influence on the early history of molecular orbital theory. The major spectral feature of these molecules is a strongly allowed singlet-singlet transition in the near ultraviolet or visible region of the spectrum. Much of the interest has developed from a desire to understand the spectral and photochemical properties of the visual pigments [107-110]. Most of the spectral studies concentrated on the calculation or measurement of λ_{max} (maximum wavelength) [110] and $\Delta\varepsilon$ (HOMO-LUMO gap) which is very closely relevant to it. λ_{max} is one of the most important properties of such conjugated compounds since they exist as embedded in the chemical structures of some natural products.

In the present work, we have also considered simple linear polyenes (Figure 18) in terms of total electronic energy, HOMO, LUMO, Δε and λ_{max}.

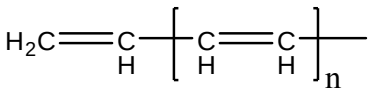

n = 1, 2, ..., 12

Figure 18. General scheme for the polyenes investigated in this study.

3.2.1.1. Method of Calculation

The initial geometry optimizations of all the structures leading to energy minima were achieved by using MM2 method followed by semi-empirical PM3 self-consistent fields molecular orbital (SCF MO) method [111,112] at the restricted level [113]. Then, geometry optimizations were achieved within the framework density functional theory (DFT, B3LYP) [114-116] at the level of 6-31G(d,p) [112]. The exchange term of B3LYP consists of hybrid Hartree-Fock and local spin density (LSD) exchange functions with Becke's gradient correlation to LSD exchange [96].The correlation term of B3LYP consists of the Vosko, Wilk, Nusair (VWN3) local correlation functional [117] and Lee, Yang, Parr (LYP) correlation correction functional [118]. The B3LYP method gives predictions which are in qualitative agreement with experiment.

The vibrational analyses were done by using the same basis set employed in the corresponding geometry optimizations. The normal mode analysis for each structure yielded no imaginary frequencies for the $3N-6$ vibrational degrees of freedom, where N is the number of atoms in the system. This indicates that the structure of each molecule corresponds to at least a local minimum on the potential energy surface (PES-see Figure 15).

The PM3 and B3LYP/6-31G(d,p) optimizations have been performed on Hyperchem 7.0 [104] and Spartan 06 [103] package programs, respectively.

The topological indices (TG Index) for the series of polyenes (n = 1-12) have been calculated as described in the previous chapter. An example of that is also presented for 1,3,5,7-octatetraene in Figure 19.

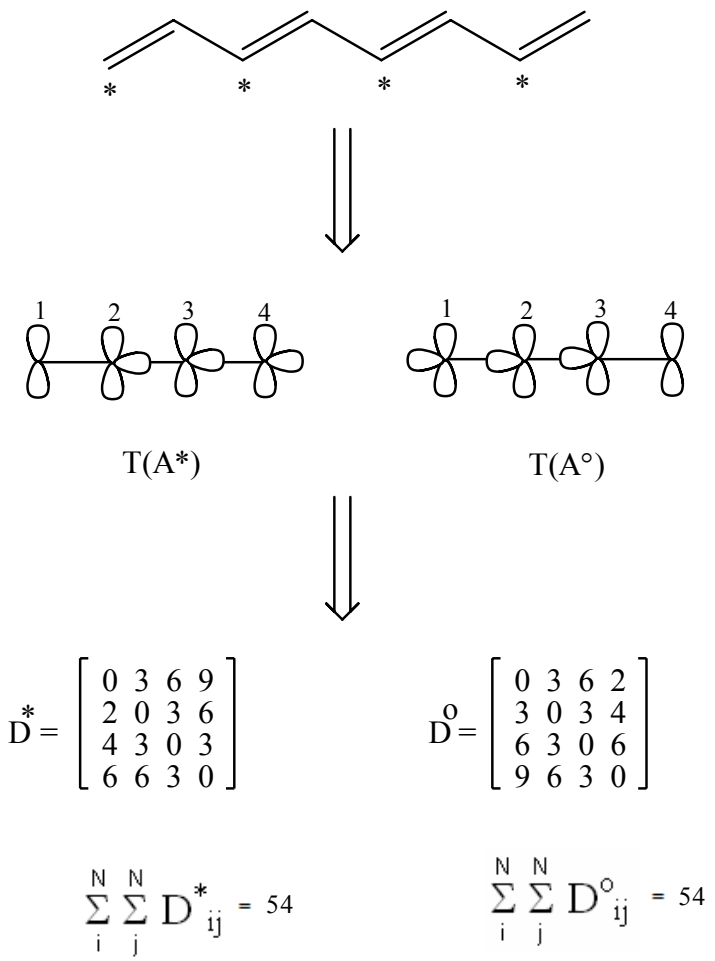

Figure 19. Calculation of the TG Index for 1,3,5,7-octatetraene.

3.2.1.2. Results and Discussion

Note that T(A*) graph is just the same with T(A°) graph for a symmetrical molecule with opposite numbering and thus, the sum of the elements of the distance-degree matrix yields the same score. When symmetrical compounds are under consideration, it is simply enough to draw one of the T(A) graphs and construct the distance-degree matrix. The sum of the elements of the corresponding T(A) graph should be squared to come up with the TG Index.

The TG Indices, data obtained from the computational calculations and the λ_{max} [110] values have been tabulated in Table 3.

Table 3. The TG Index, total energy (in Hartree), heat of formation (ΔH_f in kcal/mol), HOMO (eV), LUMO (eV), $\Delta\varepsilon$ (eV) and λ_{max} (nm) data [110] for polyene series considered in this thesis.

n	TG	Total Energy		ΔH_f	HOMO	LUMO	$\Delta\varepsilon$	λ_{max}
		PM3	B3LYP					
1	25	-20.7713	-156.0017	30.91	-6.25	-0.64	5.61	203.2
2	441	-30.5958	-233.4113	44.88	-5.71	-1.23	4.48	242.7
3	2916	-40.4205	-310.8216	58.76	-5.38	-1.59	3.79	278.8
4	12100	-50.2452	-388.2322	72.63	-5.15	-1.83	3.32	311.5
5	38025	-60.0699	-465.6430	86.49	-4.98	-2.01	2.98	340.8
6	52900	-69.8946	-543.0538	100.35	-4.86	-2.14	2.72	366.7
7	151321	-79.7193	-620.4647	114.22	-4.76	-2.24	2.52	389.2
8	356409	-89.5441	-697.8757	128.08	-4.68	-2.33	2.36	408.3
9	736164	-99.3688	-775.2867	141.94	-4.62	-2.39	2.22	424.0
10	1600225	-109.1935	-852.6968	155.80	-4.48	-2.56	1.93	436.3
11	2722500	-119.0182	-930.1075	169.66	-4.37	-2.67	1.70	445.2
12	4435236	-128.8429	-1007.5182	183.52	-4.34	-2.83	1.50	450.7

Tha data in Table 3 demonstrate that the TG Indices, total energies (absolutely), heat of formations, lowest occupied molecular orbital energy (LUMO, absolutely) and λ_{max} values increase, whereas the highest occupied

molecular orbital energy (HOMO, absolutely) and the interfrontier energy gap ($\Delta\varepsilon = \varepsilon_{LUMO}-\varepsilon_{HOMO}$) decrease with molecular size of the polyenes. The results of the correlation analyses between the natural logarithm of the TG index and the natural logarithm of the total energies (both PM3 and B3LYP), heat of formation, frontier molecular orbital energies (HOMO and LUMO), $\Delta\varepsilon$ and λ_{max} have been shown by the two-dimensional diagrams in Figures 20-26 (all with 12 entries). Note that in most of the figures presented in the thesis, the intersection points of the axes are not at O(0,0) point.

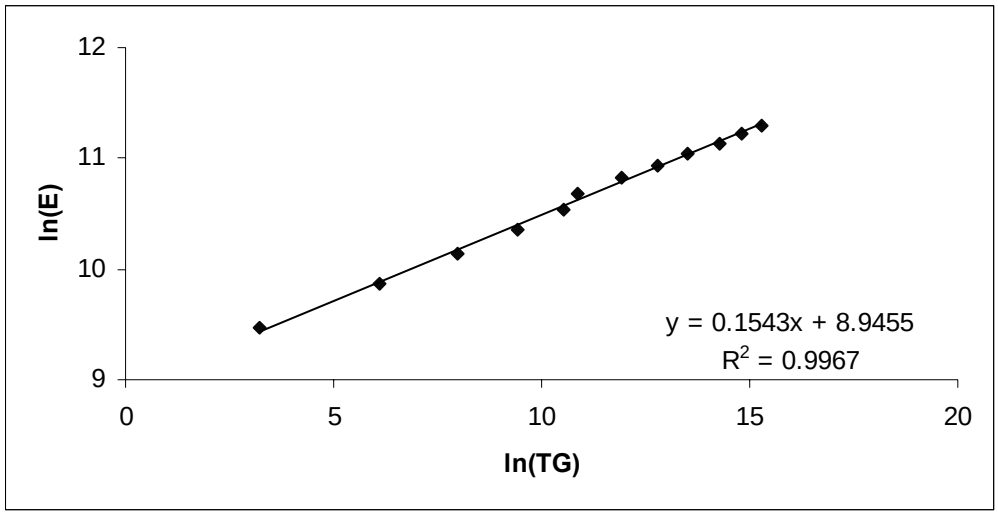

Figure 20. The plot of ln(total energy) calculated with PM3 method versus ln(TG Index)

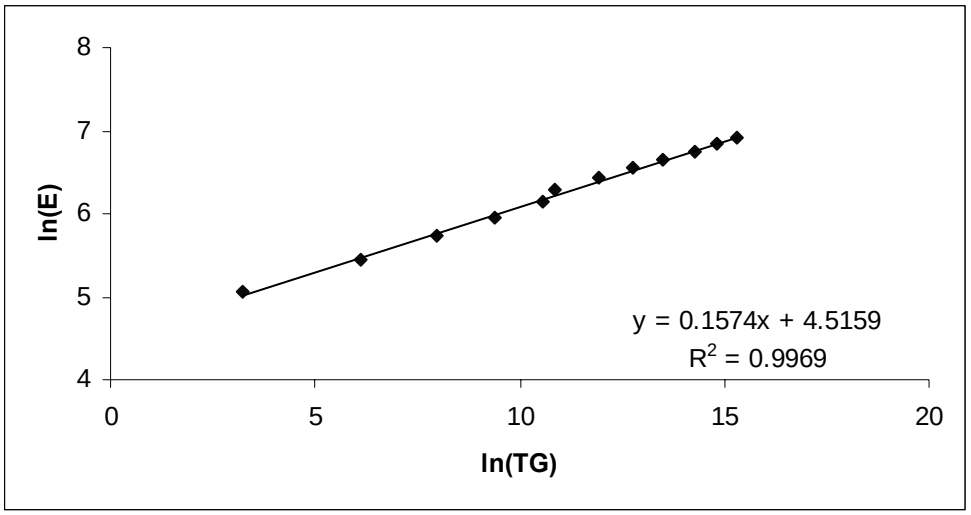

Figure 21. The plot of ln(total energy) calculated with B3LYP/6-31G(d,p) method versus ln(TG Index).

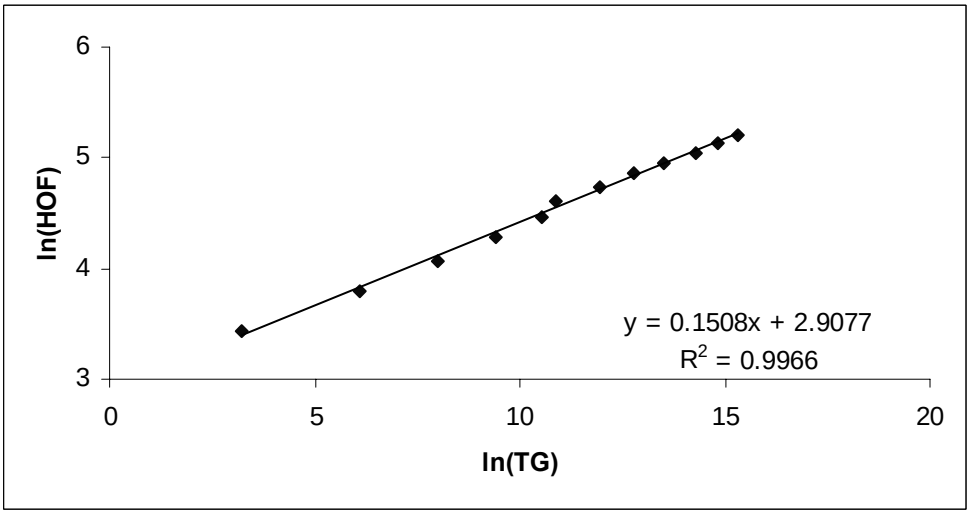

Figure 22. The plot of the ln(ΔH_f) calculated with PM3 Method versus ln(TG Index).

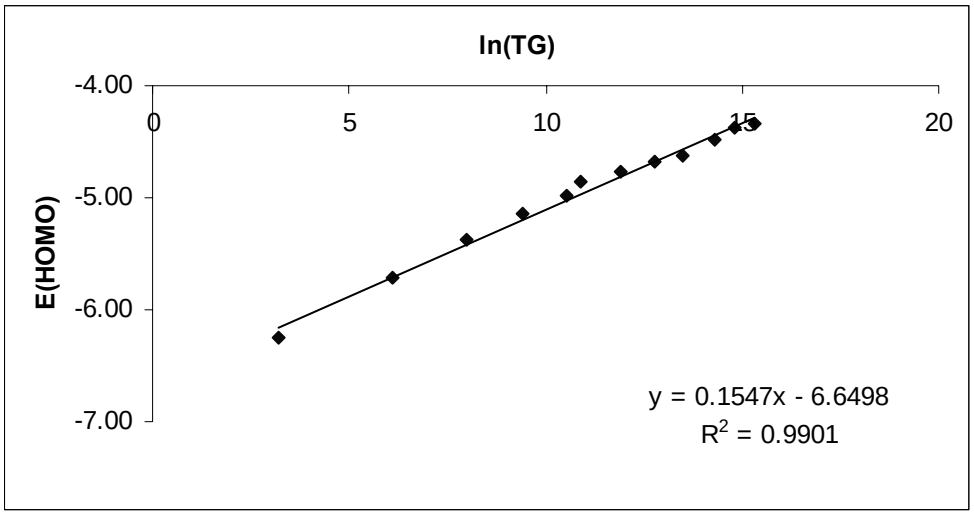

Figure 23. The plot of ε_{HOMO} calculated with B3LYP/6-31G(d,p) method versus ln(TG Index).

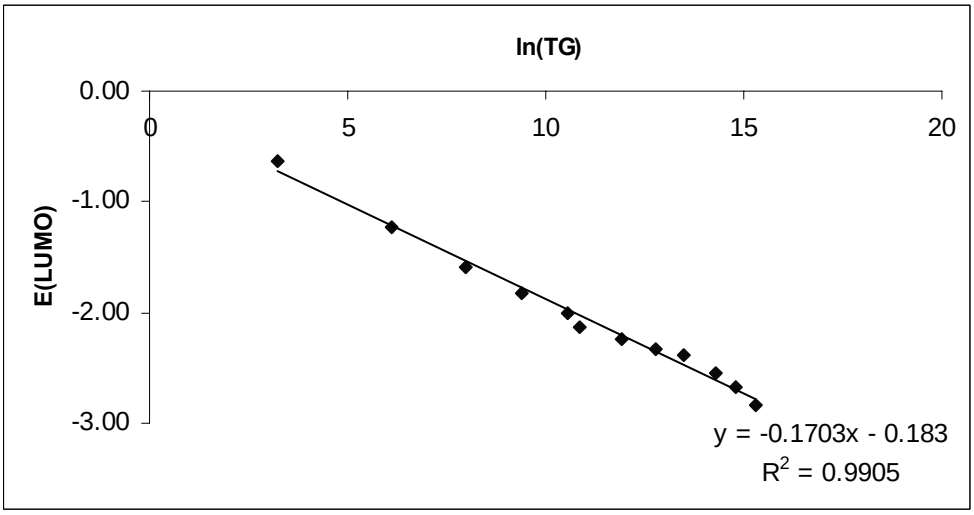

Figure 24. The plot of ε_{LUMO} calculated with B3LYP/6-31G(d,p) method versus ln(TG Index).

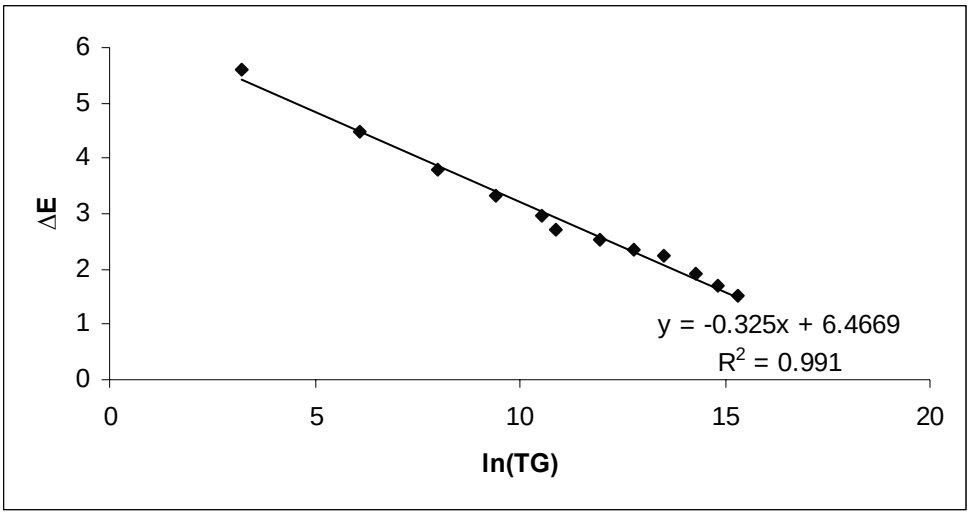

Figure 25. The plot of Δε calculated with B3LYP/6-31G(d,p) method versus ln(TG Index)

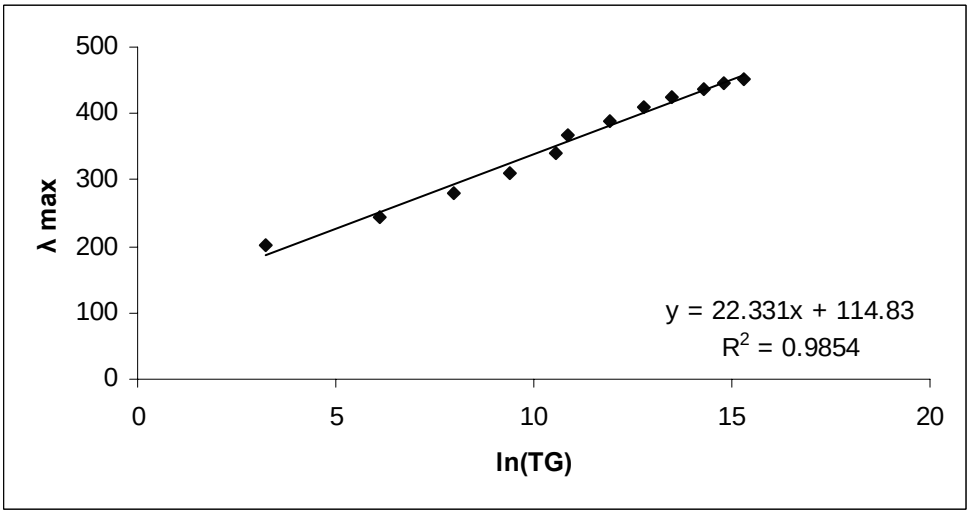

Figure 26. The plot of λ_{max} taken from Ref. [110] versus ln(TG Index).

As can be seen from the plots (Figures 20-26), all the properties considered here correlate very well with the TG index, which evidences that the TG index contains valuable structural information. Therefore, it can be regarded as successful so that the correlation equations can be extrapolated for the prediction of the properties of unknown polyenes or natural products that possess polyene moieties embedded in their structures such as β-Carotene and Lycopene (Figure 27). When the regression equation for the correlation of λ_{max} with the TG index has been used, we obtained 487 nm for β-Carotene and 513 nm for Lycopene. The deviations from the experimental data are -2.01 % and 1.58 %, respectively, which can be considered as quite acceptable.

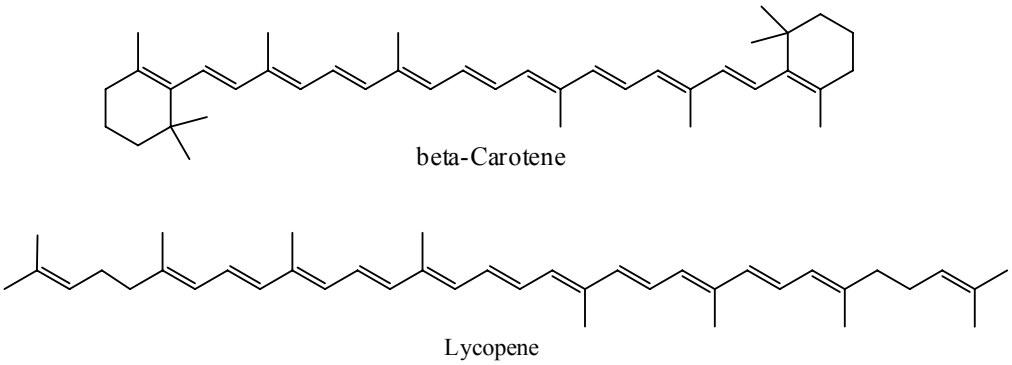

Figure 27. Chemical structures of β-Carotene (red-orange, λ_{max} = 497 nm) and Lycopene (bright red, λ_{max} = 505 nm). Both have 11 conjugated double bonds.

3.2.2. Alkanes

The alkanes represent an attractive class of compounds as a starting point for the application of graph theoretical approaches because of their non-polar characteristics and presence of just two kinds of atoms. The use of more polar compounds is avoided due to some complexities. Moreover, many properties of alkanes change in a regular manner with their mass and the extent of branching.

The aim of this part of the thesis is to investigate the possible structure-property relationships (QSPR) for the various physicochemical and electronic properties of the alkanes. Such relationships can be employed to predict yet unmeasured values for the considered properties of compounds, in addition to that, it can be extended for design of non-existent structures possessing some desirable properties.

Since the alkanes are non-polar, a number of complexities due to polarity, polarizability, and hydrogen bonding that arise with more polar compounds are avoided. Thus, the physicochemical properties of alkanes are dominated by their inherent structural features, such as molecular dimension or shape. The molecular size has an impact and influence on most properties (activities), although other factors such as branching and steric factors also have smaller influences. In the present study, we are mainly concerned with the size and branching effects on some physical, physiological and electronic properties.

3.2.2.1. Method of Calculation

The physical properties considered in this part are boiling points (bp), molar volumes at 20 ˚C (MV), molar refractions at 20 ˚C (MR), heats of vaporization at 25 ˚C (HV), critical temperatures (TC), critical pressures (PC), surface tensions at 20 ˚C (ST), melting point (mp), molar susceptibility (χ_m), polarizability (α), density (d) and parachore (PR). Values for the properties were excerpted from the literature [119]. The molar volumes were calculated as MW/d where MW is the molecular weight and d is the density (g/mL). The molar refractions were calculated by using Lorentz-Lorenz expression [120] where n_o is the index of refraction.

$$MR = \frac{n_o^2 - 1}{n_o^2 + 2} \quad \frac{MW}{d} \qquad (17)$$

In the present study, MR is considered due to its relationship to molecular polarizability [121-126]. Only liquid-phase values for MV, MR, HV and ST were used. Among the branched alkanes, the TG index of 2,2-dimethyl propane cannot be calculated since the distance-degree matrix of the unstared set has only one element which leads TG index to be zero.

For the compounds considered, additional data have been gathered from the literature [127,128] for the aqueous solubilities (S_w, expressed as log S_w), as well as the partition coefficient in octanol-water solvent system (P_{oct}, expressed as logP_{oct}).

The regression analyses between the index and the properties have been performed by the MS Excel 2003 package program.

3.2.2.2. Results and Discussion

Consequent to above we have first discussed unbranched alkanes, and the study was then extended to a large number of alkanes consisting of branched and unbranched structures. We first developed QSPR models based on boiling points (bp) and then considered several other properties of alkanes [128].

3.2.2.3. Linear Alkanes

The correlation analyses have been performed between the natural logarithm of the TG Index and the physical properties (bp, mp, χ_m, α, d, PR, log P_{oct}, log P_{16} and - log S_w) of the linear alkanes. The properties of the linear alkanes together with the calculated TG Index data, and the results of the regression analyses have been given in Tables 4 and 5, respectively.

The boiling point (bp) of a compound is related directly to the chemical structure of the molecules. Pioneering work in applying QSPR to the boiling points of alkanes was done by Wiener [129]. Since then, there have been very extensive efforts to apply structural information to fit experimental boiling points. Most of this work was centered at homologous and congeneric series of compounds. Here the boiling points of 17 linear alkanes (butane to eicosane)

have been considered for correlation with the TG index. As can be seen from Table 5 a very good fit is obtained for these class of compounds with a coefficient of determination of 0.9919.

Table 4. Calculated TG Index values and some physical properties of the linear alkanes. (Units: bp, °C; mp, °C; χ_m, m^3/mol; d, g/cm^3; α, $C \cdot m^2 \cdot V^{-1}$)

# of C atoms	Alkane	TG	bp	mp	χ_m	$logP_{oct}$
4	n-Butane	9	-0.5	-138	50.3	3.14
5	n-Pentane	40	36.1	-130	61.5	3.67
6	n-Hexane	169	68.7	-95	74.1	4.21
7	n-Heptane	448	98.4	-91	85.2	4.74
8	n-Octane	1156	125.7	-57	96.6	5.28
9	n-Nonane	2400	150.77	-54	108.1	5.82
10	n-Decane	4900	174.12	-30	119.5	6.35
11	n-Undecane	8800	196.8	-26	131.8	6.89
12	n-Dodecane	14641	216.3	-10		7.42
13	n-Tridecane	25480	235.4	-5.5		7.96
14	n-Tetradecane	41209	263.7	6		8.5
15	n-Pentadecane	62720	270.1	10		9.03
16	n-Hexadecane	97344	280	18	187.6	9.57
17	n-Heptadecane	137088	292	22		10.1
18	n-Octadecane	197136	308	28		10.64
19	n-Nonadecane	273600	320	32		11.18
20	n-Eicosane	378225	342.7	36.8		
		TG	**$-logS_w$**	**d**	**PR**	**α**
4	n-Butane	9	2.57		231	9.99
5	n-Pentane	40	3.18	0.626	270.8	11.83
6	n-Hexane	169	3.84	0.659	310.6	13.66
7	n-Heptane	448	4.53	0.684	350.4	15.5
8	n-Octane	1156	5.24	0.703	390.2	17.34
9	n-Nonane	2400	5.88	0.718	430	19.17
10	n-Decane	4900	6.98	0.73	469.7	21.01
11	n-Undecane	8800	7.59	0.74	509.5	22.85
12	n-Dodecane	14641	7.67	0.749	549.3	24.28
13	n-Tridecane	25480		0.756	589.1	26.52
14	n-Tetradecane	41209	7.96	0.763	628.9	28.36
15	n-Pentadecane	62720		0.769	668.7	30.19
16	n-Hexadecane	97344	8.4	0.773	708.4	32.03
17	n-Heptadecane	137088		0.778	748.2	33.87
18	n-Octadecane	197136		0.777	788	35.7
19	n-Nonadecane	273600		0.777	825.8	37.4
20	n-Eicosane	378225		0.789	1225.6	55.91

Table 5. The regression equations and the coefficients of determination of the regression analyses between the TG index and the experimental properties of linear alkanes.

Property	regression equation	R^2
bp (n = 17)	y = 32.602x + 92.423	0.9919
mp (n = 17)	y = 17.663x + 186.19	0.9901
χ_m (n = 9)	y = 14.194x + 186.19	0.9411
$\log P_{oct}$ (n = 16)	y = 0.793x + 0.2688	0.9466
$-\log S_w$ (n = 11)	y = 0.7015x + 0.6224	0.9693
d (n = 16)	y = 0.0169x + 0.5787	0.9735
PR (n = 16)	y = 58.809x + 18.486	0.9471
α (n = 16)	y = 2.7112x + 0.1828	0.9461

The boiling points of alkanes are determined by the forces of attraction between the molecules in the liquid form. Since the molecules in the solid state have a rigid three-dimensional structures, melting point unlike boiling point, is a solid state property and hence is influenced by properties of solids such as amorphous or crystalline nature, allotropy, polymorphism, molecular symmetry, as additional and more important factors than intermolecular forces. Hence, the melting points of alkanes are more difficult to model. The data in Table 5 for the regression of TG index with the melting point indicate that in spite of the complexities of solid state properties included in melting points, the TG index is very successful in this correlation.

In physics, the susceptibility (χ) of a material or substance describes its response to an applied field. Molar susceptibility (χ_m) is measured as m^3/mol. Magnetic susceptibility is measured by the force change felt upon the application of a magnetic field gradient [130]. Today, high-end measurement systems use a superconductive magnet. An alternative is to measure the force change on a strong compact magnet upon insertion of the sample. This system, widely used today, is called the Evans balance. For liquid samples, the susceptibility can be measured from the dependence of the NMR frequency of the sample on its shape or orientation [131]. This important property requires

expensive apparatus to be measured. Thus, being able to guess it by a simple mathematical formula is quite acceptable. As can be seen from Table 5 χ_m has a reasonable high coefficient of determination value of 0.9411. Therefore, the regression equation can be used to predict the χ_m data for the missing members of the series and the rest of linear alkanes which are not considered here.

For developing a QSPR model for the unbranched alkanes the authors have considered $\log P_{oct}$ (logarithm of octanol-water partition coefficient P_{oct}) and aqueous solubility (S_w) to represent their physiological activity. The solubility of liquids and solids in water (S_w) as well as partition coefficient of solutes in different solvents viz. partition coefficient in octanol-water (P_{oct}) are very important molecular properties that influence the release, transport, and the extent of absorption of drugs in the body. These properties are the key determinants of the environmental fate of agrochemicals and pollutants in the environment. The hydrophobic constant (logP) is used to rationalize interactions of small ligands with various macromolecules in the fields of biochemistry, medicinal chemistry, and environmental sciences. Considerable experience in the use of log P in the study of QSPR by regression analysis clearly indicated that measured log P should be used whenever possible. Nevertheless, when the number of compounds is great and the structural variations limited, experimentally simple economics makes it desirable to measure $\log P_s$ for the key structures only and to calculate the remainder.

A number of methods are also reported for estimating the aforementioned parameters (P_{oct} and S_w) using molecular descriptors other than topological indices. However, very little work is done for the estimation of aforementioned parameters using topological indices. This has prompted us to undertake the present investigation in that we have used the novel TG index for modeling, monitoring, and estimating P_{oct} and S_w. In doing so we have chosen n-alkanes (Table 4) since all these parameters for this set of compounds are easily available in the literature which can be adopted [127].

A perusal of Table 4 shows that both of the properties viz. $\log P_{oct}$ and log S_w increase with the size of the alkanes. It means that these properties are

the function of size, shape, and branching of the molecules. Hence, it appears that TG index might be appropriate for modeling, monitoring, and estimating these properties. The data presented in Table 4 show that like the presently considered properties, the magnitude of TG index also increases with the size of the alkanes under present study. This means that, TG index would be quite suitable for modeling the two properties mentioned above.

To understand the performance of the TG index, the results of regression calculations can be seen in Table 5. The TG index shows very good correlation (R^2 = 0.9466, 0.9693 for $\log P_{oct}$ and $\log S_w$, respectively) with the properties mentioned. Therefore, TG index can serve as a potential candidate for predicting the physical and physiological properties of linear alkanes.

Density is another very important physical property and easily available for the small-sized members of the series. The density of the alkanes usually increases with increasing number of carbon atoms. The R^2 value for the linear regression of ln(TG) versus density exceeds 0.97. Therefore, it can be concluded that the TG index is again capable of modeling this size dependent property, useful especially for nonexistent structures.

In this study parachor is also considered for regression analysis since it is a well known property leading to calculation of a very essential property of liquids; the surface tension. A well correlated equation will give us the ability to obtain the surface tensions of liquids.

Parachor is a quantity defined by the molecular weight of a liquid times the fourth root of its surface tension, divided by the difference between the density of the liquid and the density of the vapor in equilibrium with it; essentially constant over wide ranges of temperature. Parachor has been used in solving various structural problems [132, 133].

A small structural change in a molecular scale gives a big effect on the surface tension. The estimation of the surface tension by a rather simple empirical approach using the quantity parachor has been successful for a wide variety of molecular liquids. The accuracy of the parachor approach is quite good.

It has been known that the parachor obeys an additivity rule, i.e., parachor of a molecule is always the sum of the parachor value assigned to each part of the molecule or to the atoms existing in that molecule, regardless of the type of compound. Although corrections by assigning a small value for branching, ring formation, etc., are often made in the summation of atomic parachors, additivity rule of the atomic parachor means that the isomers essentially have similar values of the molecular parachor. Also, the success of the parachor additivity rule means that the anisotropic or structure-dependent part of the molecular interaction must give only minor effects on the surface tension of molecular liquids [134]. Considerable effort has been paid to explain the empirical relation. However, there seems to be no convincing explanation of the additivity rule of the parachor, which is the essential point for the success of parachor as a method of surface tension estimation.

The coefficient of determination for the regression analysis of parachor of linear alkanes versus the TG index is 0.9471, which is a satisfactorily good result (see Table 5).

Molecular polarizability is another important property related to electron movements. Many papers have investigated the effective polarizability effects on the properties of organic compound in gas phase (such as protonic acidities and basicities) [135-137]. Previous works showed that the molecular polarizability is an important factor affecting properties of organic compounds related to positive or negative charge. The regression equation and the coefficient of determination of the analysis of polarizability of linear alkanes have been given in Table 5.

In conclusion, the TG index is a very useful tool for the estimation of the considered properties for alkanes whose data are missing and sometimes difficult (expensive and time consuming) to measure within only a few percents of error. The molecular size of the unbranched alkanes increase steadily, so does the TG index. Therefore, the TG index can be considered as successful for the correlation of size dependent physical properties. The effect

of branching on the success of TG index will be investigated in the following part of the thesis.

3.2.2.4. Branched Alkanes

The calculated indices and the experimental values for the eight physical properties (bp, MV, MR, HV, TC, PC, ST, mp) and coefficients of determination between the eight physical properties of the alkanes under consideration can be seen in Tables 6 and 7, respectively. A representative illustration for the calculation of the TG index for branched alkanes can be seen in Figure 28.

Before starting the correlation analyses between the novel topological index and each physical property, it is instructive to examine the correlations among the properties themselves. The results of these correlation studies are given in Table 7. As can be seen from the table, it is readily apparent that most of the properties show strong internal correlation (colinearity). Melting points are exceptional, which are very weakly correlated with the other properties. In addition to melting points, surface tensions and the critical temperatures do not correlate well with the critical pressures. For the remaining properties, all the coefficients of determination are greater than 0.807, and even exceed 0.942 for the subset (bp, MV, MR, and HV). It can be anticipated that if a given set of structural parameters successfully models a given property, this parameter set should also be reasonably successful in modeling other, strongly correlated properties. The converse can also be anticipated; i.e., lack of success should be transferred to the correlated properties.

Figures 29-36 show the plots obtained by examining the relation between each property and natural logarithm of TG index (ln(TG)) separately. Each plot also shows the regression equation and the coefficients of determination. The properties are correlated with the logarithm of the index to obtain a linear plot.

Table 6. Calculated TG indices and experimental values for the physical properties of the 70 alkanes (Units: bp, °C; MV, cm^3/mol; MR, cm^3/mol; HV, kJ/mol; TC, °C; PC, atm; ST, dyn/cm; mp, °C).

Entry	Name	TG	bp	MV	MR	HV	TC	PC	ST	mp
1	n-Butane	9	-0.5	-	-	-	152.01	37.47	-	-138.35
2	n-Pentane	40	36.074	115.205	25.2656	26.42	196.62	33.31	16	-129.72
3	2-Methylbutane	32	27.852	116.426	25.2923	24.59	187.8	32.9	15	-159.9
4	n-Hexane	169	68.74	130.688	29.9066	31.55	234.7	29.92	18.42	-95.35
5	2-Methylpentane	110	60.271	131.933	29.9459	29.86	224.9	29.95	17.38	-153.67
6	3-Methylpentane	120	63.282	129.717	29.8016	30.27	231.2	30.83	18.12	-118
7	2,3-Dimethylbutane	100	57.988	132.744	29.9347	29.12	216.2	30.67	16.3	-99.87
8	2,2-Dimethylbutane	75	49.741	130.24	29.8104	29.12	227.1	30.99	17.37	-128.54
9	n-Heptane	448	98.427	146.54	34.5504	36.55	267.01	27.01	20.26	-90.61
10	2-Methylhexane	304	90.052	147.656	34.5908	34.8	257.9	27.2	19.29	-118.28
11	3-Methylhexane	285	91.85	145.821	34.4597	35.08	262.4	28.1	19.79	-119.4
12	3-Ethylpentane	288	93.475	143.517	34.2827	35.22	267.6	28.6	20.44	-118.6
13	2,2-Dimethylpentane	150	79.197	148.695	34.6166	32.43	247.7	28.4	18.02	-123.81
14	2,3-Dimethylpentane	264	89.784	144.153	34.3237	34.24	264.6	29.2	19.96	-119.1
15	2,4-Dimethylpentane	192	80.5	148.949	34.6192	32.88	247.1	27.4	18.15	-119.24
16	3,3-Dimethylpentane	252	86.064	144.53	34.3323	33.02	263	30	19.59	-134.46
17	2,2,3-Trimethylbutane	216	80.882	145.191	34.3736	32.04	258.3	24.64	18.76	-24.91
18	n-Octane	1156	125.655	162.592	39.1922	41.48	296.2	24.8	21.76	-56.79
19	2-Methylheptane	855	117.647	163.663	39.2316	39.68	288	25.6	20.6	-109.04
20	3-Methylheptane	896	118.925	161.832	39.1001	39.83	292	25.6	21.17	-120.5

Table 6 (continued)

21	4-Methylheptane	756	117.709	162.105	39.1174	39.67	290	25.74	21	-120.95
22	2,2-Dimethylhexane	703	106.84	160.072	38.9441	37.29	292	25.6	21.51	-
23	2,3-Dimethylhexane	729	115.607	164.285	39.2525	38.79	279	26.6	19.6	-121.18
24	2,4-Dimethylhexane	684	109.429	160.395	38.9808	37.76	293	25.8	20.99	-
25	2,5-Dimethylhexane	841	109.103	163.093	39.13	37.86	282	25	20.05	-137.5
26	3,3-Dimethylhexane	595	111.969	164.697	39.2596	37.93	279	27.2	19.73	-91.2
27	3,4-Dimethylhexane	676	117.725	160.879	39.0087	39.02	290.84	27.4	20.63	-126.1
28	3-Ethylhexane	783	118.534	158.814	38.8453	39.4	298	27.4	21.64	-
29	2,2,3-Trimethylpentane	476	109.84	158.794	38.8362	36.91	295	28.9	21.52	-114.96
30	2,2,4-Trimethylpentane	329	99.238	157.026	38.7171	35.13	305	28.2	21.99	-90.87
31	2,3,3-Trimethylpentane	525	114.76	159.526	38.9249	37.22	294	25.5	20.67	-112.27
32	2,3,4-Trimethylpentane	504	113.467	165.083	39.2617	37.68	271.15	29	18.77	-107.38
33	3-Ethyl-2-methylpentane	532	115.65	157.292	38.7617	38.84	303	27.6	21.56	-100.7
34	3-Ethyl-3-methylpentane	567	118.259	158.852	38.8681	38.48	295	24.5	21.14	-109.21
35	2,2,3,3-Tetramethylbutane	441	106.47	-	-	-	270.8	22.74	-	-
36	n-Nonane	2400	150.798	178.713	43.8423	46.49	322	23.6	22.92	-53.52
37	2-Methyloctane	2160	114.76	157.292	38.7617	37.22	303	29	21.56	-100.7
38	3-Methyloctane	1976	113.467	158.852	38.8681	37.61	295	27.6	21.14	-109.21
39	4-Methyloctane	1900	142.48	178.15	43.7687	45.09	318.3	23.98	22.34	-113.2
40	3-Ethylheptane	1664	143	176.41	43.642	44.96	318	23.98	22.81	-114.9
41	4-Ethylheptane	1572	141.2	175.685	43.4907	45	318.3	22.8	22.81	-
42	2,2-Dimethylheptane	1408	132.69	180.507	43.9138	41.82	302	23.79	20.8	-113

Table 6 (continued)

43	2,3-Dimethylheptane	1600	140.5	176.653	43.6269	43.51	315	22.7	22.34	-116
44	2,4-Dimethylheptane	1323	133.5	179.12	43.7393	43.31	306	22.7	21.3	-
45	2,5-Dimethylheptane	1683	136	179.371	43.8484	42.91	307.8	23.7	21.3	-
46	2,6-Dimethylheptane	1496	135.21	180.914	43.9258	42.3	306	24.19	20.83	-102.9
47	3,3-Dimethylheptane	1512	137.3	176.897	43.687	42.78	314	24.77	22.01	-
48	3,4-Dimethylheptane	1457	140.6	175.349	43.5473	43.44	322.7	23.59	22.8	-
49	3,5-Dimethylheptane	1586	136	177.386	43.6378	43.49	312.3	24.18	21.77	-
50	4,4-Dimethylheptane	1140	135.2	176.897	43.6022	43.09	317.8	24.77	22.01	-
51	3-Ethyl-2-methylhexane	1395	138	175.445	43.655	43.65	322.7	25.56	22.8	-
52	4-Ethyl-2-methylhexane	1496	133.8	177.386	43.6472	43.26	330.3	25.66	21.77	-
53	3-Methyl-3-ethylhexane	1280	140.6	173.077	43.268	43.11	327.2	23.59	23.22	-
54	3-Ethyl-4-methylhexane	1320	140.4	172.844	43.3746	43.79	312.3	25.07	23.27	-
55	2,2,3-Trimethylhexane	1271	133.6	175.878	43.6226	41.5	318.1	23.39	21.86	-
56	2,2,4-Trimethylhexane	1155	126.54	179.22	43.7638	40.83	301	22.41	20.51	-120
57	2,2,5-Trimethylhexane	1496	124.084	181.346	43.9356	40.03	296.6	25.56	20.04	-105.78
58	2,3,3-Trimethylhexane	1120	137.68	173.78	43.4347	41.91	326.1	25.46	22.41	-116.8
59	2,3,4-Tri methylhexane	1260	139	173.498	43.3917	42.45	324.2	23.49	22.8	-
60	2,3,5-Trimethylhexane	1408	131.34	177.656	43.6474	41.8	309.4	23.79	21.27	-127.8
61	2,4,4-Trimethylhexane	1080	130.648	177.187	43.6598	41.25	309.1	26.45	21.17	-113.38
62	3,3,4-Trimethylhexane	1131	140.46	172.055	43.3407	41.99	330.6	26.94	23.27	-101.2
63	3,3-Diethylpentane	1584	146.168	170.185	43.1134	43.1	342.8	25.96	23.75	-33.11
64	2,2-Dimethyl-3-ethylpentane	864	133.83	174.537	43.4571	41.63	322.6	26.94	22.38	-99.2

Table 6 (continued)

65	2,3-Dimethyl-3-ethylpentane	1008	142	170.093	42.9542	42.01	338.6	25.46	23.87	-
66	2,4-Dimethyl-3-ethylpentane	896	136.73	173.804	43.4037	42.38	324.2	27.04	22.8	-122.2
67	2,2,3,3-Tetramethylpentane	988	140.274	169.495	43.2147	40.07	334.5	25.66	23.38	-9.9
68	2,2,3,4-Tetramethylpentane	832	133.016	173.557	43.4359	40.25	319.6	24.58	21.98	-121.09
69	2,2,4,4-Tetramethylpentane	528	122.284	178.256	43.8747	38.41	301.6	26.85	20.37	-66.54
70	2,3,3,4-Tetramethylpentane	960	141.551	169.928	43.2016	40.81	334.5	29.75	23.31	-102.12

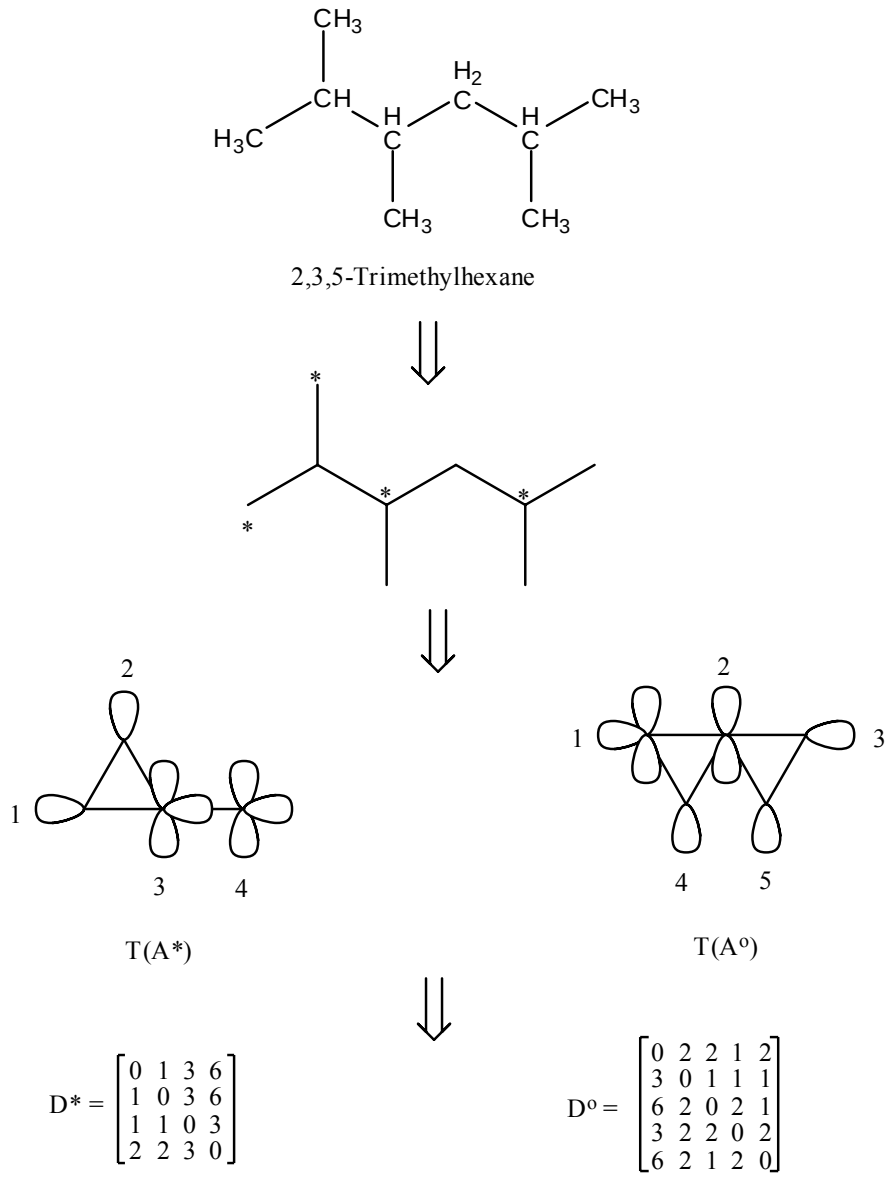

Figure 28. Calculation of the TG index for 2,3,5-trimethyl hexane (Entry 60).

Table 7. Coefficients of determination (R^2) among the properties examined, for branched alkanes considered presently.

	bp	MV	MR	HV	TC	PC	ST	mp
bp	1.000							
MV	0.956	1.000						
MR	0.975	0.992	1.000					
HV	0.981	0.946	0.952	1.000				
TC	0.975	0.909	0.951	0.930	1.000			
PC	-0.838	-0.841	-0.823	-0.842	-0.778	1.000		
ST	0.923	0.807	0.865	0.892	0.965	-0.688	1.000	
mp	0.397	0.293	0.329	0.319	0.432	-0.354	0.421	1.000

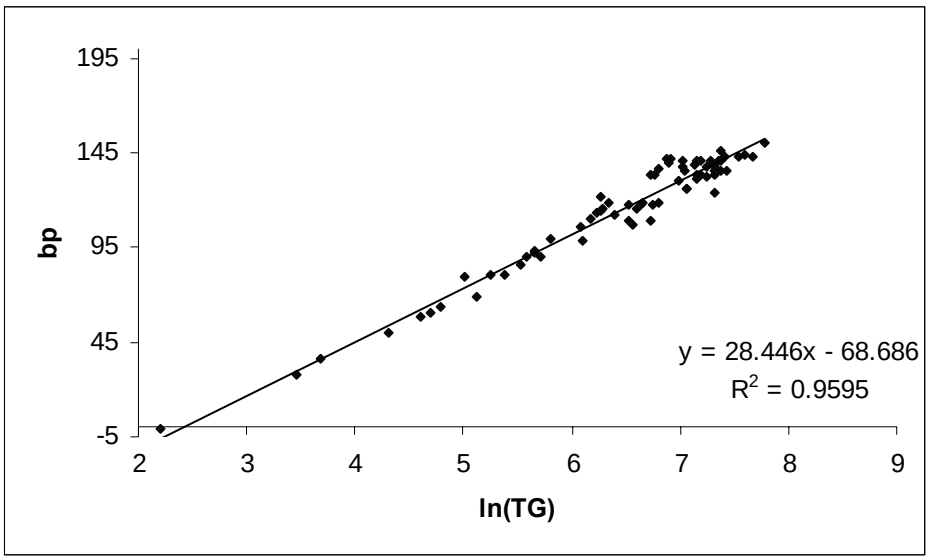

Figure 29. The plot of boiling point of branched alkanes (n = 70) (°C) versus ln(TG).

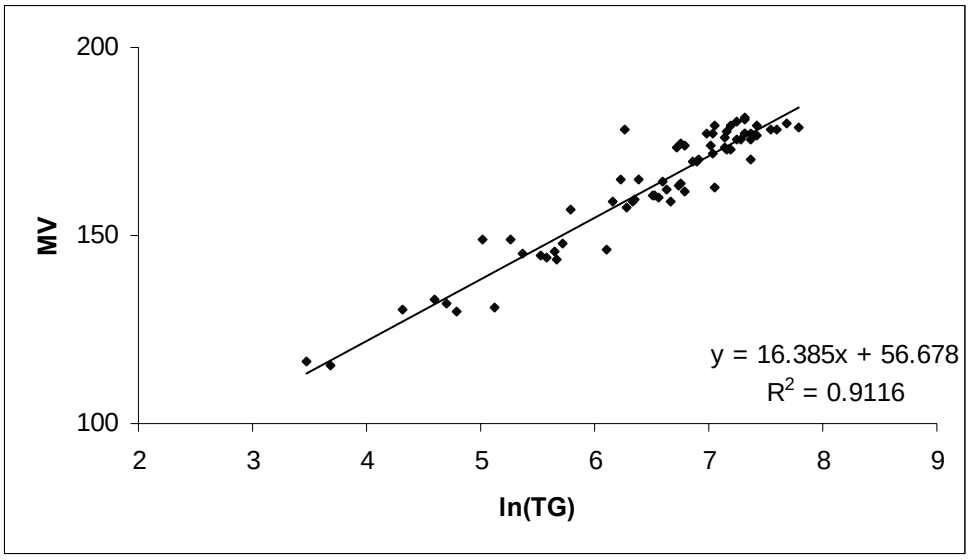

Figure 30. The plot of molecular volume (cm^3/mol) of branched alkanes (n = 68) versus ln(TG).

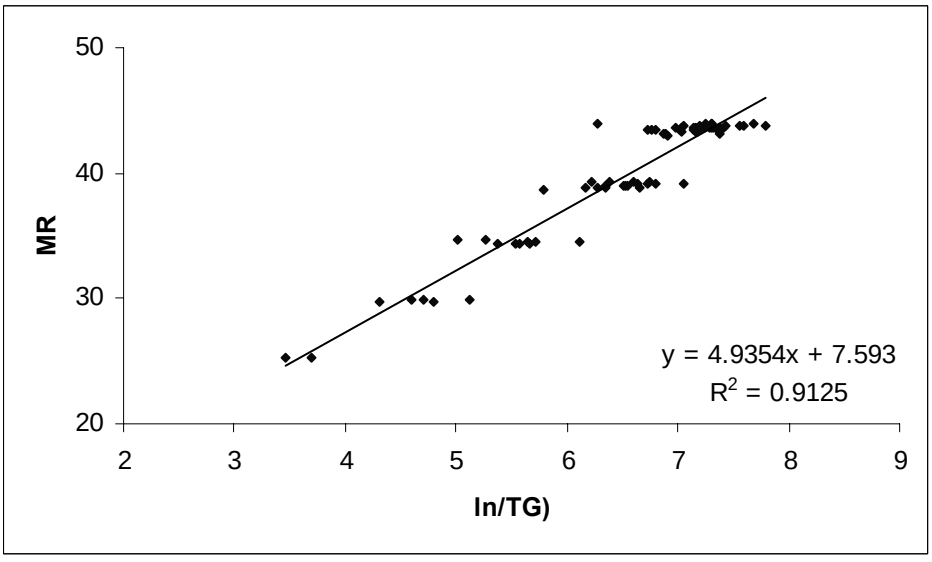

Figure 31. The plot of molar refraction (cm^3/mol) branched alkanes (n = 68) versus ln(TG).

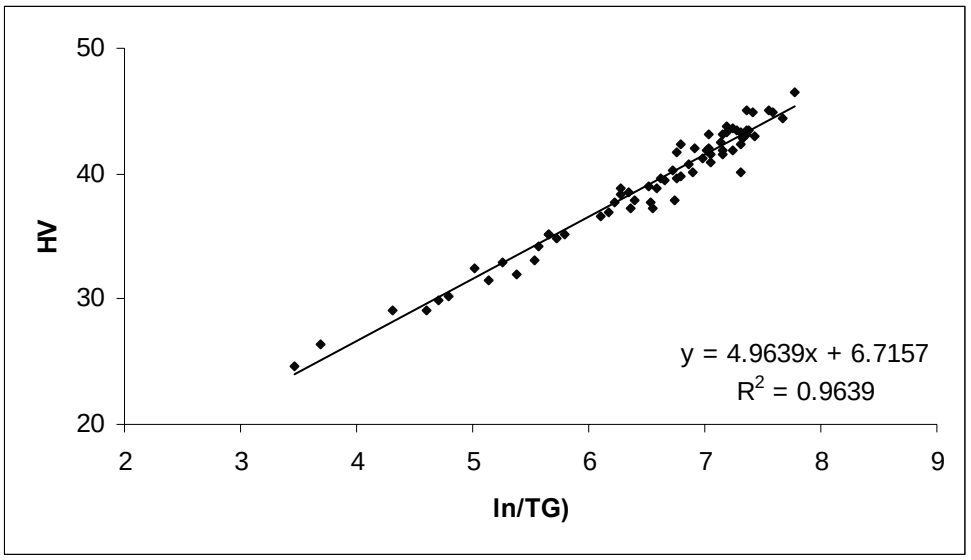

Figure 32. The plot of heat of vaporization (kJ/mol) of branched alkanes (n = 68) versus ln(TG).

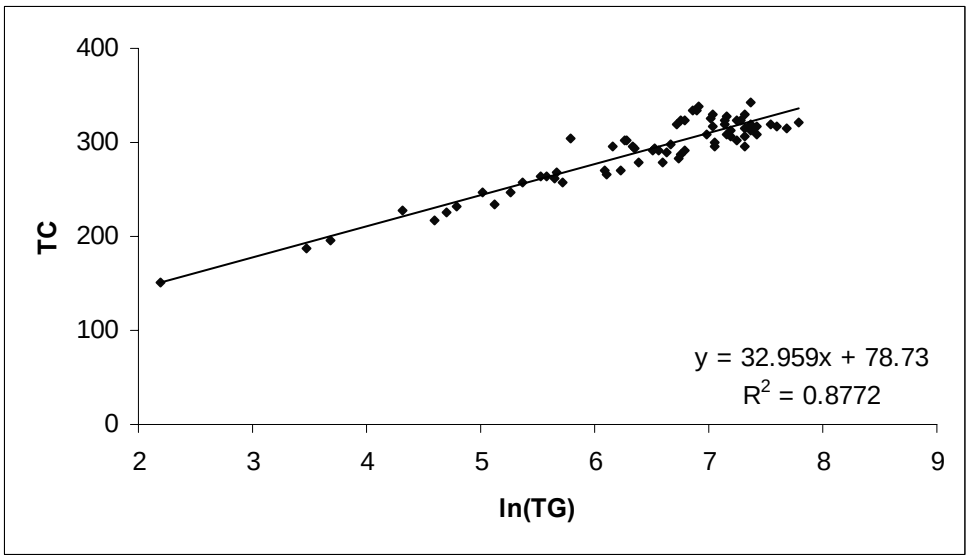

Figure 33. The plot of critical temperature (°C) of branched alkanes (n = 70) versus ln(TG).

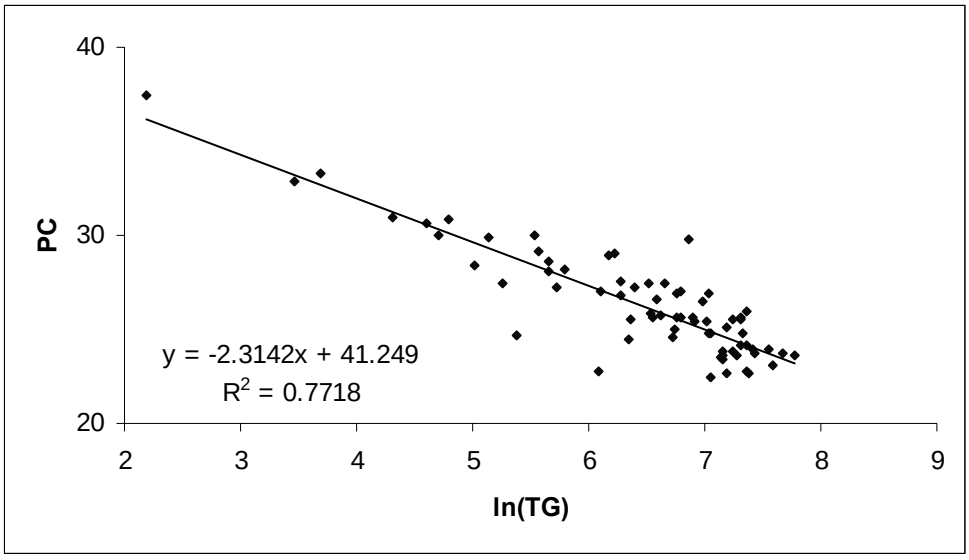

Figure 34. The plot of critical pressure (atm) of branched alkanes (n = 70) versus ln(TG)

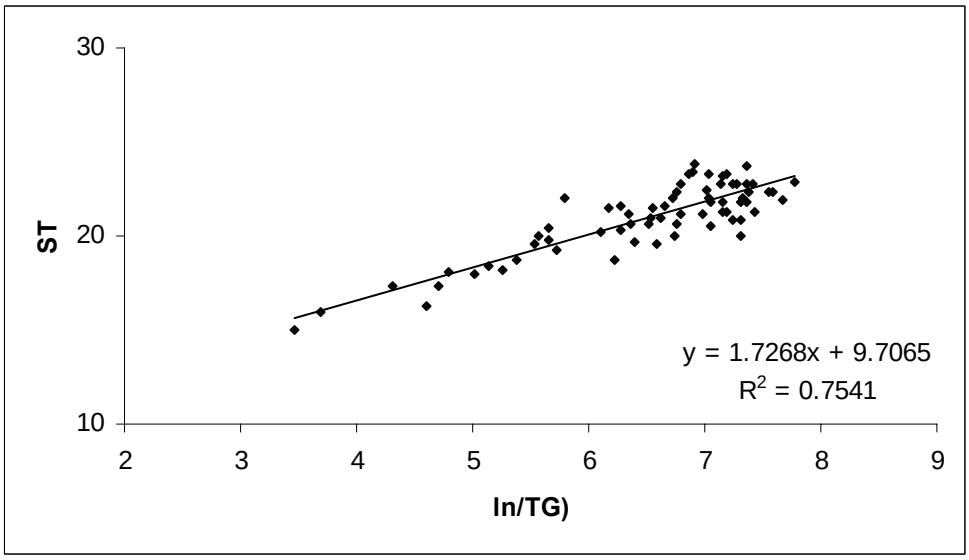

Figure 35. The plot of surface tension (dyn/cm) of branched alkanes (n = 68) versus ln(TG).

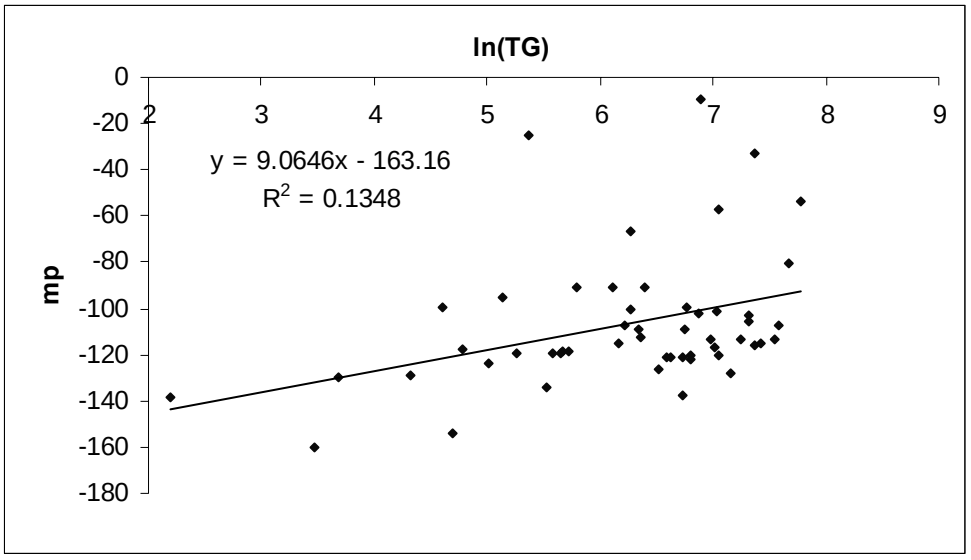

Figure 36. The plot of melting point (°C) of branched alkanes (n = 52) versus ln(TG).

According to the results of the regression analyses, the novel TG index is successful for modeling most of the properties considered. In the previous section, the success of the index had been proved over the linear alkane series. The results obtained in this part of the thesis indicate that the novel TG index is also capable of reflecting the effect of branching in molecules. Small variations in between the values of the coefficients of determination are not due to the failure of the index but the improper correlations between the properties themselves. The index correlated best with boiling point ($R^2 = 0.9595$) and heat of vaporization ($R^2 = 0.9639$).

The failure of the present index to model the melting points of the presently considered 70 alkane molecules is not surprising; a similar result was obtained by Seybold et al. [138]. A melting transition maintains a condensed phase and involves a partial disruption of intermolecular orientations. Therefore, melting might depend on some geometrical and other crystalline factors, which are not well defined with any topological descriptors, yet.

3.2.2.5. Cycloalkanes

Cycloalkanes (also called naphthenes, especially if from petroleum sources) are types of alkanes which have one or more rings of carbon atoms in the chemical structure of their molecules. Cycloalkanes consist of only carbon (C) and hydrogen (H) atoms and are saturated because there are no multiple C-C bonds to hydrogenate. A general chemical formula for cycloalkanes would be $C_nH_{2(n+1-g)}$ where n = number of C atoms and g = number of rings in the molecule. Cycloalkanes with a single ring are named analogously to their normal alkane counterpart of the same carbon count: cyclopropane, cyclobutane, cyclopentane, cyclohexane, etc. The larger cycloalkanes, with greater than 20 carbon atoms are typically called cycloparaffins.

Cycloalkanes are classified into small, common, medium, and large cycloalkanes, where cyclopropane and cyclobutane are the small ones, cyclopentane, cyclohexane, cycloheptane are the common ones, cyclooctane through cyclotridecane are the medium ones, and the rest are the larger ones. Cycloalkanes are similar to alkanes in their general physical properties, but they have higher boiling points, melting points, and densities than alkanes.

Although, boiling points of alkanes are traditionally used for testing and/or demonstrating the correlating abilities of topological indices. Boiling points of cycloalkanes have been examined to a much lesser extent [139,140]. Moreover, Rücker and Rücker [141] produced a critical compilation of experimental boiling points of cycloalkanes and reported their correlations with numerous topological indices and (linear) combinations. In this part of the thesis we have been motivated to extend our novel QSPR models over the boiling points of cycloalkanes.

The calculated TG indices (see Figure 37 for calculation of the TG index for methylcyclohexane) and the experimental boiling point data of the cyclohexanes with 6-10 carbon atoms, and the plot of bp (°C) versus ln(TG) have been given in Table 8 and Figure 38, respectively. As in the case of linear and branched alkanes, the TG index and the boiling point increases with the number of carbon atoms present in the structure. The regression analysis

yielded 0.9721 for the coefficient of determination. Consequently, the TG index has proved itself as a successful parameter for modeling the cyclic systems as well.

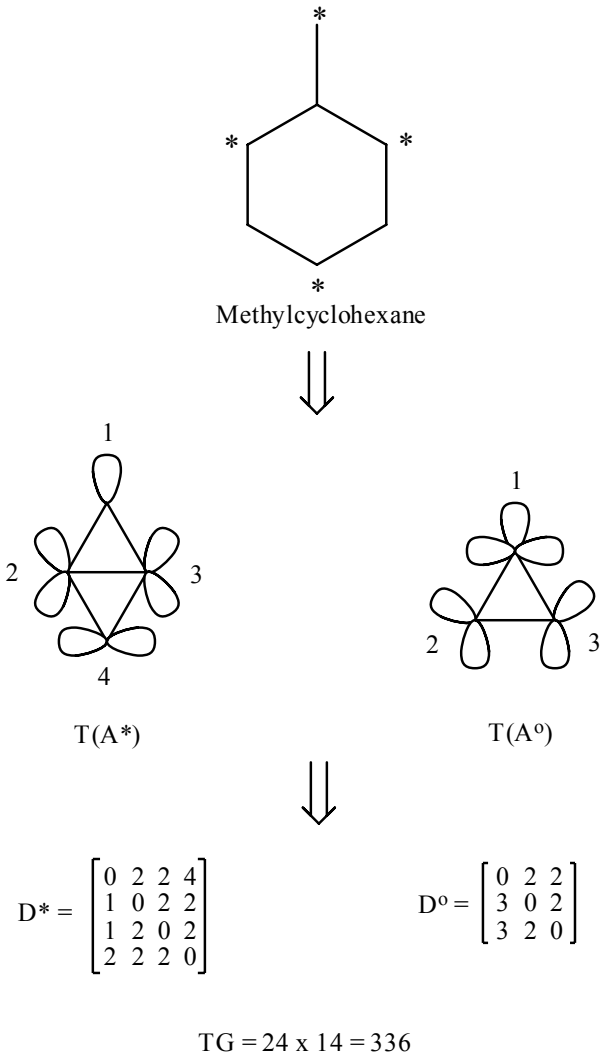

Figure 37. Calculation of the TG index for methylcyclohexane (Entry 2)

Table 8. The TG index and experimental boiling points (°C) of cyclohexane systems with 6-10 carbon atoms.

	Name	TG	bp
1	c6	144	80.7
2	1mc6	336	101
3	1ec6	840	131.8
4	14mc6	784	121.8
5	13mc6	640	122.3
6	12mc6	729	126.6
7	11mc6	640	119.5
8	1pc6	1820	156.7
9	1ipc6	1536	154.8
10	1m4ec6	1700	150.8
11	1m3ec6	1564	150
12	1m2ec6	1457	154.3
13	135mc6	1080	139.5
14	124mc6	1395	144.8
15	123mc6	1320	149.4
16	1m1ec6	1485	152
17	113mc6	1062	136.6
18	112mc6	1350	145.1
19	1bc6	3840	180.9
20	1ibc6	3078	171.3
21	1m4pc6	3481	173.4
22	1m3pc6	2964	169
23	1sbc6	3078	179.3
24	14ec6	3249	175.5
25	13ec6	3016	172
26	1m2pc6	3078	174.5
27	1m4ipc6	2664	170
28	12ec6	2809	176
29	1m3ipc6	2808	167
30	1e35mc6	2584	168.5
31	1m2ipc6	2415	171
32	1m1pc6	2774	174.3
33	1tbc6	2268	171.5
34	11ec6	2592	179.5
35	14m1ec6	2695	168
36	1245mc6	2500	167
37	13m1ec6	2516	166.6
38	1235mc6	2244	166.5
39	1234mc6	2401	172.5
40	1135mc6	1640	153

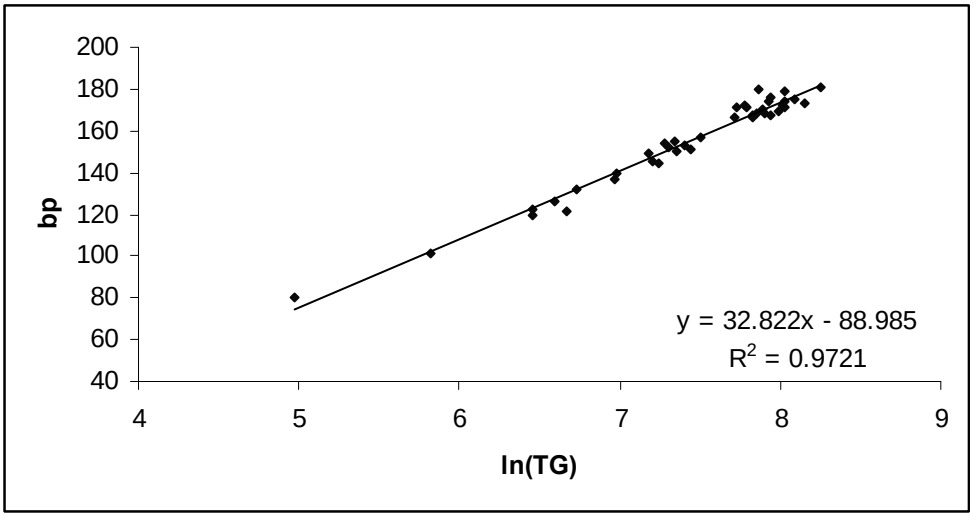

Figure 38. The plot of boiling points of cyclohexane derivatives versus ln(TG)

3.2.3. Alkenes

In the previous part, the topological descriptors have been applied to some physical and electronic properties of a set of normal and branched alkanes. In that part, it has been found that the TG index is successful in obtaining high-quality structure-property relationships. Good regression equations were obtained for most of the physical properties of the alkanes (the melting points (mp), traditionally a subtle and difficult property to handle, were an exception). In this part of the work, we employ the TG index as a structural measure for the physical and chemical properties of a set of monoalkenes, where a new structural feature, the double bond, is introduced. Only a few previous QSPR studies have been devoted to the properties of this class of compounds [142-145], and these have generally been limited to single properties.

The properties examined in this point of the study are: boiling points (bp), molar refractions (MR), molar volumes (MV) at 20°C, heats of combustion (HC), molar heats of vaporization (HV) at 25°C, flashpoints (FLASH), second virial coefficients (VIRC) at 25°C, critical temperatures

(TC), critical pressures (PC), and melting points (mp). The property values were excerpted from the reference source [146]. MV values were calculated as MW/d, where MW is the molecular weight, and d is the density (g/cm^3) at 20°C.

The calculated indices, and the experimental values for the eleven properties, of the alkenes under consideration can be seen in Tables 10 and Table 11, respectively.

Table 9. The TG indices and the experimental values for the physical properties of the alkenes series considered (Units: bp, °C; mp, °C; MV, cm^3/mol; MR, cm^3/mol; HC, kJ/mol; FLASH, K; VIRC, cm^3/mol; HV, kJ/mol; TC, °C; PC, MPa).

Name	TG	bp	mp	MR	MV	HC	HV	FLASH	VIRC	TC	PC
1-Butene	16	-6.3	-185.4	22.66	94.3	2716.8	20204	-	-650	146.5	4.02
Cis-2-butene	16	3.7	-138.9	20.59	90.3	2710.0	21963	-	-713	162.4	4.21
Trans-2-butene	16	0.9	-105.6	20.73			21483	-	-700	155.5	4.10
1-Pentene	65	30.0	-165.2	24.85	109.4	3375.4	25501	-	-1093	191.6	3.53
Cis-2-pentene	60	36.9	-151.4	24.95	107.0	3370.0	26885	-	-1150	201.8	3.70
Trans-2-pentene	60	37.0	-140.2	25.02	-	-	-	228.15	-1140	201.9	3.65
2-Methyl-1-butene	45	31.2	-137.6	24.85	107.8	3361.6	-	-	-1111	191.9	3.51
3-Methyl-1-butene	50	20.1	-168.5	24.94	111.8	3368.9	-	-	-974	191.9	3.44
2-Methyl-2-butene	50	38.6	-133.8	24.95	105.9	3355.7	27090	228.15	-1264	197.2	3.38
1-Hexene	256	63.5	-139.8	29.49	125.0	4034.1	30587	247.15	-1729	230.8	3.14
Cis-2-hexene	240	68.8	-141.1	29.53	122.5	4023.8	33744	-	-	-	-
Trans-2-hexene	240	67.9	-133.0	29.67	-		32136	253.15	-	-	-
Cis-3-hexene	225	66.4	-137.8	29.66	123.8	4028.5	31724	-	-	-	-
Trans-3-hexene	225	67.1	-113.4	29.75	-		32072	261.15	-	-	-
2-Methyl-1-pentene	138	60.7	-135.7	29.48	123.8	4016.8	31042	247.15	-	-	-
3-Methyl-1-pentene	180	54.1	-153.0	29.49	126.1	4026.1	29262	245.15	-	-	-
4-Methyl-1-pentene	144	53.9	-153.6	29.55	126.8	4024.9	29376	242.15	-	-	-
2-Methyl-2-pentene	132	67.3	-135.1	29.74	122.6	4007.3	32088	250.15	-	-	-
3-Methyl-cis-2-pentene	168	70.5	-138.4	29.55	122.2	4013.9	31812	-	-	-	-
3-Methyl-trans-2-pentene	168	67.6	-134.8	29.55	-	-	32536	-	-	-	-

Table 9 (continued)

4-Methyl-cis-2-pentene	132	56.3	-134.4	29.67	125.8	4018.7	30096	245.15	-	-	-
4-Methyl-trans-2-pentene	132	58.6	-140.8	29.75	-	-	30550	-	-	-	-
2-Ethyl-1-butene	168	64.7	-131.5	29.37	122.0	4020.2	31614	-	-	-	-
2,3-Dimethyl-1-butene	144	55.7	-157.3	29.43	124.1	4011.2	29800	255.15	-	-	-
3,3-Dimethyl-1-butene	108	41.2	-115.2	29.58	128.9	4015.4	27449	245.15	-	-	-
2,3-Dimethyl-2-butene	144	73.2	-74.3	29.59	118.8	4007.3	32476	257.15	-1929	-	-
1-Heptene	646	93.6	-119.0	34.13	140.9	4692.6	35484	272.15	-2810	264.1	-
Cis-2-heptene	608	98.5	-	34.17	138.9	4686.5	-	-	-	-	-
Trans-2-heptene	608	98.0	-109.5	34.28	-	-	-	272.15	-	-	-
Cis-3-heptene	576	95.8	-	34.31	139.7	4686.5	-	-	-	-	-
Trans-3-heptene	576	95.7	-136.6	34.43	-	-	-	-	-	-	-
2-Methyl-1-hexene	532	92.0	-102.8	34.12	139.7	4678.0	-	267.15	-	-	-
3-Methyl-1-hexene	486	84.0	-	34.16	142.0	4688.7	-	267.15	-	-	-
4-Methyl-1-hexene	504	86.7	-141.5	34.08	140.6	4688.7	-	-	-	-	-
5-Methyl-1-hexene	551	85.3	-	34.14	141.9	4686.0	-	-	-	-	-
2-Methyl-2-hexene	513	95.4	-130.4	34.40	138.7	4672.2	-	-	-	-	-
3-Methyl-cis-2-hexene	459	94.0	-	34.18	137.2	4674.9	-	-	-	-	-
3-Methyl-trans-2-hexene	459	94.0	-	34.19	137.5	4674.9	-	-	-	-	-
4-Methyl-cis-2-hexene	468	87.4	-	34.22	-	-	-	-	-	-	-
4-Methyl-trans-2-hexene	468	87.6	-126.5	34.35	-	-	-	-	-	-	-
5-Methyl-cis-2-hexene	522	91.0	-	34.20	139.9	4679.3	-	-	-	-	-
5-Methyl-trans-2-hexene	522	86.0	-	34.41	-	-	-	-	-	-	-

Table 9 (continued)

2-Methyl-cis-3-hexene	486	86.0	-	34.37	141.5	4679.3	-	-	-		
2-Methyl-trans-3-hexene	486	86.0	-	34.52	-	-	-	-	-		
3-Methyl-cis-3-hexene	494	95.4	-	34.32	137.7	4674.9	-	-	-		
3-Methyl-trans-3-hexene	494	93.6	-	34.34	-	-	-	-	-		
2-Ethyl-1-pentene	459	94.0		33.99	138.7	4680.7	-	-	-	-	-
3-Ethyl-1-pentene	406	85.1	-127.4	34.06	141.1	4691.3	-	-	-	-	-
2,3-Dimethyl-1-pentene	364	84.3	-134.8	34.00	139.2	4673.8	-	-	-	-	-
2,4-Dimethyl-1-pentene	266	81.6	-123.8	34.18	141.5	4670.9	33344	-	-	-	-
3,3-Dimethyl-1-pentene	357	77.5	-134.3	34.01	140.8	4679.4	-	-	-	-	-
3,4-Dimethyl-1-pentene	378	81.0	-	34.05	140.7	4681.7	-	-	-	-	-
4,4-Dimethyl-1-pentene	259	72.5	-136.6	34.23	143.9	4674.7	31598	-	-	-	-
3-Ethyl-2-pentene	442	96.0	-	34.11	136.3	4677.5	-	-	-	-	-
2,3-Dimethyl-2-pentene	350	97.5	-118.3	34.22	134.9	4667.1	-	-	-	-	-
2,4-Dimethyl-2-pentene	252	83.4	-	34.53	141.3	4665.1	34418	-	-	-	-
3,4-Dimethyl-cis-2-pentene	350	87.0	-	34.12	137.6	4667.9	-	-	-	-	-
3,4-Dimethyl-trans-2-pentene	350	87.0	-	34.15	-	-	-	-	-	-	-
4,4-Dimethyl-cis-2-pentene	238	80.4	-135.5	34.23	140.4	4667.9	32973	-	-	-	-
4, 4-Dimethyl-trans-2-pentene	238	76.8	-115.2	34.41	-	-	33187	-	-	-	-
2-Ethyl-3-methyl-1-butene	350	89.0	-	33.96	138.5	4673.7	34634	-	-	-	-
2,3,3-Trimethyl-1-butene	322	77.9	-119.9	33.99	139.3	4668.2	32485	256.15		-	-
1-Octene	1600	121.3	-101.7	38.78	157.0	5351.1	41224	-	-3948	-	-
Cis-2-octene	1520	125.6	-100.2	38.79	154.9	-	-	-	-	-	-

Table 9 (continued)

Trans-2-octene	1520	125.0	-87.7	38.88	-						
Cis-3-octene	1444	122.9	-	38.85	155.8						
Trans-3-octene	1444	123.3	-	39.09							
Cis-4-octene	1444	122.5	-	38.94	155.6	-	-	-	-	-	-
Trans-4-octene	1444	122.3	-	39.08		-	-	-	-	-	-
2-Methyl-1-heptene	1144	119.3	-	38.78	155.7	-	-	-	-	-	-
3-Methyl-1-heptene	1216	111.0	-	38.76	157.8	-	-	-	-	-	-
4-Methyl-1-heptene	1050	112.8	-	38.77	156.5	-	-	-	-	-	-
5-Methyl-1-heptene	1254	113.3	-	38.76	156.6	-	-	-	-	-	-
6-Methyl-1-heptene	1188	113.2	-	38.79	157.6	-	-	-	-	-	-
2-Methyl-2-heptene	1100	122.6	-	38.97	155.0	-	-	-	-	-	-
3-Methyl-cis-2-heptene	1152	122.0	-	38.87	153.9	-	-	-	-	-	-
3-Methyl-trans-2-heptene	1152	122.0	-	38.87		-	-	-	-	-	-
4-Methyl-cis-2-heptene	987	114.0	-	38.83	156.7	-	-	-	-	-	-
4-Methyl-trans-2-heptene	987	114.0	-	38.83		-	-	-	-	-	-
5-Methyl-cis-2-heptene	1188	118.0	-	38.78	155.2	-	-	-	-	-	-
5-Methyl-trans-2-heptene	1188	118.0	-	38.78		-	-	-	-	-	-
6-Methyl-cis-2-heptene	1122	117.0	-	38.89	156.3	-	-	-	-	-	-
6-Methyl-trans-2-heptene	1122	117.0	-	38.89		-	-	-	-	-	-
2-Methyl-cis-3-heptene	1050	112.0	-	39.12	158.9	-	-	-	-	-	-
2-Methyl-trans-3-heptene	1050	112.0	-	39.12		-	-	-	-	-	-
3-Methyl-cis-3-heptene	1116	121.0	-	38.84	154.1	-	-	-	-	-	-

Table 9 (continued)

3-Methyl-trans-3-heptene	1116	121.0	-	38.84		-	-	-	-	-	-
4-Methyl-cis-3-heptene	980	122.0	-	38.92	154.8	-	-	-	-	-	-
4-Methyl-trans-3-heptene	980	122.0	-	38.92		-	-	-	-	-	-
5-Methyl-cis-3-heptene	1116	112.0	-	38.99	157.4	-	-	-	-	-	-
5-Methyl-trans-3-heptene	1116	112.0	-	38.99		-	-	-	-	-	-
6-Methyl-cis-3-heptene	1071	115.0	-	38.99	157.4	-	-	-	-	-	-
6-Methyl-trans-3-heptene	1071	115.0	-	38.99		-	-	-	-	-	-
2-Ethyl-1-hexene	1152	120.0	-	38.71	154.3	-	-	-	-	-	-
3-Ethyl-1-hexene	1054	110.3	-	38.63	156.9	-	-	-	-	-	-
4-Ethyl-1-hexene	1088	113.0	-	38.46	154.6	-	-	-	-	-	-
2,3-Dimethyl-1-hexene	961	110.5	-	38.70	155.5	-	-	-	-	-	-
2,4-Dimethyl-1-hexene	924	111.2	-	38.70	155.8	-	-	-	-	-	-
2,5-Dimethyl-1-hexene	1122	111.6	-	38.80	156.5	-	-	-	-	-	-
3,3-Dimethyl-1-hexene	800	104.0	-	38.69	157.2	-	-	-	-	-	-
3,4-Dimethyl-1-hexene	930	112.0	-	38.65	155.0	-	-	-	-	-	-
3,5-Dimethyl-1-hexene	924	104.0	-	38.76	158.5	-	-	-	-	-	-
4,4-Dimethyl-1-hexene	840	107.2	-	38.64	155.9	-	-	-	-	-	-
4,5-Dimethyl-1-hexene	1024	109.0	-	38.52	154.1	-	-	-	-	-	-
5,5-Dimethyl-1-hexene	968	102.5	-	38.78	158.3	-	-	-	-	-	-
3-Ethyl-cis-2-hexene	992	121.0	-	38.85	152.3	-	-	-	-	-	-
3-Ethyl-trans-2-hexene	992	121.0	-	38.85		-	-	-	-	-	-
4-Ethyl-cis-2-hexene	1020	113.0	-	38.51	154.8	-	-	-	-	-	-

Table 9 (continued)

4-Ethyl-trans-2-hexene	1020	113.0	-	38.51		-	-	-	-	-	-
2,3-Dimethyl-2-hexene	837	121.8	-115.1	38.87	151.5	-	-	-	-	-	-
2,4-Dimethyl-2-hexene	882	110.6	-	38.69	155.6	-	-	-	-	-	-
2,5-Dimethyl-2-hexene	1054	112.2	-	38.94	155.8	-	-	-	-	-	-
3,4-Dimethyl-cis-2-hexene	870	116.0	-	38.37	152.3	-	-	-	-	-	-
3,4-Dimethyl-trans-2-hexene	870	116.0	-	38.37		-	-	-	-	-	-
3,5-Dimethyl-cis-2-hexene	880	112.0	-	38.84	154.8	-	-	-	-	-	-
3,5-Dimethyl-trans-2-hexene	880	112.0	-	38.84		-	-	-	-	-	-
4,4-Dimethyl-cis-2-hexene	780	106.0	-	38.75	155.4	-	-	-	-	-	-
4,4-Dimethyl-trans-2-hexene	780	106.0	-	38.75		-	-	-	-	-	-
4,5-Dimethyl-cis-2-hexene	960	110.0	-	38.59	154.8	-	-	-	-	-	-
4,5-Dimethyl-trans-2-hexene	960	110.0	-	38.59		-	-	-	-	-	-
5,5-Dimethyl-cis-2-hexene	924	106.9	-	38.89	156.5	-	-	-	-	-	-
5,5-Dimethyl-trans-2-hexene	924	104.1	-	38.96		-	-	-	-	-	-
3-Ethy1-3-hexene	870	116.0		38.79	153.9	-	-	-	-	-	-
2,2-Dimethyl-cis-3-hexene	861	105.4	-137.4	38.99	157.4	-	-	-	-	-	-
2,2-Dimethyl-trans-3-hexene	861	100.9	-	39.18		-	-	-	-	-	-
2,3-Dimethyl-cis-3-hexene	900	114.0	-	38.68	154.1	-	-	-	-	-	-
2,3-Dimethyl-trans-3-hexene	900	114.0	-	38.68		-	-	-	-	-	-
2,4-Dimethyl-cis-3-hexene	840	109.0	-	39.06	156.3	-	-	-	-	-	-
2,4-Dimethyl-trans-3-hexene	840	107.6	-	39.13		-	-	-	-	-	-
2,5-Dimethyl-cis-3-hexene	1024	102.0	-	38.82	158.0	-	-	-	-	-	-

Table 9 (continued)

2,5-Dimethyl-trans-3-hexene	1024	102.0	-	38.82		-	-	-	-	-	-
3,4-Dimethyl-cis-3-hexene	841	122.0	-	38.80	150.2	-	-	-	-	-	-
3,4-Dimethyl-trans-3-hexene	841	122.0	-	38.80		-	-	-	-	-	-
2-n-Propyl-1-pentene	960	117.7	-	38.70	155.0	-	-	-	-	-	-
2-Isopropyl-1-pentene	930	113.0	-	38.67	154.8	-	-	-	-	-	-
2-Ethyl-3-methyl-1-pentene	870	112.5	-	38.48	15.9	-	-	-	-	-	-
2-Ethyl-4-methyl-1-pentene	880	110.3	-	38.68	156.0	-	-	-	-	-	-
3-Ethyl-2-methyl-1-pentene	856	110.0	-	38.49	153.7	-	-	-	-	-	-
3-Ethyl-3-methyl-1-pentene	768	112.0	-	38.71	153.6	-	-	-	-	-	-
3-Ethyl-4-methyl-1-pentene	720	107.5	-	38.59	155.8	-	-	-	-	-	-
2,3,3-Trimethyl-1-pentene	696	108.3	-69.0	38.41	152.6	-	-	-	-	-	-
2,3,4-trimethyl-1-pentene	672	108.0	-	38.54	153.9	-	-	-	-	-	-
2,4,4-Trimethyl-1-pentene	440	101.4	-93.5	38.77	156.9	-	-	-	-	-	-
3,3,4-Trimethyl-1-pentene	720	105.0	-	38.50	153.9	-	-	-	-	-	-
3,4,4-Trimethyl-1-pentene	560	104.0	-	38.83	156.1	-	-	-	-	-	-
3-Ethyl-2-methyl-2-pentene	672	117.0	-	38.80	151.8	-	-	-	-	-	-
3-Ethyl-4-methyl-cis-2-pentene	672	116.0	-	38.74	151.8	-	-	-	-	-	-
3-Ethyl-4-methyl-trans-2-pentene	672	114.3	-	38.71		-	-	-	-	-	-
2,3,4-Trimethyl-2-pentene	640	116.3	-133.3	38.79	150.9	-	-	-	-	-	-
2,4,4-Trimethyl-2-pentene	364	104.9	-106.3	39.01	155.5	-	37224	-	-	-	-
3,4,4-Trimethyl-cis-2-pentene	608	112.0	-	38.66	151.8	-	-	-	-	-	-
3,4,4-Trimethyl-trans-2-pentene	608	112.0	-	38.66		-	-	-	-	-	-

Table 9 (continued)

2-Isopropyl-3-methyl-1-butene	640	104.0	-	38.38	155.4	-	-	-	-	-	-
2-Ethyl-3,3-dimethyl-1-butene	608	110.0	-	38.67	154.1	-	-	-	-	-	-
1-Nonene	3220	146.9	-81.4	43.45	173.2	6010.1	-	-	-	320.1	2.33
Cis-2-nonene	3082	150.8	-	-	-	-	-	-	-	-	-
Trans-2-nonene	3082	150.1	-	-	-	-	-	-	-	-	-
Cis-3-nonene	2992	148.4	-	-	-	-	-	-	-	-	-
Trans-3-nonene	2992	148.2	-	-	-	-	-	-	-	-	-
Cis-4-nonene	2904	147.4	-	-	-	-	-	-	-	-	-
Trans-4-nonene	2904	147.8	-	-	-	-	-	-	-	-	-

Table 10. Coefficients of determination among the properties of the alkene series examined.

	bp	**MR**	**MV**	**HC**	**HV**	**FLASH**	**VIRC**	**TC**	**PC**	**mp**
bp	1.000									
MR	0.967	1.000								
MV	0.946	0.992	1.000							
HC	0.970	0.996	0.992	1.000						
HV	0.993	0.921	0.903	0.938	1.000					
FLASH	0.933	0.905	0.844	0.897	0.878	1.000				
VIRC	-0.960	-0.981	-0.969	-0.976	-0.974	-0.975	1.000			
TC	0.996	0.965	0.979	0.989	0.998	0.997	-0.942	1.000		
PC	-0.950	-0.940	-0.958	-0.958	-0.920	-0.825	0.903	-0.954	1.000	
mp	0.664	0.640	0.614	0.525	0.482	0.518	-0.543	0.607	-0.467	1.000

The correlations among the properties examined are shown in Table 12. As can be seen, most of the properties are highly correlated with one another, with the exception of mp, which is poorly correlated with the other properties. The remaining nine properties all have coefficients of determination greater than 0.82, and the subset of bp, MR, MV, and HV all have correlations greater than 0.90.

Table 13 gives the regression equations and the coefficients of determination (R^2) values obtained by examining the relation between each property of the alkenes and ln(TG) separately. In Figure 39, the plot of boiling point values versus ln(TG) for the 161 alkenes studied can be seen for the representation of the acceptable scattering of the data.

Table 11. The regression equations and the coefficients of determination (R^2) for the eleven properties of the alkene series obtained by the application of the index.

	regression equation	**R^2**
bp (n=117)	y = 28.06x - 79.59	0.949
MR (n=114)	y = 4.47x + 7.82	0.911
MV (n=114)	y = 15.54x + 47.79	0.909
HC (n=49)	y = 590.14x + 1079.51	0.940
HV (n=27)	y = 4275.20x + 9208.43	0.903
FLASH (n=14)	y = 14.83x + 173.78	0.806
VIRC (n=11)	y = -663.95x + 1427.25	0.921
TC (n=10)	y = 29.99x + 73.25	0.983
PC (n=9)	y = -0.32x + 4.85	0.921
mp (n=48)	y = 13.52x - 202.85	0.423

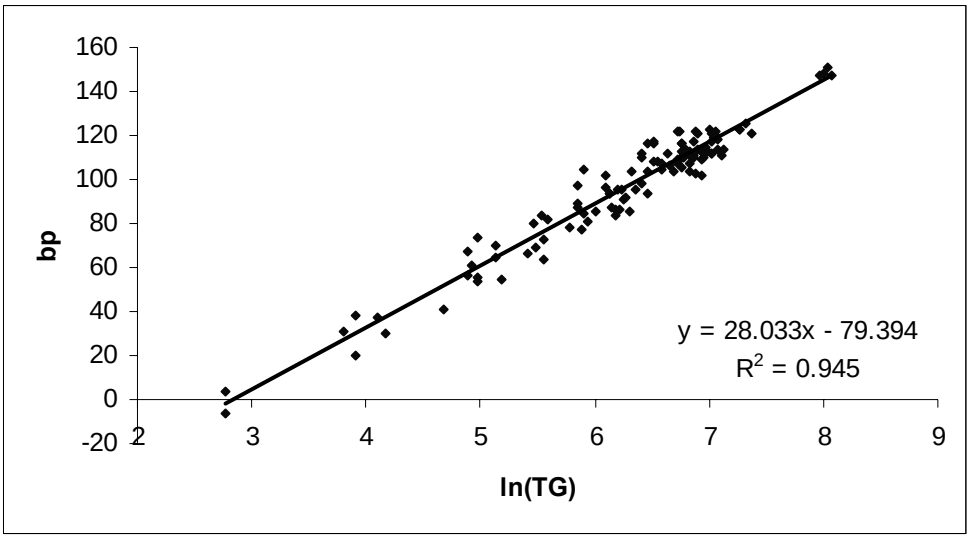

Figure 39. The plot of ln(TG) versus the boiling points of alkene derivatives (n = 117)

The regression equations presented in Table 13 are generally of high-quality for properties other than the mp. Therefore, property values estimated on the basis of these equations, with the exception of mp, should be sufficiently accurate for many practical purposes.

As can be seen from the Table, the molecular mass/bulk clearly exerts the dominant influence on the properties other than mp, suggesting that dispersion forces play a dominant role for those properties which depend on intermolecular forces. A similar conclusion was reached in the earlier alkane study (see the previous part). This is a reasonable conclusion in the present case for bp, HV, VIRC, TC, PC, and VISC. For MV the 'mass/bulk' dependence can be attributed directly to the larger volume of compounds with higher number of carbon atoms. Likewise, MR depends largely on the higher number of electrons in larger compounds. For the two strictly "chemical" properties, the HC and the flashpoints (FLASH), the dependence on the mass/bulk dimension is more accurately attributed to the larger number of

reacting bonds in the larger, higher number of carbon atoms containing compounds.

Branching, steric factors, and the double bond environment exert smaller influences on the properties, as demonstrated by the coefficients in the regression equations. Molecular branching sequesters interior parts of these compounds and reduces the extent of contact between neighboring molecules. The latter effect is reflected on the MVs. Because dispersion forces are strongly dependent on distance -the interaction energies fall as $1/r^6$, where r is the separation- a decrease in the amount of close contact decreases the cohesive forces experienced by the compounds. Therefore, bp and HV decrease as molecular branching increases.

The failure of the TG index to model the mp in this case is not surprising, either since this property was also not well modeled by these same topological parameters in the previous section, which deals with the alkanes. This illustrates the greater subtlety of the melting transition as compared to the boiling and critical transitions. The latter transitions involve a direct dependence on the operative intermolecular forces, and so directly reflect the strengths of these forces. The melting transition, in contrast, maintains a condensed phase and involves a partial disruption of intermolecular orientations. Melting, thus, depends on geometric factors, and other factors as well that are not well addressed by the present topological parameters (The TG index is directly influenced by the molecular shape and size.). This dependence on shape and entropic factors, in contrast to a simple intermolecular force dependence, is reflected in the melting point rather than the mass/bulk related factor. Dearden [147] has given a comprehensive review of mp predictions.

3.2.4. Alcohols and Amines

After obtaining successful results in the application of the TG index to the alkanes and monoalkenes, the index has been applied to heteroatom containing species; alcohols and amines, initially. In this part of the study, the index has been applied to predict the boiling points of certain linear and

branched, alcohols and amines (see Table 14 for alcohols and Table 15 for amines), at the standard pressure using the novel TG index.

The normal boiling points of liquids reflect the strength of the intermolecular forces (among other forces present) that hold them together. The stronger the intermolecular forces, the more tightly the molecules will be held together and, therefore, the higher the normal boiling point. The boiling point can be directly correlated to the chemical structure of a molecule [148]. Normal boiling points can be measured relatively easily, but having predictive boiling point models can be a useful adjunct, especially for predicting boiling points for large number of compounds. Otherwise, it would seem arduous to first synthesize and then experimentally determine the boiling point of each.

Calculated TG indices (see Figure 14 for the calculation of the TG index for alcohols and amines) and experimental boiling points of 71 alcohol and 20 amine derivatives are listed in Table 14 and Table 15, respectively. Since the present systems contain heteroatoms (N and O), in the calculation of the indices here, the *Z* weighting scheme has been applied. One application of this method can be seen in the method part of the thesis.

When the results of the correlation analysis are carefully inspected the following statement is hold; while the correlations for the boiling point values of the linear primary alcohols and linear primary amines with ln(TG) are satisfactorily good (R^2 = 0.995 and R^2 = 0.987, respectively), these values degrease to R^2 = 0.854 and R^2 = 0.862 when all the alcohols and all the amines in the list have been considered (see Figures 40 and 41). The decrease in the value of coefficient of determination when branching is considered is not very surprising in the case of alcohols and amines, because apart from the molecular weight, some additional factors (such as steric factors which may result in a decrease in hydrogen bonding) affect the boiling point of the species.

Although the effect of the extent of branching for alcohols and amines could not be perfectly pictured by the TG index for the boiling points, the correlation analysis show promising results for the prediction of at least long chain linear alcohols and amines. The estimation of the boiling points of

branched alcohols and amine will still give admissible data within the limits of small percent errors.

Table 12. The TG indices and the normal boiling points (°C) of the alcohols considered in this thesis.

Entry	Alcohol	TG	bp
1	2-butanol	38	99.5
2	Pentanol	198.25	138
3	3-methyl-1-butanol	113.75	131
4	2-methyl-1-butanol	142.5	128
5	2-pentanol	110	119.3
6	3-pentanol	138	116.2
7	3-methyl-2-butanol	115	112.9
8	2-methyl-2-butanol	100	102.3
9	Hexanol	520	157.6
10	3-methyl-1-pentanol	401.25	153
11	4-methyl-1-pentanol	438	151.9
12	2-methyl-1-pentanol	396.75	149
13	2-ethyl-1-butanol	333	147
14	3,3-dimethyl-1-butanol	223.5	144.5
15	2,3-dimethyl-1-butanol	309	143
16	2-hexanol	432	140
17	2,2-dimethyl-1-butanol	325	136.5
18	3-hexanol	390	135
19	3-methyl-2-pentanol	307.5	134.3
20	4-methyl-2-pentanol	219	131.6
21	2-methyl-3-pentanol	297	126.5
22	3-methyl-3-pentanol	322	122.4
23	2-methyl-2-pentanol	182.5	121.1
24	3,3-dimethyl-2-butanol	270	120.4
25	2,3-dimethyl-2-butanol	267	118.4
26	Heptanol	1309	176.4
27	4-methyl-1-hexanol	1022	173
28	5-methyl-1-hexanol	983.25	170
29	3-methyl-1-hexanol	864	169
30	2-methyl-1-hexanol	1022	164
31	2,4-dimethyl-1-pentanol	769.5	159
32	2-methyl-2-hexanol	954.75	143
33	5-methyl-2-hexanol	826.5	151
34	2,3-dimethyl-2-pentanol	928	139.7

Table 12 (continued)

35	2,4-dimethyl-2-pentanol	567	133.1
36	2,3,3-trimethyl-2-butanol	385	131
37	3-heptanol	598	157
38	2-methyl-3-hexanol	992	143
39	3-methyl-3-hexanol	810	143
40	5-methyl-3-hexanol	705.5	148
41	3-ethyl-3-pentanol	765	142
42	2,2-dimethyl-3-pentanol	730.75	135
43	2,3-dimethyl-3-pentanol	558	139.7
44	2,4-dimethyl-3-pentanol	650	138.7
45	4-heptanol	558	156
46	Octanol	837	195.3
47	4-methyl-1-heptanol	2700	188
48	6-methyl-1-heptanol	2071	188.6
49	2,5-dimethyl-1-hexanol	2370	179.5
50	2,4,4-trimethyl-1-pentanol	1905.75	168.5
51	2-octanol	1312	180
52	2-methyl-2-heptanol	2370	156
53	3-methyl-2-heptanol	1600.5	166.1
54	5-methyl-2-heptanol	1768	170
55	2,3-dimethyl-2-hexanol	1856.25	160
56	2,5-dimethyl-2-hexanol	1472.5	154.5
57	3,4-dimethyl-2-hexanol	1717	165.5
58	2-methyl-3-ethyl-2-pentanol	1395	156
59	2,3,4-trimethyl-2-pentanol	992	147.5
60	3-octanol	960	171
61	2-methyl-3-heptanol	2175.5	167.5
62	3-methyl-3-heptanol	1750	163
63	6-methyl-3-heptanol	1494	174
64	2-methyl-3-ethyl-3-pentanol	1598	160
65	2,2,4-trimethyl-3-pentanol	1843	150.5
66	2,3,4-trimethyl-3-pentanol	1836	156.5
67	4-octanol	1218	176.3
68	2-methyl-4-heptanol	910	164
69	Nonanol	5425	213.3
70	Decanol	9700	231.1
71	Undecanol	17031.25	245

Table 13. The TG indices and the normal boiling points (°C) of the amines under treatment.

Entry	Amine	TG	bp
1	propylamine	11.57	78
2	butylamine	50.29	104
3	pentylamine	202.43	131
4	hexylamine	530.29	155
5	heptylamine	1330.86	176
6	octylamine	2742.86	201
7	nonylamine	5500	217
8	decylamine	9828.57	240
9	2-butylamine	38.86	67.75
10	3-methyl-1-butylamine	139.71	96
11	3-methyl-2-butylamine	117.14	85.5
12	2-methyl-2-butylamine	122.14	77
13	3-penthylamine	140.57	89
14	2-ethyl-1-hexylamine	1915.43	169.2
15	3-methyl-1-hexylamine	879.43	149
16	4-methyl-2-hexylamine	776.57	132.5
17	2-heptylamine	969	142
18	3-heptylamine	848.57	139.5
19	6-methyl-2-heptylamine	1662.57	155
20	2-octylamine	2400	164

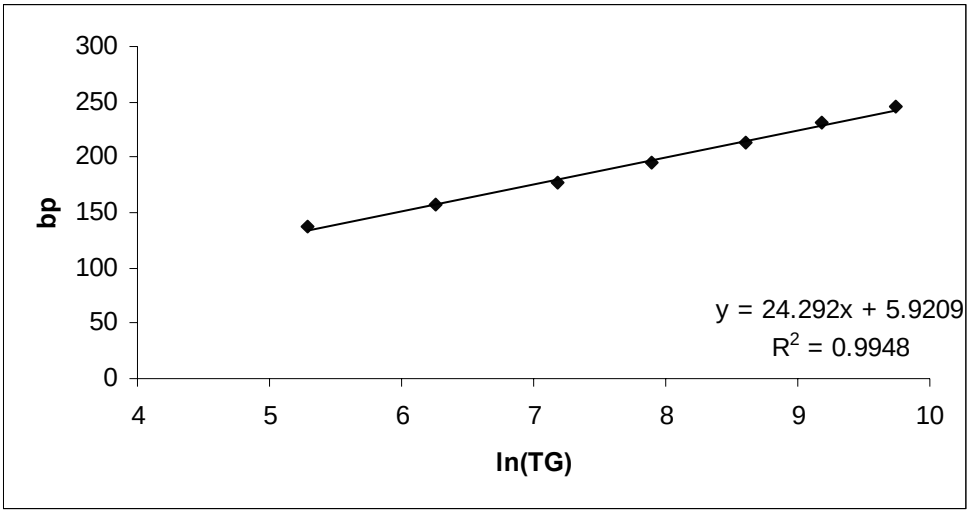

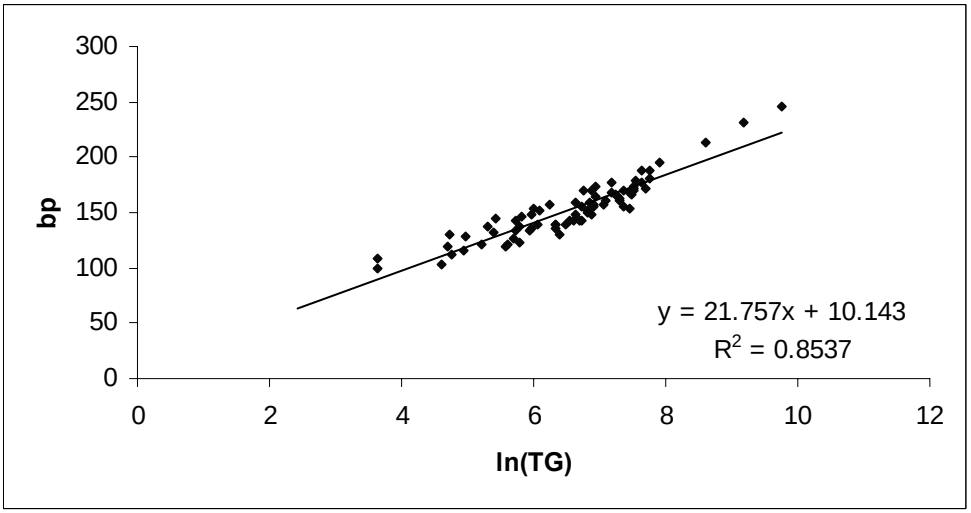

Figure 40. Results of the correlation analysis for linear and branched alcohols.

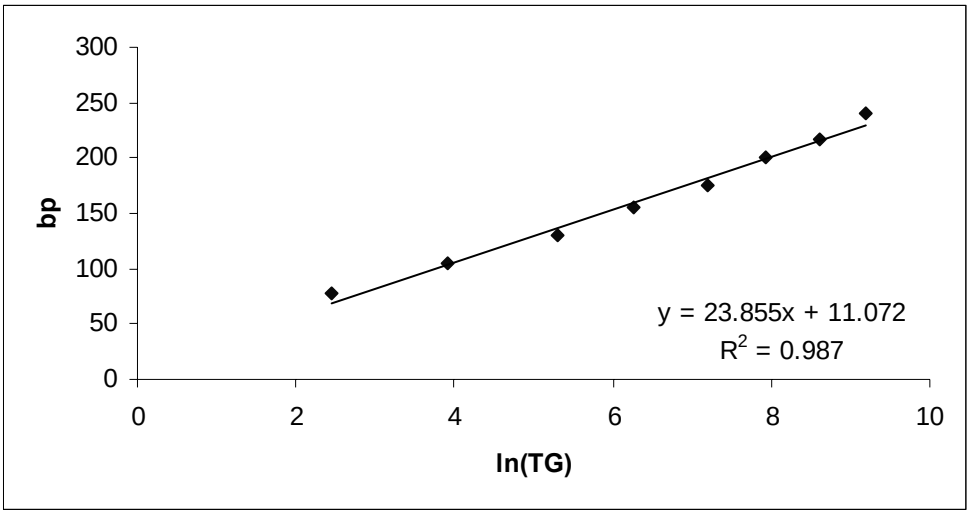

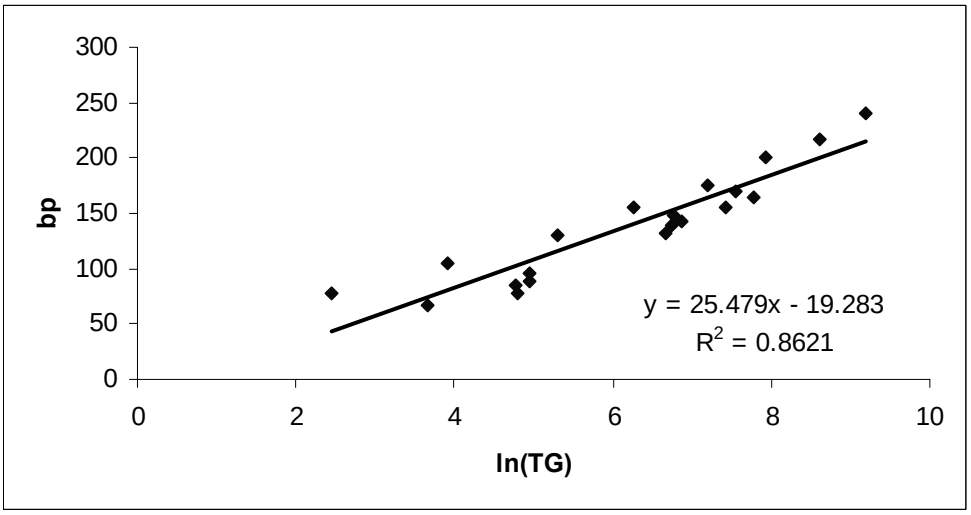

Figure 41. Results of the correlation analysis for linear and branched amines.

3.2.5. Explosives

After obtaining reasonably well correlation with the properties of the linear polyenes, alkanes, alkenes, alcohols and amines, the TG index is thought to be potentially good enough to be applied for the estimation of properties of more complex systems, such as explosives.

To be able to predict the detonation properties (detonation pressure, energy and velocity) from a given molecular structure and know the crystal density is of vital importance for especially in designing new explosive materials. Quantitative estimation of the properties of compounds, such as heats of formation, density, detonation parameters and sensitivity would permit the selection of the most promising high energy density material (HEDM) candidates for laboratory synthesis and further considerations [149].

3.2.5.1. Nitropyridines

The pyridine ring system occurs in the structures of many natural products, pharmaceutical and agrochemical compounds, and other commercial substances. A wide range of synthetic methods has, therefore, been developed, both for construction of the pyridine ring and for its substitution [150]. However, nitration of pyridine and its simple C-alkyl derivatives at a ring carbon atom with common nitrating systems, generally results in a very low yield of nitropyridine and is of little synthetic value [151]. Unfortunately, one of the most important classes of aromatic substitution reactions, electrophilic aromatic substitution, takes place with great difficulty and only under forcing conditions [152], owing to the electron-deficient character of the pyridine ring. Thus, many simple nitropyridines, which are synthetic precursors of potential pharmaceutical and agrochemical importance [153-158] are not available by conventional direct nitration of the parent pyridine. Katritzky et al. [159] and Bakke [150] have reported the synthesis of β-nitro (3-nitro) pyridine.

The search for new potential high-energy density materials (HEDMs) is on going [160-164]. Good high-energy materials possess high-density, have a fast velocity of detonation, and are energetically unstable with respect to their

reaction products. They are also expected to have relatively high positive heat of formation values. With the idea that nitropyridines can be candidates for HEDMs, the authors have performed a theoretical analysis on all possible nitro derivatives of pyridine.

3.2.5.1.1. Method of Calculation

Computations were performed via the Gaussian 03 package program. The geometry optimizations of all the structures have been performed by the application of density functional theory (DFT) calculations with B3LYP exchange correlation function and various basis sets (6-31G(d,p), 6-31++G(d,p), 6-311G(d,p) and cc-pvdz).

Geometrical optimization of the molecules was performed by the above-mentioned methods without any geometrical restriction. For each set of calculations, vibrational analyses were done (using the same basis set employed in the corresponding geometry optimizations). The normal mode analysis for each structure yielded no imaginary frequencies for the $3N-6$ vibrational degrees of freedom, where N is the number of atoms in the system. This indicates that the structure of each molecule corresponds to at least a local minimum on the potential energy surface.

Nucleus independent chemical shift calculations at the center of rings (NICS(0)) were also performed on all the molecules using the gauge invariant atomic orbital (GIAO) approach at the B3LYP/6-31G(d,p) level. The B3LYP/6-311G(d,p) optimized geometries were used for the NICS calculations.

Various isodesmic reaction schemes were selected for the calculation of the heats of formation of (1) 2-nitropyridine, (2) 3-nitropyridine, (3) 4-nitropyridine, (4) 2,3-dinitropyridine, (5) 2,4-dinitropyridine, (6) 2,5-dinitropyridine, (7) 2,6-dinitropyridine, (8) 3,4-dinitropyridine, (9) 3,5-dinitropyridine, (10) 2,3,4-trinitropyridine, (11) 2,3,5-trinitropyridine, (12) 2,3,6-trinitropyridine, (13) 3,4,5-trinitropyridine, (14) 3,4,6-trinitropyridine, (15) 2,4,6-trinitropyridine, (16) 2,3,4,5-tetranitropyridine, (17) 2,3,4,6-

tetranitropyridine, (18) 2,3,5,6-tetranitropyridine, (19) 2,3,4,5,6-pentanitropyridine (see Figure 42 for the calculation of the TG index for 3-nitropyridine and Figure 43 for all the structures considered).

The explosive properties of the present systems have also been calculated and the correlation analysis of them have been performed against the novel TG index.

3.2.5.1.2. Results and Discussion

3.2.5.1.2.1. Energetics

The total energies (zero point corrected) of the molecules under present consideration with different basis sets are given in Table 16. According to the results of the calculations, the lowest energies are obtained by 6-311G(d,p) basis set. When the total energies of all the molecules are considered, 2-nitropyridine (1) is found to be the most favorable isomer among the mono nitro pyridines, 2,6-dinitropyridine (7), is found to be the most favorable isomer among the di nitro pyridines, 3,4,5-trinitropyridine (13) is found to be the most favorable isomer among the tri nitro pyridines and 2,3,4,5-tetranitropyridine (16) is found to be the most favorable isomer among the tetra nitro pyridine derivatives. The most stable isomer of each one of the series showed that when the nitro groups are close to the heteroatom of the main skeleton, the stability of that isomer increases (except for the tri-nitro derivatives). This is quite reasonable since the electrons located on the electronegative nitrogen atom can be pulled over the ring more evenly by the attachment of very strong electron withdrawing nitro groups. The nitro groups increase the electron density as well as the aromatic character of the main skeleton which was partially lost by the insertion of one nitrogen into a benzene ring.

3.2.5.1.2.2. NICS

Aromaticity continues to be an actively investigated area of chemistry. The simplest criteria for aromatic compounds are that they possess cyclic

conjugated π-systems containing the proper number of π-electrons (i.e., the Hückel rule). While these criteria are robust enough to predict the aromaticity of a host of neutral and charged ring systems, it is not always a clear indicator of aromaticity for more complex systems (as in our case).

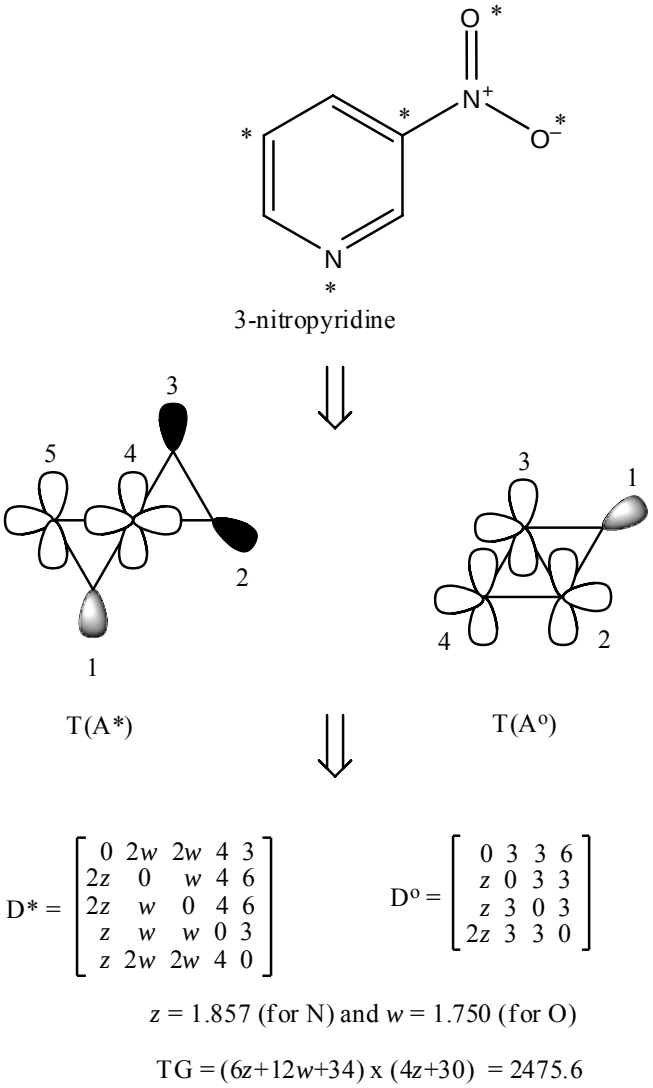

Figure 42. Calculation of the TG index for 3-nitropyridine (2)

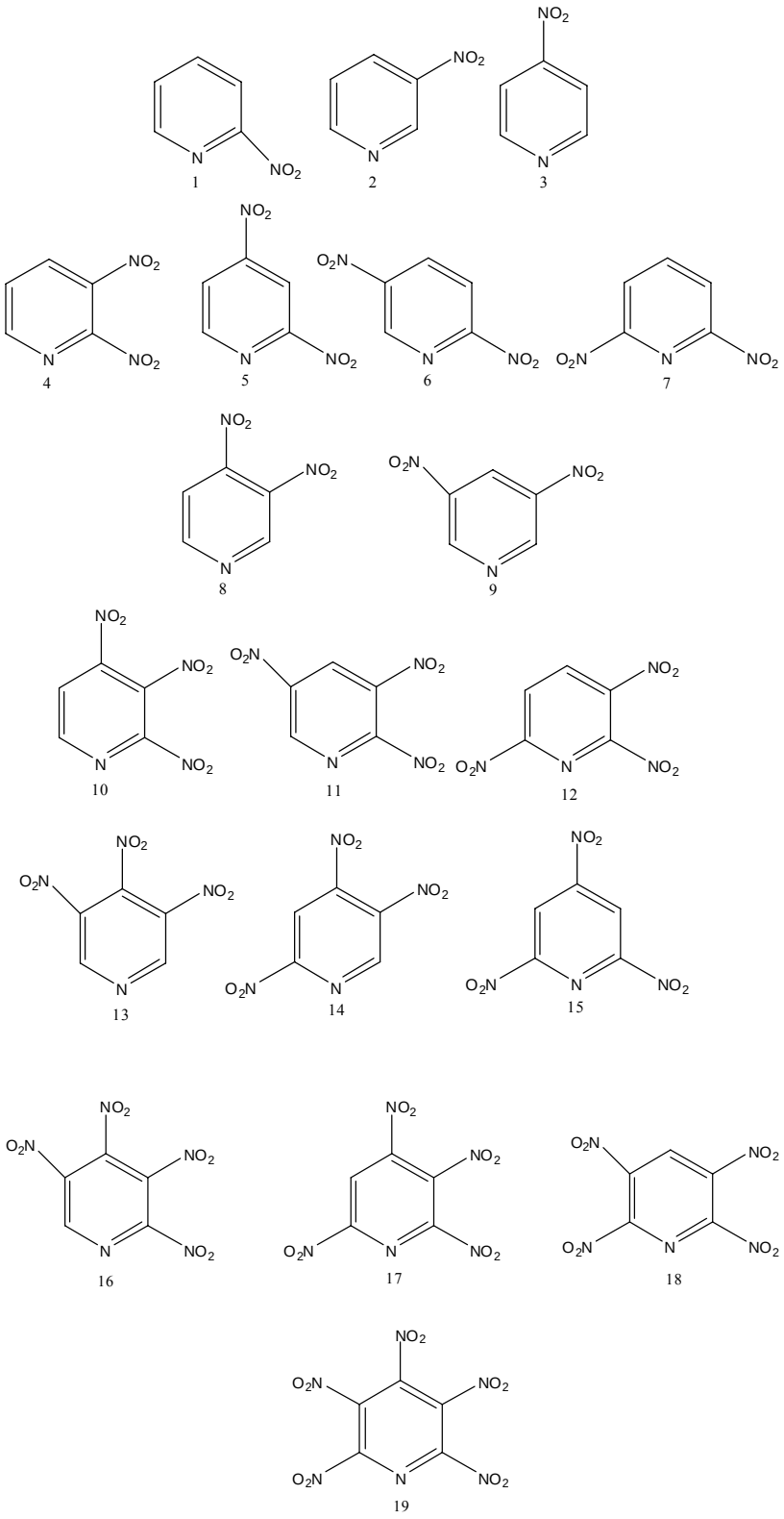

Figure 43. Structures of the considered nitropyridine species.

Table 14. The zero point energy corrected total electronic energies of the nitropyridine derivatives, calculated with B3LYP correlation function with different basis sets. (Energies are in Hartrees)

	Basis set			
	6-31G(d,p)	**6-31++G(d,p)**	**6-311G(d,p)**	**cc-pvdz**
1	-452.689532	-452.709845	-452.801130	-452.717338
2	-452.689602	-452.709798	-452.800617	-452.717122
3	-452.688901	-452.709160	-452.800036	-452.716564
4	-657.047314	-657.075353	-	-657.144494
5	-657.174446	-657.203641	-657.342775	-657.223184
6	-657.174836	-657.204063	-657.343051	-657.218521
7	-657.174686	-	-657.341403	-657.223462
8	-657.145160	-657.173299	-657.312698	-657.194370
9	-657.174884	-657.203899	-657.342522	-657.223279
10	-861.580508	-861.616593	-861.806221	-861.652558
11	-861.626906	-861.663862	-861.851957	-861.697594
12	-861.626781	-861.664090	-861.852224	-861.697568
13	-861.655015	-861.692949	-861.880401	-861.725182
14	-861.579520	-861.615112	-861.804144	-861.651299
15	-861.626347	-861.663222	-861.851214	-861.697103
16	-1066.099564	-1066.147338	-1066.382092	-1066.190398
17	-1066.058708	-1066.103500	-1066.341774	-1066.152564
18	-1066.078437	-1066.123341	-1066.360738	-1066.170578
19	-1270.226295	-1270.274305	-1270.546198	-1270.329301

Aromaticity is expressed by a combination of properties in cyclic delocalized systems. In general, aromaticity is discussed in terms of energetic, structural and magnetic criteria [165-170]. In 1996, Schleyer introduced a simple and efficient probe for aromaticity: Nucleus-independent chemical shift (NICS) [171], which is the computed value of the negative magnetic shielding at some selected point in space, generally, at a ring or cage center. Negative NICS values denote aromaticity (-11.5 for benzene, -11.4 for naphthalene) and positive NICS values denote antiaromaticity (28.8 for cyclobutadiene) while small NICS values indicate non-aromaticity (-2.1 for cyclohexane, -1.1 for adamantane). NICS may be a useful indicator of aromaticity that usually correlates well with the other energetic, structural and magnetic criteria for

aromaticity [172-175]. Resonance energies and magnetic susceptibilities are measures of the overall aromaticity of a polycycle, but do not provide information about the individual rings. However, NICS is an effective probe for local aromaticity of individual rings of polycyclic systems.

In the present case, NICS values of the various nitro pyridine derivatives have been calculated by the application of density functional theory using the standard 6-31G(d,p) basis set (Table 17). All the molecules have been found to be aromatic. The aromaticity of pyridine itself is expected to be improved by the substitution of nitro groups due to the following reasoning; due the presence of electronegative nitrogen, the ring of the pyridine suffers from homogeneous electron distribution and thus, exhibit poor aromaticity. Insertion of a nitro group into the system will pull the electrons located on the nitrogen atom of the pyridine ring and let these electrons delocalize over the ring better which will lead to an improved aromaticity. Therefore, the greater the number of nitro groups properly oriented in the system, more aromatic the structure will be. As can be seen in Table 17 the NICS values of the systems increase (absolutely) as the number of nitro groups in the structures increase.

Table 15. NICS(0) values (ppm) of the pyridine and nitropyridine systems

Structures	B3LYP/6-31G(d,p)
Pyridine	-8.08
1	-9.45
2	-9.22
3	-9.51
4	-10.54
5	-10.81
6	-10.12
7	-10.78
8	-10.44
9	-9.84
10	-12.61
11	-12.00
12	-12.46
13	-11.91
14	-11.99
15	-11.87
16	-12.79
17	-13.47
18	-13.61
19	-13.08

3.2.5.1.2.3. Heat of Formations by Isodesmic Reactions

Thermochemical and molecular properties are critical parameters in many aspects of gas kinetics, and the accuracy to which these parameters are determined can greatly affect the determination of a variety of parameters including rate coefficients, rates of heat release, and branching ratios, all of which are critical in the accurate simulation of reactive gas-phase systems.

Heat of formation of a molecule has significant practical application to explore reactivity and equilibrium of a chemical reaction. It is important to find the heats of formation of various related compounds correctly. For the aromatic nitro compounds, although some of their heats of formation can be found experimentally, certain nitro compounds are very difficult to synthesize and some of them are highly unstable. Hence, it would be useful to develop a

reliable theoretical means to calculate the heats of formation of these energetic materials.

Heat of formation values have been calculated by the *ab initio* methods for many years, especially using some high level theories, such as G2, G3, QCISD (T), CCSD (T), MP4SDTQ approaches [176-182]. However, these approaches need huge computation time and can only be used for small to medium-sizes molecules. Density functional theory (DFT) has emerged as a very reliable theoretical method to calculate geometries of molecules. Hence, it has been used to evaluate the heats of formation of some interested molecules [183-187] and the results indicate that DFT is a reliable method. Rice et al. [36] reported methods to predict gas phase heats of formation of energetic materials using quantum mechanical calculations. Among these methods, predictions for gas-phase heats of formation are based on Hess' Law [188], combined with quantum mechanical and experimental information. The application of the Hess' Law requires building a chemical reaction scheme. The isodesmic reaction, in which numbers of electron pairs and chemical bond types are conserved in the reaction, allows canceling of errors inherent in the approximate treatment of electron correlation in the solutions to quantum mechanic equations. Hence, various reports of the heats of formation of the molecules have been given by various isodesmic reaction schemes [180-194]. Ventura et al. [195,196] have pointed out that DFT methods using modest basis sets and isodesmic reactions can produce very accurate thermo-chemical information, in many cases superior to results from G2 and even CCSD (T).

Chen et al. [197] investigated the heat of formation values of various aromatic nitro compounds and they found that the results were quite close to the experimental data. In this study, the complete series of nitro pyridine derivatives were selected to calculate the heats of formation through the selected isodesmic reaction, using various DFT methods and basis sets. Since these kinds of calculation are reliable as pointed out before, the heat of formation of compounds whose heat of formation cannot be determined by experimental technique can be found theoretically.

As indicated by Foresman and Frisch [198], different isodesmic reactions would predict different values of heat of formation for the same molecule. Therefore, it is necessary to select properly the isodesmic reaction of the studied molecule. Since isodesmic reactions require as many experimental data as possible in order to be applied conveniently, we have chosen the isodesmic reaction shown in Scheme 1 because of its convenience to get the required experimental data. We could find the experimental heat of formation values for pyridine, methane and nitromethane from the literature. Additionally, in an isodesmic reaction, the bonding in the both sides of the reaction must be as similar as possible. Therefore, after a detailed survey of various possible isodesmic reactions, the following isodesmic reaction (Scheme 1) has been selected in order to calculate the heat of formation values of, nitropyridine systems (1-19) presently considered.

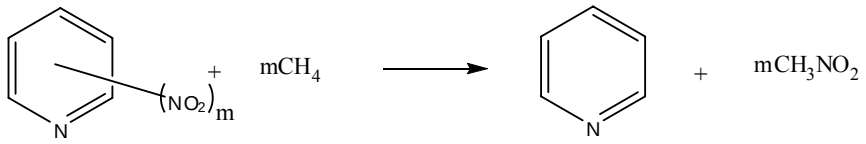

Scheme 1

The general bond separation reaction of the systems under consideration is presented in Scheme 1 and the calculated energies of all species are listed in Table 16. The energy difference between the products and reactants shown in Scheme 1 has been calculated as the heat of reaction, ΔH_{rxn}. From the calculated, ΔH_{rxn} and experimental heats of formation at 298 K of methane, pyridine, and nitromethane, heats of formation (ΔH_f) values of all the molecules (1-19) can be calculated and the results are listed in Table 18. It is well known that DFT methods underestimate the energies by 1-3 kcal/mol [199]. The experimental gas phase enthalpies of formation values of the present

systems are not available in the literature since they are all difficult to synthesize. Thus, no comparison with the experimental values can be done. The heat of formation values obtained by different basis sets are mostly close to each other.

Table 16. B3LYP calculated heat of formation values of the nitropyridine derivatives, with different basis sets (Energies are in kJ/mol)

	Basis set			
	6-31G(d,p)	**6-31++G(d,p)**	**6-311G(d,p)**	**cc-pvdz**
1	118.8	129.0	125.2	123.5
2	118.6	129.1	126.5	124.1
3	120.4	130.8	128.1	125.5
4	447.4	472.0	-	328.4
5	113.6	135.2	126.9	121.8
6	112.6	134.1	126.2	134.1
7	112.9	-	130.5	121.1
8	190.5	214.8	205.9	197.5
9	112.4	134.5	127.6	121.6
10	315.4	353.6	334.0	320.9
11	193.6	229.5	213.9	202.7
12	193.9	228.9	213.2	202.8
13	119.8	153.1	139.2	130.3
14	318.0	357.5	339.4	324.3
15	195.1	231.2	215.8	204.0
16	220.6	262.7	245.8	235.3
17	327.9	377.8	351.7	334.6
18	276.1	325.8	301.9	287.3
19	1155.8	1232.0	1238.8	1197.0

3.2.5.1.2.4. Predicted Densities and Detonation of the Nitropyridine Derivatives

Detonation velocity (D), and detonation pressure (P) are the important parameters to evaluate the explosive performances of energetic materials and

can be predicted by the empirical Kamlet-Jacobs [200-205] equations as follows:

$$D = 1.01\ (N\ M^{1/2}\ Q^{1/2})^{1/2}\ (1+130\ \rho) \qquad (18)$$

$$P = 1.558\ \rho^2\ N\ M^{1/2}\ Q^{1/2} \qquad (19)$$

where each term in esq. 18 and 19 is defined as follows: D, detonation velocity (km/s); P, detonation pressure (GPa); ρ, density of a compound (g/cm^3); N, moles of gaseous detonation products per gram of explosive; M, average molecular weight of gaseous products; Q, chemical energy of detonation (kJ/g). The parameters N, M, and Q are calculated according to the chemical composition of each explosive as listed in Table 19.

Table 17. Formulas for calculating the N, M and Q parameters of the $C_aH_bO_cN_d$ explosives.

	Stoichiometric ratio		
Parameters	**c ≥ 2a+b/2**	**2a+b/2 > c ≥ b/2**	**b/2 > c**
N	(b+2c+2d)/4MW	(b+2c+2d)/4MW	(b+d)/2MW
M	4MW/(b+2c+2d)	(56d+88c-8b) /(b+2c+2d)	(2b+28d+32c) /(b+d)
Q	(28.9b+94.05a +0.239ΔHf)/MW	[28.9b+94.05(c/2-b/4)+ 0.239ΔHf]/MW	(57.8c+0.239ΔHf) /MW

In the table, $C_aH_bO_cN_d$ denotes the empirical formula of the compound. N is moles of gaseous detonation products per gram of explosive (in mol/g); M is the average molecular weight of the gaseous products (in g/mol); Q is the chemical energy of detonation (in kJ/g); MW in the formula is the molecular weight of the title compounds (in g/mol); ΔH_f is the heat of formation of the studied compound (in kJ/mol).

It is clear from the equations (18 and 19) that density has been considered as the primary physical parameter in detonation performance, because detonation velocity and pressure of the explosives increase proportionally with packing density and square of it, respectively. The simplest and earliest method used for the prediction of density is the "group or volume additivity" method, where the molar volume is obtained by summing up the volume of appropriate atoms or functional groups [206]. However, this method has the drawback that it cannot readily account for the molecular conformation, isomerization and crystal packing efficiency. That is, it yields the same density values for different isomers or conformations of the same compound or even for different compounds with the same functional group composition, and ignores the density differences due to crystal polymorphism. So, it is not efficient to predict the density of HEDMs by using the volume additivity method. In this thesis, a convenient methodology already used in the literature for predicting the crystalline densities of energetic materials not limited only for some classes but valid for nearly all organic explosives has been applied. It is based on quantum chemical computations. The density of each compound was predicted from the molecular weight divided by molecular volume, while the molecular volume of each molecule was obtained from the statistical average of 100 single-point molar volume calculations for each optimized structure. The molar volume was defined as inside a contour of 0.001 electrons/Bohr^3 density that was evaluated by using a Monte Carlo integration implemented in the Gaussian 03 W program. In the literature, this method has been successfully tested on various molecules and accurately predicts the densities. Using this density and by the help of Kamlet-Jacobs equations, detonation velocities, and detonation pressures of the explosives were accurately determined [207-212].

In order to calculate detonation parameters, heat of formation values in gas phase have been calculated using the semiempirical molecular orbital method, PM3. It has been reported in the literature that PM3 method provide excellent values for simple 23 nitrogen heterocyclic compounds [190]. Also

previous studies [214-219] have reported and proved that ΔH_f calculated by the PM3 method could replace the experimental data reasonably well in evaluating the D and P of the energetic compounds due to above mentioned reasons. PM3 is also very fast method so computational cost is so low compared to high level of theories such as DFT and *ab initio* methods.

Table 20 collects the predicted densities and detonation properties of the nitropyridine derivatives together with the TG index. The heats of formation (ΔH_f) values were also calculated and listed in the table. All these data in Table 20, gave some clue about the explosive character of the molecules derived from pyridine.

Table 18. Predicted densities and detonation properties of the nitropyridine derivatives (ΔH_f values are obtained from PM3 calculations, V data are obtained from 100 single point calculations at the 6-31G(d,p) level)

	ΔH_f (kJ/mol)	**Q (kJ/g)**	**V (cm^3/mol)**	**ρ (g/cm^3)**	**D (km/s)**	**P (GPa)**	**TG Index**
1	117.25	1158.24	79.09	1.57	7.17	23.46	2482
2	103.93	1132.58	78.25	1.58	7.21	23.32	2475
3	108.59	1141.57	78.76	1.57	7.18	23.34	2398
4	145.82	1414.87	101.03	1.67	8.87	32.56	11363
5	113.08	1368.58	101.96	1.66	8.72	31.87	10425
6	112.66	1367.99	103.56	1.63	8.58	31.62	12544
7	122.59	1382.02	102.25	1.65	8.71	31.99	10095
8	160.28	1435.33	104.77	1.61	8.58	32.20	10647
9	102.78	1354.01	101.42	1.67	8.74	31.79	10708
10	249.99	1648.01	121.30	1.76	10.16	39.49	31926
11	163.92	1551.88	124.71	1.72	9.74	37.79	34283
12	178.55	1568.23	121.95	1.75	9.98	38.42	35437
13	129.24	1513.15	123.98	1.73	9.73	37.43	31658
14	241.85	1638.91	125.01	1.71	9.85	38.79	35018
15	179.11	1568.85	124.07	1.72	9.82	38.10	30539
16	190.48	1649.08	140.37	1.85	10.91	42.58	81158
17	293.20	1743.87	141.58	1.83	10.97	43.60	78592
18	241.09	1695.79	143.26	1.81	10.77	42.75	86254
19	512.22	1949.58	159.91	1.90	11.93	48.66	170430

It is clear that from mono-substituted to penta-substituted nitropyridines, density (ρ), velocity of detonation (D) and detonation pressure (P) all increase with the increasing number of the nitro groups. This might show good group additivity on the detonation properties and also supports the claim that introducing more nitro substituents into a molecule usually helps to increase its detonation performance. For RDX and HMX, experimental value of D and P are 8.75 km/s, 9.10 km/s and 34.70 GPa, 39.00 GPa [220], respectively. Furthermore, at the same theoretical level, the calculated performance parameters D and P of RDX and HMX were found to be 8.83 km/s, 8.998 km/s and 34.11 GPa, 35.92GPa, respectively. Comparing these values with tri-nitropyridine compounds; compound (13) has velocity of detonation value of 9.73 km/s and detonation pressure value of 37.43 GPa. All the other tri-nitro derivatives, tetra-nitro and penta-nitro derivatives possess D and P values greater than that of compound (13). Therefore, one finds them to be more powerful explosives than the famous explosives HMX and RDX. Furthermore, the relative position of the nitro substituent in the pyridine compounds affects the detonation properties (see Table 20). Especially di- and tri-nitro substituted pyridines will be novel potential candidates for high energy density materials (HEDMs) when they are successfully synthesized.

3.2.5.1.2.5. Correlation Analysis with TG Index

As in the case of alcohols and amines, the TG index for nitropyridines have been calculated using the vertex-weighted graphs. The results of the correlation analysis of the TG index with the total energies and the explosive properties are given in Table 21. The data in the table reveal that TG index can successfully be used for the prediction of the explosive properties of HEDMs, since the coefficient of determination exceeds 0.98 for Q and 0.99 for P. Therefore there is no need for the time consuming computational calculations for the estimation of the explosion characteristics of the explosives. The regression equations maybe extrapolated and the desired property for an explosive material can be determined with a very small error.

Table 19. The regression equation and the coefficient of determination between the natural logarithm of the TG index and the explosive properties. (Q: Heat of explosion, V: Volume of explosion, D: Velocity of detonation, P: Pressure of explosion)

Property	Regression Equation	R^2
Total Energy	y = -178.41x + 973.41	0.9704
Q	y = 166.96x - 158.21	0.9540
V	y = 18.12x - 64.127	0.9864
ρ	y = 0.0723x + 0.9921	0.9178
D	y = 1.0532x - 1.039	0.9846
P	y = 5.6048x - 20.03	0.9903

3.2.5.2. Nitropyrimidines

Pyrimidine, also known as m-diazine, is the parent substance of a large group of heterocyclic compounds which have attracted much attention for a long time. Compounds belonging to this group were known as breakdown products of uric acid at a very early date in the history of organic chemistry, but the systematic study of the ring system really began with work of Elderfield [213], who first applied the name pyrimidine to the unsubstituted parent heterocyclic skeleton. Pyrimidine derivatives play a vital role in many biological processes, the ring system being present in, for example, the nucleic acids, several vitamins and coenzymes, and uric acid and other purines. Many synthetic members of the group are also important as synthetic drugs (e.g., barbituric acid derivatives) and chemotherapeutic agents (e.g., sulfadiazine).

Like imidazole (five-membered ring analog of pyrimidine), which also plays an important part in biological processes, pyrimidine can be regarded as a cyclic amidine, and the chemical behavior of its derivatives is dominated by this fact. Thus, although positions 4 and 6 are similar as regards reactivity, positions 2 and 5 stand somewhat apart. The equivalence of positions 4 and 6, which are symmetrically placed, has led to the use of various numbering systems which at times appear confusing [213]. The isomeric nitropyrimidines

here will be numbered according to positional numbers of the nitro groups, eg. 2,4-dinitropyrimidine is called structure **24** etc.

The known mononitro derivative of pyrimidine compound, 4-amino-2,6-dichloro-5-nitropyrimidine [214], is a key intermediate in the synthesis of a purine scaffold, as nucleophilic substitution of the chlorides allows access to a diverse array of potentially biologically active compounds. Furthermore the mono substituted nitropyrimidines were studied theoretically in the literature [215].

Nitropyrimidines are also known as explosive compounds but there have not been any study (to the best knowledge of the authors), both theoretical and experimental, on dinitro, trinitro and tetranitro substituted pyrimidine derivatives (see Figure 44 for the structures). This part of the thesis aims to investigate the stabilities of the nitropyrimidine systems in terms of total energy and NICS data in addition to calculation of the detonation parameters and correlation of them with the TG index.

3.2.5.2.1. Method of Calculation

All the calculations have been performed with Gaussian 03 program package. B3LYP/6-31G(d,p) density functional theory method has been applied for the geometry optimizations, NICS and molecular volume calculations.

3.2.5.2. Results and Discussion

3.2.5.2.1. Energetics

The nitro substituents in the structure of pyrimidine change its electronic character as well as its chemistry. Theoretically nitro-group can be either coplanar or not with the aromatic nucleus. In the case of coplanar nitro group, shift of electrons from the aromatic ring to the nitro group occurs through resonance. This effect produces a flat geometry for the NO_2 group with an sp^2 hybridized nitrogen atom and a relatively short C-N bond of "partially double" character. The exact balance of these processes is subtle and

depends on the possibility of forming resonance structures (the statistical weight of the contributing canonical structures).

Table 22 shows the calculated energies (including zero point energies) and NICS data of the compounds at B3LYP/6-31G(d,p) level. In terms of the energy considerations, the stability order is 5>4>2 for mono-nitro substituted pyrimidines, for dinitrated pyrimidines 46>25>24>45, and for the three nitro substituted pyrimidines 246>245>456 at this performed theoretical levels (see Table 22). The stability order in the case of mono-substituted systems can be explained easily by resonance structures. Also it is well known that electrophilic substitution of pyrimidine results mainly the 5-substituted product, e.g nitration. Among the isomeric dinitro pyrimidine structures, it is clear that the least stable molecule is 45 due to the presence of vicinal nitro groups which causes electronic and steric repulsion. Stability of 46 can be attributed to the symmetrical charge distribution in the system.

The aromaticity of pyrimidine itself is expected to be improved by the substitution of nitro groups due to the following reasoning; due the electro negativity of nitrogen the ring of the pyrimidine suffers from homogeneous electron distribution and thus, poor aromaticity. Insertion of a nitro group into the system will pull the electrons located on the nitrogen atoms of the pyrimidine ring and let these electrons delocalize over the ring which will lead to an improved aromaticity. Therefore, the greater the number of nitro groups properly oriented in the system exists, more aromatic will be the structure. As can be seen in Table 22 pyrimidine has lower (absolutely) NICS value than the nitro counterparts. The NICS values of the nitro substituted systems increase (absolutely) as the number of nitro groups in the structures increases. The NICS values, therefore, the aromaticity of the systems increase in the case where the nitro substitution is at the symmetrical positions 4 and 6. On the other hand, when the nitro group is located in position 5, NICS values decrease. This is quite reasonable, since the distance between nitrogens of the ring and the nitro group increase, the electron withdrawing effect of the nitro group decreases.

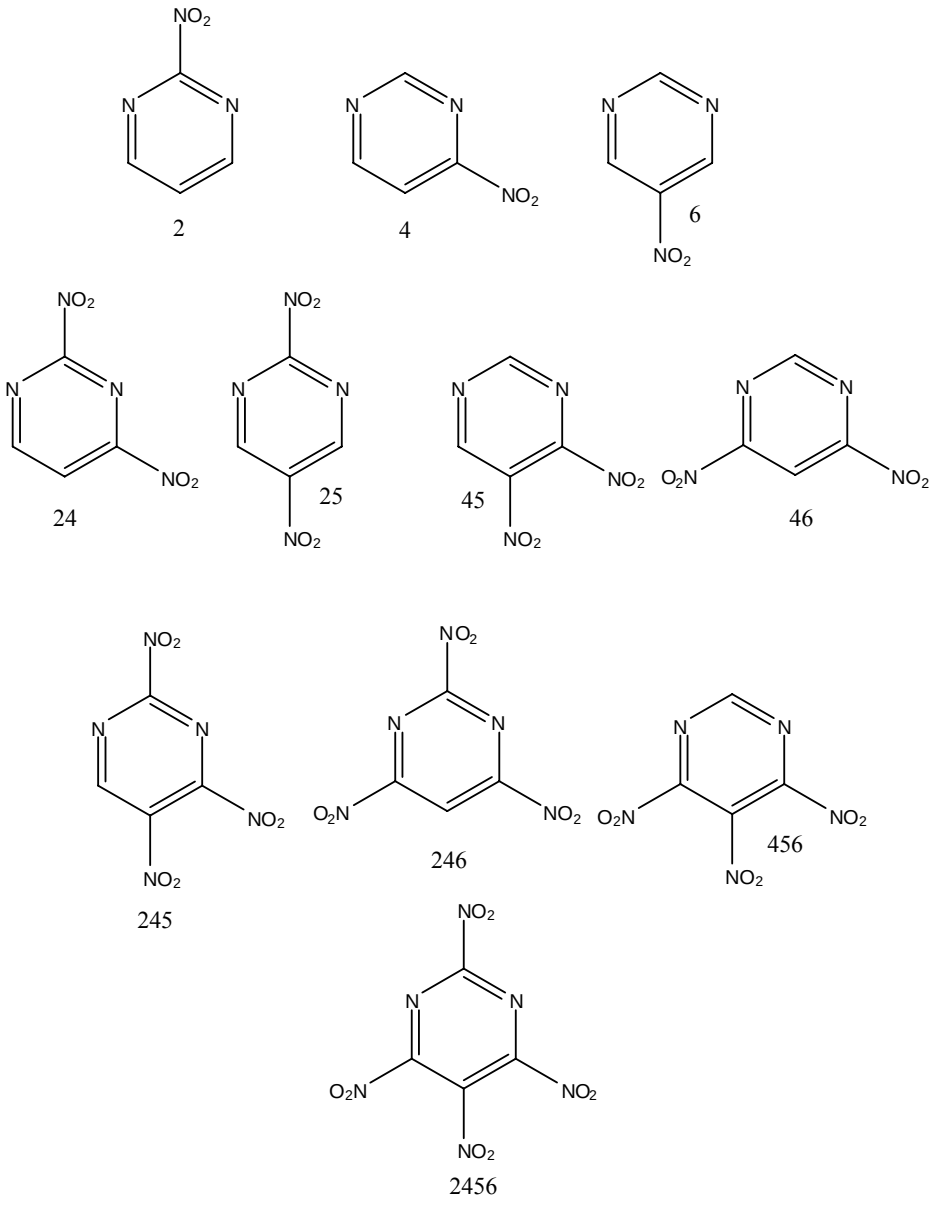

Figure 44. The structures of all possible nitropyrimidine derivatives

Table 20. The zero point energy corrected total energies (Hartree) and NICS (ppm) data for nitropyrimidines.

Structures	Total Energy	NICS
Pyrimidine	-	-6.71
2	-468.8178125	-8.05
4	-468.8211169	-8.63
5	-468.8214355	-7.59
24	-673.3036858	-9.68
25	-673.3043570	-8.73
45	-673.2965086	-9.02
46	-673.3072528	-10.09
245	-877.7751052	-10.01
246	-877.7849952	-11.24
456	-877.7693889	-8.98
2456	-1082.2445560	-11.88

3.2.5.2.2. Predicted Densities and Detonation of the Nitropyrimidine Derivatives

Presently, the detonation parameters of nitropyrimidine derivatives have been calculated using the Kamlet-Jacobs [200-205] equations (see the previous part) and the data have been presented in Table 23.

From mono-substituted to tetra-substituted nitro pyrimidines, density (ρ), velocity of detonation (D) and detonation pressure (P) all increase with the increasing number of the nitro groups. This might show good group additivity on the detonation properties and also supports the claim that introducing more nitro substituents into a molecule usually helps to increase its detonation performance. The tetra-substituted nitro pyrimidine compound which has velocity of detonation value of 9.23 km/s and detonation pressure value of 39.81 GPa, which make it more powerful explosive than the famous explosives HMX and RDX. Furthermore, the relative position of the nitro substituent in the pyrimidine compounds affects the detonation properties (see Table 23). Especially di-, tri- and tetra-nitro substituted pyrimidines might be novel

potential candidates for high energy density materials (HEDMs) when they are successfully synthesized [216].

3.2.5.2.3. Correlation Analysis with TG Index

The results of the correlation analysis of the TG index with the total energies and the explosive properties are given in Table 24. The data in the table reveal that TG index can successfully be used for the prediction of the explosive properties of HEDMs, since the coefficient of determination exceeds 0.985 for Q and P.

Table 21. Predicted densities and detonation properties of the nitropyrimidine derivatives (ΔH_f values are obtained from PM3 calculations, V data are obtained from 100 single point calculations at the 6-31G(d,p) level)

	ΔH_f (kJ/mol)	Q (kJ/g)	V (cm^3/mol)	ρ (g/cm^3)	D (km/s)	P (GPa)	TG Index
2	148.83	1165.46	79.67	1.57	6.44	16.90	2232
4	143.97	1156.18	80.04	1.56	6.41	16.68	2148
5	130.10	1129.67	79.02	1.58	6.43	16.91	2219
24	127.32	1348.19	96.18	1.77	7.76	26.40	9611
25	120.01	1337.91	97.14	1.75	7.69	25.78	11615
45	139.72	1365.60	96.46	1.76	7.77	24.56	9784
46	142.58	1369.63	95.73	1.78	7.81	26.87	9408
245	140.77	1493.30	115.20	1.87	8.54	33.08	32855
246	133.50	1485.22	114.71	1.88	8.56	33.28	28256
456	159.55	1514.17	112.85	1.91	8.70	34.72	29578
2456	169.46	1602.20	131.83	1.97	9.23	39.81	75365

Table 22. The regression equation and the coefficient of determination between the natural logarithm of the TG index and the explosive properties. (Q: Heat of explosion, V: Volume of explosion, D: Velocity of detonation, P: Pressure of explosion)

Property	Regression Equation	R^2
Total Energy	y = -164.54x + 817.18	0.9809
Q	y = 129.66x - 156.81	0.9855
V	y = 14.009x - 30.172	0.9775
ρ	y = 0.1164x + 0.6826	0.9795
D	y = 0.8078x - 0.2577	0.9846
P	y = 6.457x - 33.133	0.9851

3.2.5.3. Nitrotriazines

The six-membered heterocycle consisting of three nitrogen atoms and three carbon atoms alternately located in the ring is known as the symmetrical triazine ring system (**1**) [217]. This heterocycle is ordinarily abbreviated as *s-triazine* (or sym-triazine). The other two isomeric six-membered heterocycles containing three nitrogen and three carbon atoms in the ring are asymmetrical triazine (**2**) [217], designated *as-triazine* (or asymm-triazine) and vicinal triazine (**3**) [217], designated *v-triazine* (or vic-triazine) (see Figure 45).

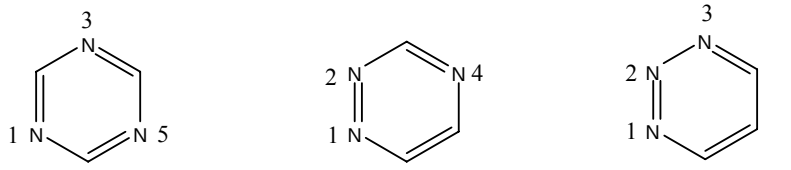

s-triazine (1,3,5-triazine) | as-triazine (1,2,4-triazine) | v-triazine (1,2,3-triazine)

Figure 45. Nomenclature and structures of triazines

One can come across with several reports on the synthesis or theoretical properties of nitro derivatives of triazine systems [218,219,221-224]. Attachment of nitro groups to the possible positions of the different triazine structures will yield 15 structures (see Figure 46 for the structures).

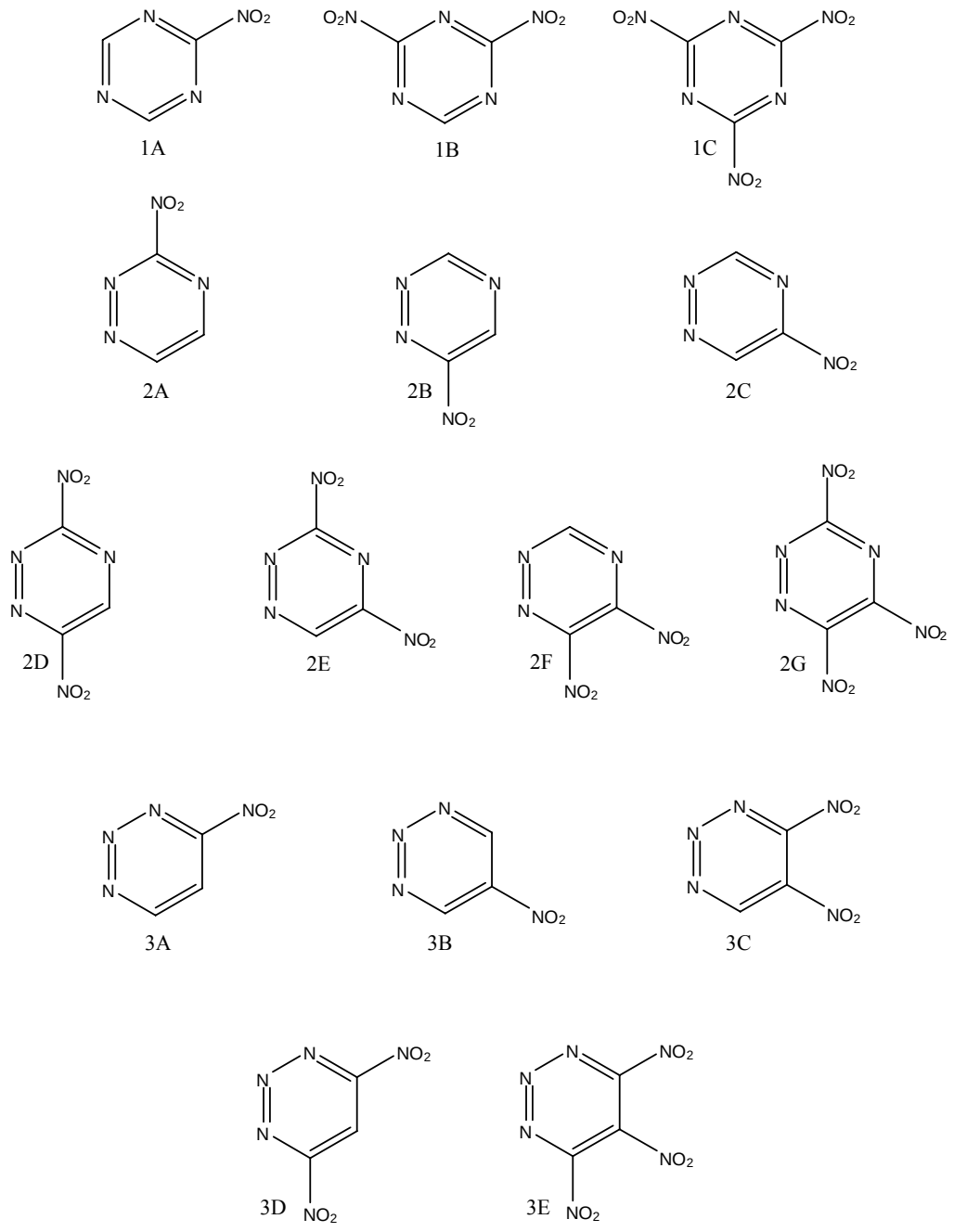

Figure 46. Chemical structures of nitrotriazine structures

3.2.5.3.1. Method of Calculation

All the calculations have been performed with Gaussian 03 program package. B3LYP/6-31G(d,p) density functional theory method has been applied for the geometry optimizations, NICS and molecular volume calculations.

3.2.5.3.2. Results and Discussion

3.2.5.3.2.1. Energetics

The electronic character and the chemistry of triazines change by the substitution of nitro groups. Nitro-groups can be either coplanar or nonplanar with the aromatic nucleus, theoretically. In the case of coplanar nitro group, shift of electrons from the aromatic ring to the nitro group occurs through resonance producing a flat geometry for the NO_2 group with an sp^2 hybridized nitrogen atom with a $C(NO_2)$-N bond of partially double bond character. Table 25 shows the calculated total energies of the compounds within the framework of density functional theory (DFT, B3LYP) at the level of 6-31G(d,p) together with the NICS data of the present systems. Total energies are corrected for zero-point vibrational energy (ZPVE). In terms of the energy considerations, the stability order is 1A>2C>2B>2A>3B>3A for the mono-nitro substituted triazines, for the dinitrated triazines 1B>2E>2D>2F>3D>3C, and for the three-nitro substituted triazines 1C>2G>3E at the performed theoretical level. In summary, the most stable isomeric structures belong to the s-triazine series.

In the present case, NICS values of the various nitrotriazine derivatives have been calculated by the application of density functional theory using the standard 6-31G(d,p) basis set (Table 25). All the molecules have been found to be aromatic. When the NICS data in Table 25 are considered, one can see a drastic increase of the aromaticity going from mono to tri nitro derivatives of s-triazine. Since the parent molecule is highly symmetric, the π-electrons of the ring are strongly withdrawn with the electronegative ring nitrogen atoms. Therefore, s-triazine has the least aromatic character among the triazine isomers. However, the symmetric nature of s-triazine allows the system to be

more and more aromatic by the attachment of increasing number of nitro substituents. At last, the aromaticity of the system (-10.7) reaches almost that of benzene (-11.5) for 2,4,6-trinitrotriazine.

According to the NICS data the most aromatic, thus the most stable compound among the series is 1C, which can be explained by the symmetry present in this structure. The nitrogens of the triazine system and the three nitro groups are arranged symmetrically in this structure, so that the pulling of ring nitrogen electrons into the ring (which presents them to be localized on nitrogens) by the electron withdrawing nitro groups is most effective in this case. Therefore, the ring current has been quite strongly increased; producing a NICS which has the greatest negative value. According to the calculated NICS results, the stability order in three most aromatic nitro triazine derivatives is; 1C>2G>3E in very good agreement with the total energies calculated (see Table 26 also for the total energies). The same argument can hold for the other series.

Table 23. The zero point energy corrected total energies (Hartree) and NICS (ppm) data for nitrotriazines.

Structures	Total Energy	NICS
s-triazine	-	-4.49
as-triazine	-	-4.91
v-triazine	-	-4.77
1A	-484.785890	-6.37
1B	-689.263187	-7.59
1C	-893.734860	-10.68
2A	-484.743161	-5.54
2B	-484.746039	-5.86
2C	-484.747221	-6.30
2D	-689.222241	-6.67
2E	-689.223176	-7.25
2F	-689.217477	-7.40
2G	-893.689908	-8.13
3A	-484.721427	-6.20
3B	-484.721882	-5.94
3C	-689.191306	-7.21
3D	-689.200595	-7.82
3E	-893.659274	-7.96

3.2.5.3.2.2. Predicted Densities and Detonation of the Nitrotriazine Derivatives

The detonation parameters of nitrotriazine derivatives have been calculated using the Kamlet-Jacobs [200-205] equations and the data have been presented in Table 26.

The density (ρ), velocity of detonation (D) and detonation pressure (P) all increase with the increasing number of the nitro groups for nitrotriazines. This might show good group additivity on the detonation properties and also supports the claim that introducing more nitro substituents into a molecule usually helps to increase its detonation performance. 1C has velocity of detonation value of 9.30 km/s and detonation pressure value of 39.23 GPa, 2G has velocity of detonation value of 9.43 km/s and detonation pressure value of 40.68 GPa, 3E has velocity of detonation value of 9.30 km/s and detonation

pressure value of 39.91 GPa, which are found to be more powerful explosives than the famous explosives HMX and RDX [220], theoretically. Moreover, the relative position of the nitro substituent in the triazine compounds affects the detonation properties (see Table 26). Especially di- and tri-nitro substituted triazines will be novel potential candidates for high energy density materials (HEDMs) when they are successfully synthesized [224].

3.2.5.3.2.3. Correlation Analysis with TG Index

The results of the correlation analysis of the TG index with the total energies and the explosive properties are given in Table 27. The data in the table reveal that TG index correlated very well with the investigated data. It can successfully be used for the prediction of the explosive properties of HEDMs except for Q where the coefficient of determination is found to be relatively low.

Table 24. Predicted densities and detonation properties of the nitropyrimidine derivatives (ΔH_f values are obtained from PM3 calculations, V data are obtained from 100 single point calculations at the 6-31G(d,p) level)

	ΔH_f (kJ/mol)	Q (kJ/g)	V (cm^3/mol)	ρ (g/cm^3)	D (km/s)	P (GPa)	TG Index
1A	176.29	1165.14	74.34	1.7	7.2	22.24	1898
1B	173.20	1372.77	95.19	1.8	8.18	29.67	8594
1C	227.52	1861.59	115.44	1.87	9.3	39.23	25972
2A	256.27	1514.72	78.7	1.6	7.41	22.62	2022
2B	257.86	1486.59	78.03	1.62	7.41	22.8	2016
2C	266.56	1498.8	77.11	1.63	7.49	23.44	1946
2D	253.76	1733.89	95.84	1.78	8.63	32.89	10814
2E	256.98	1743.66	94.9	1.8	8.7	33.64	8994
2F	270.60	1732.49	93.54	1.83	8.78	34.51	9058
2G	276.30	1890.69	113.81	1.9	9.43	40.68	31108
3A	329.77	1593.1	78.8	1.6	7.49	23.14	1946
3B	326.14	1552.92	77.75	1.62	7.51	23.47	1948
3C	341.44	1607.83	94.57	1.81	8.55	32.53	8954
3D	340.77	1800.32	96.62	1.77	8.67	32.98	8804
3E	366.08	1710.64	112.06	1.93	9.3	39.91	27801

Table 25. The regression equation and the coefficient of determination between the natural logarithm of the TG index and the explosive properties. (Q: Heat of explosion, V: Volume of explosion, D: Velocity of detonation, P: Pressure of explosion)

Property	Regression Equation	R^2
Total Energy	y = -148.1x + 644.84	0.9871
Q	y = 133.13x – 455.16	0.5284
V	y = 13.084x - 22.471	0.9757
ρ	y = 0.1032x + 0.8493	0.9290
D	y = 0.7303x - 1.8929	0.9682
P	y = 6.3591x - 25.278	0.9787

CHAPTER 4

CONCLUSION

After the pioneering work of Wiener, the importance of graph theoretical descriptors, for use in QSAR and QSPR studies, have been accepted by the scientific community.

Later on, these graph theoretical descriptors have been named as topological indices by Hosoya. Today, there are about a hundred topological indices reported in the literature. However, there is still no topological index that can be applied on each and every molecule or can be used to model all the properties of a substance.

The need for a universal topological index for organic compounds was the motivation of the present study. In this study, a novel topological index has been developed for modeling the physical, chemical and molecular properties of organic compounds.

The novel topological index has been named as the TG Index (Türker-Gümüş Index). The computation of the index is based on familiar concepts of the chemical graph theory, the connectivity and the distance between vertices. Moreover, the index makes use of the T(A) graphs derived by Türker in order to model the alternant hydrocarbons. In addition, the calculation of the index includes the construction of the distance-degree matrix, which is not pronounced in the literature before.

A good topological index must correlate as many properties as of a substance so that it can be used to estimate the properties of unknown compounds. Therefore, the next step, after the construction of the index, was

the application of it on organic compounds. Since the T(A) graphs are based on alternant hydrocarbons, the polyenes have been considered as candidates for correlation analysis. The TG index was quite successful for modeling the total energy, ΔH_f, and HOMO, LUMO, $\Delta\varepsilon$ and λ_{max} data for polyene series.

Thereafter, the index has been found to correlate successfully with the physical properties of linear and branched alkanes together with the cycloalkanes, alkenes, alcohols and amines.

After obtaining reasonably well correlation with the properties of the basic organic systems, the TG index is thought to be good enough to be applied for the estimation of properties of more complex systems, such as explosives.

To be able to predict the detonation properties (detonation pressure, energy and velocity) from a given molecular structure and know the crystal density is of vital importance for especially for designing new explosive material. Quantitative estimation of the properties of compounds, such as heats of formation, density, detonation parameters and sensitivity would permit the selection of the most promising high energy density material (HEDM) candidates for laboratory synthesis and further considerations

For this reason, the molecular orbital and detonation properties of yet nonexistent explosives nitropyridines, nitropyrimidines and nitrotriazines have been calculated theoretically. The computational calculations have been performed using density functional theory and B3LYP correlation function together with several different basis sets.

In the literature, the detonation parameters of explosives have been calculated using the Kamlet-Jacobs equation which need huge computation time and computational resources. However, the strong correlation between the calculated detonation properties and the TG index suggests that the equations from the correlation analyses can replace the Kamlet Jacobs equations. One should still keep in mind that, the ballistic properties obtained by means of any calculation method are helpful for the design purposes. The real behavior of an explosive is to be determined by field tests.

In conclusion, a novel topological index has been constructed and applied for modeling organic compounds. A novel topological matrix (distance-degree matrix) and atomic number weighting (for heteroatom containing species) scheme have been developed The correlation analyses showed quite successful results so that the TG index may replace huge computational effort and can be used to estimate various properties of unknown compounds including the explosives.

REFERENCES

[1] A. C. Brown, Rept. Brit. Assoc. Sci. (1874) 45.

[2] F.M. Flavitsky, J. Russ. Soc. 3 (1871) 160.

[3] R.J. Wilson, Introduction to Graph Theory, Oliver and Boyd, Edinburg, 1972.

[4] G. Avondo-Bodino, Economic Applications of the Theory of Graphs, Gordon and Breach, New York, 1962.

[5] F. Capra, Am. J. Phys. 47 (1979) 11.

[6] D. Cartright, F. Harary, Psychol. Rev. 63 (1963) 277.

[7] R.D. Mattuck, A Guide to Feynman Diagrams in the Many-Body Problem, McGrawhill, New York, 1967.

[8] S. Even, Graph Algorithms, Pitman, London, 1979.

[9] A. Cliff, P. Haggett, K. Ord, in Applications of Graph Theory, (Eds: R.J. Wilson, L.W. Beineke), Academic Press, London, 1979, p.293.

[10] F. Roberts, Applications of Conbinatorics and Graph Theory to the Biological and Social Sciences, Springer-Verlag, New York, 1989.

[11] N.J. Turro, Angew. Chem. Int. Ed. Engl. 25 (1986) 882.

[12] N. Trinajstic, Chemical Graph Theory, CRC Press, Florida, 2000.

[13] D.H. Rouvray, Roy. Inst. Chem. Rev. 4 (1971) 173.

[14] I. Gutman, N. Trinajstic, Topics Curr. Chem. 42 (1973) 49.

[15] A.T. Balaban, Chemical Applications of Graph Theory. Academic Press, London, 1976.

[16] Z. Slanina, Chem. Listy. 72 (1978) 1.

[17] D.H. Rouvray, A.T. Balaban, in Applications of Graph Theory, (Eds: R.J. Wilson, L.W. Beineke), Academic Press, London, 1979, p.177.

[18] R.B. King, Chemical Applications of Topology and Graph Theory, Elsevier, Amsterdam, 1983.

[19] A.T. Balaban, J. Mol. Struct. (Theochem) 120 (1985) 117.

[20] N. Trinajstic, D.J. Klein, M. Randic, Int. J. Quantum Chem. 20 (1986) 699.

[21] V. Prelog, Science 193 (1976) 17.

[22] G. Chartrand, Graphs as Mathematical Models. Prindle, Weber and Schmidt, Boston, 1977.

[23] D.H. Rouvray, Computational Chemical Graph Theory, NovaScience Publishers, New York, 1990.

[24] M.J. Lynch, J.M. Harrison, V.G. Town, J.E. Ash, Computer Handling of Chemical Structure Information, Macdonald, London, 1971.

[25] R.E. Carthart, D.H. Smith, H. Brown, N.S. Sridharan, J. Chem. Inf. Comput. Sci. 15 (1975) 124.

[26] N. Trinajstic, S. Nikolic, J.V. Knop, W.R. Müller, K. Szymanski, Computational Chemical Graph Theory, Simon and Schuster, Chichester, 1991.

[27] E.J. Corey, Q. Rev. Chem. Soc. 25 (1971) 455.

[28] J.B. Hendrickson, D.L. Grier, A.G. Toczko, J. Am. Chem. Soc. 107 (1985) 5288.

[29] B. Ruscic, P. Krivka, N. Trinajstic, Theor. Chim. Acta 69 (1986) 107.

[30] S.J. Cyvin, I. Gutman, Kekule Structures in Benzenoid Hydrocarbons, Springer-Verlag, Berlin, 1988.

[31] L.B. Kier, L.H. Hall, Molecular Connectivity in Chemistry and Drug Research, Academic Press, New York, 1976.

[32] L.B. Kier, L.H. Hall, Molecular Connectivity in Structure-Activity Analysis. Research Studies Press, Hertfordshire, 1986.

[33] D.H. Rouvray, Sci. Am. 254 (1986) 40.

[34] N. Trinajstic, S. Nikolic, S. Carter, Kem. Ind. (Zagreb) 38 (1989) 469.

[35] F. Harary, Graph Theory, Addison-Wesley, Reading, 1971.

[36] L. Euler, Comment. Acad. Sci. Imp. Petropolitanae 8 (1736) 128.

[37] L. Spialter, J. Chem. Doc. 4 (1964) 269.

[38] D.H. Rouvray, in Chemical Applications of Graph Theory, (Ed: A.T. Balaban) Academic Press, London, 1976, p. 175.

[39] A.T. Balaban, Pure Appl. Chem. 55 (1983) 189.

[40] H. Kopp, Ann. Chem. Pharm. 50 (1844) 71.

[41] E. Heilbronner, The HMO Model and Its Application, Wiley, London, 1976.

[42] J. Devillers, A.T. Balaban, Topological Indices and Related Descriptors in QSAR and QSPR. Gordon and Breach Science Publishers, Amsterdam, 1999.

[43] F.S. Roberts, Discrete Mathematical Models. Prentice-Hall, CA, 1975.

[44] M. Barysz, D. Plavsic, N. Trinajstic, Math. Chem. 19 (1986) 89.

[45] H. Wiener, J. Am. Chem. Soc. 69 (1947) 17.

[46] H. Wiener, J. Am. Chem. Soc. 69 (1947) 2636.

[47] J.R. Platt, J. Chem. Phys. 15 (1947) 419.

[48] J.R. Platt, J. Phys. Chem. 56 (1952) 328.

[49] M. Gordon, G.R. Scantlebury, Trans. Faraday, 60 (1964) 604.

[50] H. Hosoya, Bull. Chem. Soc. Japan, 44 (1971) 2332.

[51] I. Gutman, B. Ruscic, N. Trinajstic, C.F. Wilcox, J. Chem. Phys. 62 (1975) 3399.

[52] M. Randic, J. Am. Chem. Soc. 97 (1975) 6609.

[53] W.C. Herndon, Tetrahedron Lett. 8 (1971) 671.

[54] I. Gutman, E. Polansky, Mathematical Concepts in Organic Chemistry, Springer, Berlin, 1977.

[55] A. Groavac, I. Gutman, N. Trinajstic, Topological Approach to the Chemistry of Conjugated Molecules, Springer, Berlin, 1977.

[56] I.V. Proskuryakov, Problems in Linear Algebra, Mir Publishers, Moscow, 1978.

[57] L. Türker, Match 25 (1990) 195.

[58] H. Wiener, J. Chem. Phys. 15 (1947) 766.

[59] L.Türker, Ind. J. of Chem. 42A (2003) 1295.

[60] S. Nikolic, A. Milicevic, N. Trinajstic, Croat. Chem. Acta 78 (2005) 241.

[61] P. Dankelmann, I. Gutman, S. Mukwembi, H.C. Swart, Discrete Math. 309 (2009) 3452.

[62] N. Trinajstic, J. Math. Chem. 2 (1988) 197.

[63] A. Juric, M. Gagro, S. Nikolic, N. Trinajstic, J. Math. Chem. 11 (1992) 179.

[64] M. Medic-Saric, S. Nikolic, J. Matijevic-Sosa, Acta Pharm. 42 (1992) 153.

[65] S. Nikolic, M. Medic-Saric, J. Matijevic-Sosa, Croat. Chem. Acta 66 (1993) 151.

[66] S. Nikolic, N. Trinajstic, Z. Mihalic, J. Math. Chem. 12 (1993) 251.

[67] M. Medic-Saric, S. Rendic, V. Vestemar, S. Saric, Acta Pharm. 43 (1993) 15.

[68] O. Ivanciuc, A. T. Balaban, Match 30 (1994) 117.

[69] A. T. Balaban, Match 21 (1986) 115.

[70] P.A. Philip, T.-S. Balaban, A.T. Balaban, J. Math. Chem. 1 (1987) 61.

[71] H.P. Schultz, E.B. Schultz, T.P. Schultz, J. Chem. Inf. Comput. Sci. 34 (1994) 1151.

[72] G. Klopman, C. Raychaudhury, J. Chem. Inf. Comput. Sci. 30 (1990) 12.

[73] A. T. Balaban, Chem. Phys. Lett. 80 (1982) 399.

[74] A. T. Balaban, Pure Appl. Chem. 55 (1983) 199.

[75] M. Barysz, G. Jashari, R. S. Lall, V. K. Srivastava, N. Trinajstic, in Chemical Applications of Topology and Graph Theory, (Ed: R. B. King), Elsevier, Amsterdam, 1983, pp. 222–227.

[76] A. T. Balaban, MATCH–Commun. Math. Comput. Chem. 21 (1986) 115.

[77] A. T. Balaban, O. Ivanciuc, in MATH/ CHEM/COMP (Ed: A. Graovac), Elsevier, Amsterdam, 1989, pp. 193–211.

[78] O. Ivanciuc, T. Ivanciuc, A. T. Balaban, J. Chem. Inf. Comput. Sci. 38 (1998) 395.

[79] O. Ivanciuc, T. Ivanciuc, A. T. Balaban, in Topological Indices and Related Descriptors in QSAR and QSPR, (Ed: J. Devillers, A. T. Balaban), Gordon and Breach, Amsterdam, 1999, pp. 169–230.

[80] M. Barysz, G. Jashari, R.S. Lall, V.K. Sarivastava, N. Trinajstic, in Chemical Applications of Topology and Graph Theory, (Ed: R.B. King), Elsevier, Amsterdam, 1983, pp. 222-227.

[81] C.J. Cramer, Essentials of Computational Chemistry, John-Wiley, 2004.

[82] J.J.P. Stewart, Encyl. Comput. Chem. 3 (1998) 2080.

[83] D.C. Young, Computational Chemistry, Wiley-Interscience, New York, 2001.

[84] F. Jensen, Introduction to Computational Chemistry, John Wiley and Sons, New York, 1999.

[85] C. Møller, M.S. Plesset, Phys. Rev. 46 (1934) 618.

[86] J. Cizek, J. Chem. Phys. 45 (1966) 4256.

[87] J. Cizek, Adv. Chem. Phys. 14 (1969) 35.

[88] R.J. Bartlett, J. Phys. Chem. 93 (1989) 1697.

[89] E. Fermi, Rend. Accad. Naz. Lincei 6 (1927) 602.

[90] L.H. Thomas, Proc. Cambridge Philos. Soc. 23 (1927) 542.

[91] P. Hohenberg, W. Kohn, Phys. Rev. B 136 (1964) 864.

[92] W. Kohn, L. Sham, J. Phys. Rev. A 140 (1965) 1133.

[93] A.D. Becke, J. Chem. Phys. 98 (1993) 1372.

[94] J.P. Perdew, J. Chem. Phys. 105 (1996) 9982.

[95] A.D. Becke, J. Chem. Phys. 104 (1996) 1040.

[96] A.D. Becke, Phys. Rev. A 38 (1998) 3098.

[97] J.P. Perdew, in Electronic Structure of Solids, (Eds: P. Ziesche, H. Esching) Akademie Verlag, Berlin, 1991.

[98] C. Lee, W. Yang, R.G. Parr, Phys. Rev. B 37 (1998) 785.

[99] I.N. Levine, Quantum Chemistry. Englewood Cliffs, Prentice Hall, New Jersey, 1991, pp. 461–466.

[100] W.J. Hehre, R. Ditchfield, J. Pople, J. Chem. Phys. 56 (1972) 2257.

[101] T.H. Dunning, J. Chem. Phys. 90 (1989) 1007.

[102] M.F. Frisch, G.W. Trucks, H.B. Schleged, G.E. Scuseria, et al., Gaussian 03, Gaussian Inc., Pittsburg, PA, 2003.

[103] Spartan 06, Wavefunction, Inc. Irvine, USA, 2006.

[104] Hyperchem program, Hypercube, Canada, 2002.

[105] J.C.J. Bart, Acta Crystal/ogr. B 24 (1968) 1587.

[106] W. Drenth, E.H. Wiebenga, Acta Crystal. 8 (1955) 755.

[107] E.W. Abrahamson, S.E. Ostroy, Progr. Mol. BioI. 17 (1967) 179.

[108] B. Honig, T. Ebrey, Ann. Rev. Biophys. Bioeng. 3 (1974) 151.

[109] J.A. Dartnall, Handbook of Sensory Physiology, Springer, New York, 1972.

[110] A. Taherpour, F. Shafiei, J Mol. Struct.(Theochem) 726 (2005) 183.

[111] J.J.P. Stewart, J Comput Chem 10 (1989) 209.

[112] J.J.P. Stewart, J Comput Chem 10 (1989) 221.

[113] A.R. Leach, Molecular Modelling, Longman, Essex, 1997.

[114] W. Kohn, L.J. Sham, Phys Rev 140 (1965) 1133.

[115] R.G. Parr, W. Yang, Density Functional Theory of Atoms and Molecules, Oxford University Press, London, 1989.

[116] Hyperchem 7 User's Manual, Tools for Molecular Modeling, Hypercube, Inc., 2002.

[117] S.H. Vosko, L. Vilk, M. Nusair, Can J Phys 58 (1980) 1200.

[118] C. Lee, W. Yang, R.G. Parr, Phys Rev B 37 (1988) 785.

[119] D.E. Needham, I.C. Wei, P.G. Seybold, J. Am. Chem. Soc. 110 (1988) 4186.

[120] R. Sayre, The Molar Refraction of Liquid Organosilicon Compounds. J. Chem. Eng. Data, 9 (1964) 146.

[121] K.G. Denbigh, Trans. Faraday Soc. 36 (1940) 936.

[122] A.I. Vogel, J. Chem. Soc. (1948) 1833.

[123] K.J. Miller, J.A. Savchic, J. Am. Chem. Soc. 101 (1979) 7206.

[124] R.R.Driesbach, Physical Properties of Chemical Compounds, Advances in Chemistry 22, American Chemical Society, Washington DC, 1959.

[125] L. Pauling, D. Pressman, J. Am. Chem. Soc. 67 (1945) 1003.

[126] W.J. Dunn, Eur. J. Med. Chem.-Chim. Ther. 12 (1977) 109.

[127] P.V. Khadikar, D. Mandloi, A.V. Bajaj, S. Joshi, Bioorg. Med. Chem. Lett. 13 (2003) 419.

[128] P.V. Khadikar, S. Karmarkar, J. Chem. Inf. Comput. Sci. 41 (2001) 934.

[129] H. Wiener, J. Am. Chem. Soc. 69 (1947) 17.

[130] L.N. Mulay, A. Weissberger, B. W. Rossiter, Techniques of Chemistry 4, Wiley-Interscience, New York, 1972, p. 431.

[131] R.E. Hoffman, J. Magn. Reson. 163 (2003) 325.

[132] http://en.wikipedia.org/wiki/parachor, August 2009.

[133] O. Exner, Nature, 196 (1962) 890.

[134] T. Sakka, Y.H. Ogata, J. Fluorine Chem. 126 (2005) 371.

[135] R.W. Taft, R.D. Topsom, Prog. Phys. Org. Chem. 16 (1987) 1.

[136] R.W. Taft, Prog. Phys. Org. Chem. 14 (1983) 247.

[137] R.W. Taft, I.A. Koppel, R.D. Topsom, F. Anivia, J. Am. Chem. Soc. 112 (1990) 2047.

[138] D.E. Needham, I.C. Wei, P.G. Seybold, J. Am. Chem. Soc. 110 (1988) 4186.

[139] A. Das, G. Domotor, I. Gutman, S. Joshi, S. Karmarkar, D. Khaddar, T. Khaddar, P.V. Khadikar, L. Popovic, N.S. Sapre, N. Sapre, A.A. Shirhatti, J. Serb. Chem. Soc. 62 (1997) 235.

[140] T. Zeljko, I. Gutman, J. Chem. Inf. Comput. Sci. 41 (2001) 1041.

[141] G. Rücker, C. Rücker, J. Chem. Inf. Comput. Sci. 39 (1999) 788.

[142] R.H. Rohrbaugh, P.C. Jurs, Anal. Chem. 57 (1985) 2770.

[143] P.J. Hansen, P.C. Jurs, Anal. Chem. 59 (1987) 2322.

[144] S. Liu, R. Zhang, M. Liu, Z.J. Hu, Chem. Info. Comput. Sci. 37 (1997) 1146.

[145] S.P. Verevkin, D. Wandschneider, A. Heintz, J. Chem. Eng. Data 45 (2000) 618.

[146] S.D. Nelson, P.G. Seybold, J. Mol. Graph. and Model. 20 (2001) 36.

[147] J.C. Dearden, in Advances in Quantitative Structure Property Relationships, (Ed: M. Charton), Vol. 2, J.A.I. Press, New York, 1999, pp. 127-175.

[148] L.M. Egolf, M.D. Wessel, P.C. Jurs, J. Chem. Inf. Comput. Sci. 34 (1994) 947.

[149] P. Politzer, P. Lane, E.M. Grice, M.C. Concha, P.C. Redfren, J. Mol. Struct. (Theochem) 38 (1995) 249.

[150] J.M. Bakke, Pure Appl. Chem., 75 (2003) 1403.

[151] F. Friedl, Chem. Ber., 45 (1912) 428.

[152] E.F.V. Scriven, G. Jones, in Comprehensive Heterocyclic Chemistry, (Eds: A. J. Boulton, A. McKillop), Vol. 2, Pergamon, Oxford, 1984.

[153] J.M.Bakke, Pure Appl. Chem. 75 (2003) 1403.

[154] J.M. Bakke, H.S.H. Gautun, C. Rømming, I. Sletvold, ARKIVOC x (2001) 26.

[155] J. Chen, G. Ling, S. Lu, Tetrahedron 59 (2003) 8251.

[156] D.L. Romero, R.A. Morge, C. Biles, N. Berrios-Pena, P.D. May, J.R. Palmer, P.D. Johnson, H.W. Smith, M. Busso, C.-K. Tan, R.L. Voorman, F. Reusser, I.W. Althaus, K.M. Downey, A.G. So, L. Resnick, W.G. Tarpley, P.A. Aristoff, J. Med. Chem.37 (1994) 999.

[157] R.W. Millar, R.P. Claridge, J.P.B. Sandall, C. Thompson, ARKIVOC iii (2002) 19.

[158] S. Youssif, ARKIVOC i (2001) 242.

[159] A.R. Katritzky, E.F.V. Scriven, S. Majumder, R.G. Akhmedova, A.V. Vakulenko, N.G. Akhmedov, R. Murugan, K.A. Abboud, Org . Biomol. Chem. 3 (2005) 538.

[160] L.E. Fried, M.R. Manaa, P.F. Pagoria, R.L. Simpson, Annu. Rev. Mater. Res. 31 (2001) 291.

[161] D.E. Chavez, M.A. Hiskey, R.D. Gilardi, Angew. Chem. 39 (2000) 1971.

[162] L. Türker, T. Atalar, J. Hazard. Mater. 137 (2006) 1333.

[163] M.A. Johnson, T.N. Truong, J. Phys. Chem. B 103 (1999) 9392.

[164] S. Zeman, W.A. Trcinski, R. Matyas, J. Hazard. Mater. 154 (2008) 192.

[165] V.I. Minkin, M.N. Glukhovtsev, B.Y. Simkin, Aromaticity and Antiaromaticity: Electronic and Structural Aspects, Wiley, New York, 1994.

[166] P.R. Schleyer, H. Jiao, Pure Appl. Chem., 68 (1996) 209.

[167] M.N. Glukhovtsev, J. Chem. Educ., 74 (1997) 132.

[168] T.M. Krygowski, M.K. Cyranski, Z. Czarnocki, G. Hafelinger, A.R. Katritzky, Tetrahedron, 56 (2000) 1783.

[169] P.R. Schleyer, Chem. Rev. 101 (2001) 1115.

[170] M.K. Cyranski,T. M. Krygowski, A.R. Katritzky, P.R. Schleyer, J. Org. Chem., 67 (2002) 1333.

[171] P.R. Schleyer, C. Maerker, A. Dransfeld, H. Jiao, N.J.R.E. Hommes, J. Am. Chem. Soc., 118 (1996) 6317.

[172] H. Jiao, P.R. Schleyer, J. Phys. Org. Chem. 11 (1998) 655.

[173] P.R. Schleyer, B. Kiran, D.V. Simion, T.S. Sorensen, J. Am. Chem. Soc. 122 (2000) 510.

[174] D. Quinonero, C. Garau, A. Frontera, P. Ballaster, A. Costa, P.M. Deya, Chem. Eur. J. 8 (2002) 433.

[175] S. Patchkovskii, W. Thiel, J. Mol. Model., 6 (2002) 67.

[176] R.J. Berry, C.J. Ehlers, D.R. Burgess Jr., M.R. Zachariah, M.R. Nyden, M. Schwartz, J. Mol. Struct. (Theochem) 422 (1998) 89.

[177] J.S. Francisco, Chem. Phys. Lett. 294 (1998) 319.

[178] K.P. Sudlow, A.A. Woolf, J. Fluorine Chem. 96 (1999) 141.

[179] T.S. Cheung, C.K. Law, W.K. Li, J. Mol. Struct. (Theochem) 572 (2001) 243.

[180] M.F. Cheng, H.O. Ho, C.S. Lam, W.K. Li, Chem. Phys. Lett. 356 (2002) 109.

[181] C.J. Cobos, J. Mol. Struct. (Theochem) 581 (2002) 17.

[182] D. Yu, G. Orlov, V.V. Bouchoux, D.A. Takhistov, J. Ponomarev, J. Mol. Struct. 608 (2002) 109.

[183] B.S. Jursic, J. Mol. Struct. (Theochem) 417 (1997) 99.

[184] D.W. Ball, J. Mol. Struct. (Theochem) 417 (1997) 107.

[185] B.M. Rice, S.V. Pai, J. Hare, Combust. Flame 118 (1999) 445.

[186] E. Vayner, D.W. Ball, J. Mol. Struct. (Theochem) 496 (2000) 175.

[187] P.A. Denis, O.N. Ventura, Chem. Phys. Lett. 344 (2001) 221.

[188] P.W. Atkins, Physical Chemistry, Oxford University Press, Oxford, 1990.

[189] W.J. Hehre, L. Radom, P.V.R. Schleyer, J.A. Pople, Ab Initio Molecular Orbital Theory, Wiley, New York, 1986.

[190] C.I. Williams, M.A. Whitehead, J. Mol. Struct. (Theochem) 393 (1997) 9.

[191] J.P. Guthrie, J. Phys. Chem. A 105 (2001) 9196.

[192] J.S. Webber, R. Woolley, J. Mol. Struct. (Theochem) 341 (1995) 171.

[193] A.El. Hammadi, M.El. Mouhtadi, J. Mol Struct. (Theochem) 497 (2000) 241.

[194] O.V. Dorofeeva, V.S. Yungman, Fluid Phase Equilib. 199 (2002) 147.

[195] O.N. Ventura, M. Kieninger, P.A. Denis, R.E. Cachau, J. Phys. Chem. A 105 (2001) 9912.

[196] O.N. Ventura, M. Kieninger, Chem. Phys. Lett. 245 (1995) 488.

[197] P.C. Chen, Y.C. Chieh, S.C. Tzeng, J. Mol. Struct. (Theochem) 634 (2003) 215.

[198] J.B. Foresman, A. Frisch, Exploring Chemistry with Electronic Structure Methods, Gaussian, Inc, Pittsburgh, 1996.

[199] B.S. Jursic, J.W. Timberlake, P.S. Engel, Tetrahedron Lett. 37 (1996) 6473.

[200] M.J. Kamlet, S.F. Jacobs, J. Chem. Phys. 48 (1968) 36.

[202] M.J. Kamlet, C. Dickenson, J. Chem. Phys. 48 (1968) 43.

[203] M.J. Kamlet, H.J. Hurwitz, J. Chem. Phys. 48 (1968) 3685.

[204] H.J. Hurwitz, M.J. Kamlet, Israel J. Tech. 7 (1968) 431.

[205] M.J. Kamlet, J.M. Short, Combust. Flame 38 (1980) 221.

[206] S. Zeman, Thermochim. Acta. 31 (1979) 269.

[207] L. Qiu, H.M. Xiao, X.H. Ju, X.D. Gong, Int, J. Quantum Chem. 105 (2005) 48.

[208] X.J. Xu, H.M. Xiao, X.D. Gong, X.H. Ju, Z.X. Chen, J. Phys. Chem. A 109 (2005) 11268.

[209] L. Qiu, H. Xiao, X. Gong, X. Ju, W. Zhu, J. Phys. Chem. A 110 (2006) 3797.

[210] G.S. Chung, M.W. Schimidt, M.S. Gordon, J. Phys. Chem. A 104 (2000) 5647.

[211] J.J. Xiao, J. Zhang, D.Yang, H.M. Xiao, Acta Chim. Sinica 60 (2002) 2110.

[212] P.E. Eaton, R.L. Gilardi, M.X. Zhang, Advanced Materials, 12 (2000) 1143.

[213] R.C. Elderfield, Heterocyclic Compounds, John Wiley and Sons Inc, New York, 1957, pp. 234-235.

[214] D. McKeveney, R.J. Quinn, C.O. Janssen, P.C. Healy, Acta Cryst. E 60 (2004) 241.

[215] P. Politzer, J.S. Murray, M.C. Concha, J. Phys. Chem. A. 102 (1998) 6697.

[216] L. Türker, S. Gümüş, T. Atalar, Y. Çamur, in New Research on Hazardous Materials, Nova Publishers, 2007.

[217] C. Patterson, The Ring Index, American Chemical Society, Washington D.C., 1960, p. 27.

[218] A.V. Shastin, T.I. Godovikova, B.L. Korsunskii, Russ. Chem. Rev. 72 (2003) 279.

[219] V.L. Rusinov, O.N. Chupakhin, Rossiiskii Khimicheskii Zhurnal 41 (1997) 103.

[220] P.W Cooper, Explosive Engineering, Wiley-VCH, New York, 1996.

[221] V.L. Rusinov, A.Y. Petrov, G.G. Aleksandrov, O.N. Chupakhin, Khimiya Geterotsiklicheskikh Soedinenii 1 (1994) 52.

[222] G.G. Moskalenko, V.F. Sedova, V.R. Akhmetova, V.N. Odinokov, V.P. Mamaev, Khimiya Geterotsiklicheskikh Soedinenii 5 (1990) 657.

[223] T.A. Andreeva, V.P. Krivopalov, V.I. Eroshkin, V.P. Mamaev, Izvestiya Akademii Nauk SSSR, Seriya Khimicheskaya 5 (1987) 1196.

[224] L. Türker, S. Gümüş, T. Atalar, Y. Çamur, J. Hazard. Mater. 167 (2009) 440.

CURRICULUM VITAE

PERSONAL INFORMATION

Surname, Name: Gümüş, Selçuk
Nationality: Turkish (TC)
Date and Place of Birth: 14 December 1977, Bursa
Marital Status: Married
Phone: +90 312 210 51 44
Fax: +90 312 210 32 00
email: sgumus@metu.edu.tr

EDUCATION

Degree	Institution	Year of Graduation
PhD	METU Department of Chemistry	2009
BS	METU Department of Chemistry	2000
High School	Bursa Tophane Anadolu Meslek Lisesi	1995

WORK EXPERIENCE

Year	Place	Enrollment
2000-	METU Department of Chemistry	Research Assistant

FOREIGN LANGUAGES

Fluent English

PUBLICATIONS

1. Türker, L., Atalar, T. Gümüş, S., "A DFT study on nitrotriazines", Journal of Hazardous Materials, Vol. 167, pp. 440-448 2009.

2. Türker, L., Tapan, A., Gümüş, S., "Electroluminescent properties of certain polyaromatic compounds: Part 2 Organic Emitters", Polycyclic Aromatic Compounds, Vol. 29, pp. 139-159 2009.

3. Türker, L., Tapan, A., Gümüş, S., "Electroluminescent properties of certain polyaromatic compounds: Part 1 Characteristics of OLED Devices Based on

Fluorescent Polyaromatic Dopants", Polycyclic Aromatic Compounds, Vol. 29, pp. 123-138 2009.

4. Türker, L., Gümüş, S., "A Theoretical Study on Some (1,4)Cyclophanes", Polycyclic Aromatic Compounds, Vol. 29, pp. 103-122 2009.

5. Türker, L., Gümüş, S., "1,3-Dipolar cycloaddition reactions of 1-Methyl-3-oxidopyridinium betaine with C_{70}-A theoretical study", Journal of Computational and Theoretical Nanoscience, Vol. 6, pp.873-879 2009.

6. Türker, L., Gümüş, S., "DFT Studies on η^6-Coronene-$Cr(CO)_3$ Complexes", Acta Chimica Slovenica, Vol. 56, pp.246-253 2009.

7. Türker, L., Gümüş, S., "A theoretical study on vomitoxin and its tautomers", Journal of Hazardous Materials, Vol. 163, pp.285-294 2009.

8. Türker, L., Gümüş, S., Tapan, A., "Biohydrogen production: molecular aspects", Journal of Scientific and Industrial Research, Vol. 67, pp. 994-1016, 2008.

9. Türker, L., Gümüş, S., Atalar, T., Atlanel, S., "A Theoretical Study on Nitrourea and its Tautomers", Journal of Energetic Materials, Vol. 26, pp. 181-195, 2008.

10. Türker, L., Gümüş, S., "Quantum chemical treatment of nivalenol and its tautomers", Journal of Hazardous Materials, Vol. 153, pp. 329-339, 2008.

11. Türker, L., Gümüş, S., "Positional Effect of Nitrogen Substitution on a Certain Perylene Chromophore-A semiempirical treatment", Polycyclic Aromatic Compounds, Vol. 28, pp. 4-14, 2008.

12. Türker, L., Gümüş, S., Atalar, T., Atlanel S., "Theoretical Study on Nitrourea and its Tautomers", Journal of Energetic Materials, Vol. 28, pp.181-195 2008.

13. Türker, L., Gümüş, S., "AM1, MNDO and MINDO/3 treatments of Hückel type cyclacenes", Polycyclic Aromatic Compounds, Vol. 26, pp. 367-384, 2006.

14. Türker, L., Gümüş, S., "Molecular orbital treatment of some endohedrally doped C_{60} systems", Polycyclic Aromatic Compounds, Vol. 26, pp. 145-162, 2006.

15. Türker, L., Gümüş, S., "Hydrogen storage capacity of $Mg@C_{120}$ system", Journal of Molecular Structure: THEOCHEM, Vol. 719, pp. 103-107, 2005.

16. Türker, L., Gümüş, S., "Peripherally B and N substituted cyclacenes", Journal of Molecular Structure: THEOCHEM, Vol. 686, pp. 91-95, 2004.

17. Türker, L., Gümüş, S., "Cyclacenes", Journal of Molecular Structure: THEOCHEM, Vol. 685, pp. 1-33, 2004.

18. Türker, L., Gümüş, S., "A quire behavior of $(Li+nH_2)@C_{58}$ systems-an AM1 treatment ", Journal of Molecular Structure: THEOCHEM, Vol. 684, pp. 205-209, 2004.

19. Türker, L., Gümüş, S., "AM 1 treatment of endohedrally hydrogen doped C_{56} systems, $nH_2@C_{56}$ ", Journal of Molecular Structure: THEOCHEM, Vol. 681, pp. 21-25, 2004.

20. Türker, L., Gümüş, S., "Mono, B, N, Si, or Ge substituted cyclacenes. A theoretical study", Journal of Molecular Structure: THEOCHEM, Vol. 679, pp. 143-147, 2004.

21. Türker, L., Gümüş, S., "An AM1 study on $C_{60}@C_{180}$ system", Journal of Molecular Structure: THEOCHEM, Vol. 674, pp. 15-18, 2004.

22. Türker, L., Gümüş, S., "Cyclacenes having mono boron or nitrogen atom in the backbone-A theoretical study", Journal of Molecular Structure: THEOCHEM, Vol. 674, pp. 185-189, 2004.